MULTINUCLEAR MAGNETIC RESONANCE AND CALORIMETRIC STUDIES OF SODIUM CATION COMPLEXES WITH SOME CROWN ETHERS AND CRYPTANDS IN VARIOUS SOLVENTS

By

Jy Dale Lin

A DISSERTATION

Submitted to
Michigan State University
in partial fulfillment of the requirements
for the degree of

DOCTOR OF PHILOSOPHY

Department of Chemistry

1980

ABSTRACT

MULTINUCLEAR MAGNETIC RESONANCE AND CALORIMETRIC STUDIES OF SODIUM CATION COMPLEXES WITH SOME CROWN ETHERS AND CRYPTANDS IN VARIOUS SOLVENTS

By

Jy Dale Lin

Sodium (^{23}Na), carbon (^{13}C) and proton (^{1}H) nuclear magnetic resonance methods were used to study sodium cation complexes with three crown ethers; 18-crown-6 (18C6), 15-crown-5 (15C5) and monobenzo-15-crown-5 (MB15C5), in aqueous and in several nonaqueous solvents. Concentration formation constants of these complexes were determined from the variation of the ^{23}Na chemical shift as a function of ligand/Na^+ mole ratio or from the variations of the ^{13}C chemical shifts with Na^+/ligand mole ratios. In general, the stability of the complex varies inversely with the solvating ability of solvent as expressed by the Gutmann donor number. For example, the formation constants for $Na^+ \cdot 18C6$ complex are log $K \geq 4$ in tetrahydrofuran (THF), acetone (Me_2CO), propylene carbonate (PC) and nitromethane ($MeNO_2$), log K = 3.8 $\pm$ 0.2 in acetonitrile (MeCN), log K = 1.41 $\pm$ 0.07 in dimethylsulfoxide (DMSO), log K = 2.31 $\pm$ 0.05

in dimethylformamide (DMF) and log K = 0.82 ± 0.05 with NaI salt in water. The relative stabilities of the complexes are in the order $Na^+ \cdot 18C6 > Na^+ \cdot 15C5 > Na^+ \cdot MB15C5$.

The formation of a 2:1 (ligand:Na^+ ion) complex is more favorable in a poorly solvating solvent such as $MeNO_2$ if the ligand cavity size is smaller than the cation size. The 2:1 complex formation constants in $MeNO_2$ solution were found to be K_2 = 1.6 ± 0.2 and K_2 = 0.8 ± 0.2 for sodium-15C5 and sodium-MB15C5 complexes respectively.

The apparent exchange rate of the sodium cation between the bulk solution and the $Na^+ \cdot 18C6$ complex in solvents of low dielectric constant such as THF and 1,3-dioxolane was found to be dependent on the anion. The exchange is slower with tetraphenylborate anion than with perchlorate or iodide anions.

Complexation of the sodium cation by four cryptands, C211, C221, C222 and C222B, in water and in several nonaqueous solvents was studied by the sodium-23 NMR technique. In most cases studied, the cation exchange between the bulk solution and the complex is slow on the NMR time scale since two resonances of the ^{23}Na nucleus were observed when the Na^+ ion was present in excess. In all solvents used in this study, the three cryptands, C221, C222 and C222B, form very stable 1:1 complexes (log K ≥ 4) with the sodium cation. The resonance linewidth of the $Na^+ \cdot C211$ complex is so broad (about 150 Hz to 300 Hz) that no definite conclusion about

the stability of the complex can be made.

For all the cryptates, the chemical shifts of the complexed Na^+ ion are solvent-dependent indicating that the Na^+ ion is not completely shielded by the cryptands from the external medium. The chemical shifts of the individual cryptate in the various solvents studied are in the same general area and the values are around +11 ppm, -4 ppm, -9 ppm and -11 ppm for $Na^+ \cdot$C211, $Na^+ \cdot$C221, $Na^+ \cdot$C222B and $Na^+ \cdot$C222 cryptates respectively.

The thermodynamic parameters of sodium cation complexes with three crown ethers, 18C6, 15C5 and MB15C5, were determined by ^{23}Na NMR and calorimetric techniques in several nonaqueous solvents. For $Na^+ \cdot$15C5 complex in DMF solution the values obtained from both methods agree within experimental error. The values are ΔH^o = -4.7 $\pm$ 0.8 kcal/mole and ΔS^o = -7 $\pm$ 3 e.u. from the NMR method, and ΔH^o = -4.2 $\pm$ 0.4 kcal/mole and ΔS^o = -5 $\pm$ 1 e.u. from the heat of complexation determined calorimetrically and the stability constant determined by ^{23}Na NMR. In most cases, the sodium-crown complexes are enthalpy stabilized but entropy destabilized. However, in few cases the complexes were found to be entirely entropy stabilized.

To My Parents.

ACKNOWLEDGMENTS

The author wishes to thank Professor Alexander I. Popov for his constant guidance throughout this study.

Professor James L. Dye is acknowledged for his helpful suggestions as second reader.

Gratitude is extended to the Department of Chemistry, Michigan State University and the National Science Foundation for financial aid. Many thanks go to all the members of Dr. A. I. Popov's research group for their friendship and stimulation.

Deep appreciation to my parents, brother and sisters for their love and encouragement during the course of this study. To my parents, I dedicate this thesis.

TABLE OF CONTENTS

LIST OF TABLES

Table | Page

Table | Page

LIST OF FIGURES

CHAPTER I

HISTORICAL REVIEW

1. Introduction

Since Pedersen's first synthesis of macrocyclic polyethers (called crowns) which form stable complexes with the alkali and alkaline earth cations (1), the properties of these ligands and related synthetic macrocyclic compounds and their complexes have been under active investigation in many laboratories (2). Typical examples of some crown ethers are given in Figure 1.

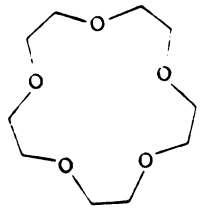

15-Crown-5 (I)
cavity: 1.7-2.2 Å

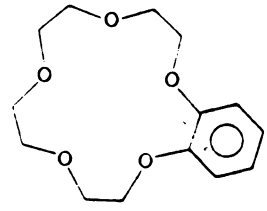

Monobenzo-15-Crown-5 (II)

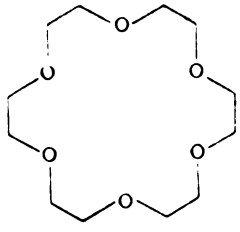

18-Crown-6 (III)
cavity: 2.6-3.2 Å

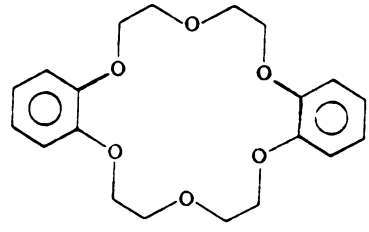

Dibenzo-18-Crown-6 (IV)

Figure 1. Structural formulas and cavity sizes of some macrocyclic polyethers.

The cavity size and the properties of the crown ether can be modified by changing the number of methylene groups as well as the number and the nature of the heteroatoms in the ring. Some of the polyethers have the useful property of solubilizing ionic compounds in organic solvents (1). The macrocyclic compounds not only form stable complexes with various ions but also can selectively bind certain cations in the presence of others in solution (3).

Shortly after Pedersen's publications, Lehn and his co-workers introduced the diazapolyoxa-macrobicyclic ligands, termed cryptands (4), which form three dimensional inclusion complexes (cryptates) with various metal cations. If the size of the cation is equal to or somewhat smaller than the size of the cryptand cavity, the complexed cation is essentially insulated from the medium. The cavity size and the properties of cryptands can also be varied by changing the number and type of the binding sites. The stabilities and selectivities of the cryptand complexes with suitable alkali and alkaline earth cations are several orders of magnitude larger than those of naturally occurring or synthetic monocyclic ligands (5). Some typical cryptands are shown in Figure 2.

One of the remarkable properties of crown ethers and cryptands is that they can dissolve alkali metals in solvents in which the latter are normally insoluble or only slightly soluble (6, 7). Dye and co-workers first

synthesized a salt containing an alkali metal anion, $(Na^{+}\cdot C222)Na^{-}$, as gold colored crystals with a shiny metallic appearance by dissolving metallic sodium in ethylamine in the presence of C222 (8). They studied the properties of various alkali metal anions in solutions and in solids by spectroscopic methods (9-11). The current status of research in this field has been recently reviewed by Dye (12).

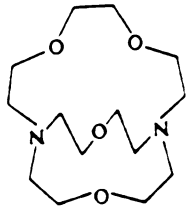

C211 cavity: 1.6 Å (V)

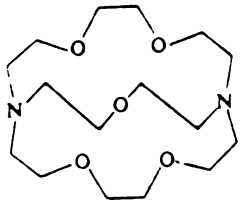

C221 cavity: 2.2 Å (VI)

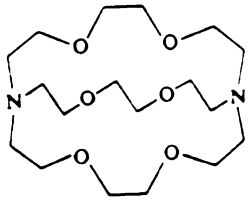

C222 cavity: 2.8 Å (VII)

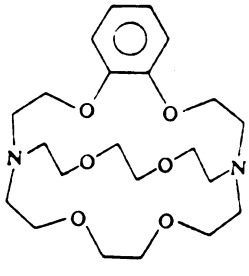

C222B (VIII)

Figure 2. Structural formulas and cavity sizes of some macrobicyclic cryptands.

Ligands containing three and four macrocycles have also been synthesized (13, 14). The properties and applications of the complexation reactions of these cryptands with various metal cations, anions and molecules in solids and in solutions have been extensively studied and reviewed by Lehn et al. (15-17). Several useful and important review articles (3, 18-22) have been published on the studies of macrocyclic ligands and their complexes. In this thesis, only studies on the alkali metal complexes of small crowns ($\leq$ 18-membered ring) and 2-cryptands will be discussed. The literature up to early 1978 on complexes of large crown ethers can be found in the Ph.D. thesis of M. Shamsipur (23).

2. Complexation of alkali metal cations with macromonocyclic compounds - crown ethers ($\leq$ 18 member ring)

The macrocyclic polyethers have been found to form primarily two-dimensional, one to one (1:1) polyether-metal ion complexes with a large variety of metal ions both in solutions and in the crystalline form (1, 3). However, depending on the ratio of the polyether cavity to metal ion diameter, as well as on the solvents and the counterions, complexes with other stoichiometries such as 2:1, 3:2, and 1:2 (ether:metal ion) complexes are also formed (24, 25). The crystal structures of a number of crown complexes have been determined (26-32). It was shown that for all 1:1 complexes except the 18-crown-6·NaSCN complex, the alkali metal cation is located approximately

in the center of and sometimes slightly above a planar ring of the ether oxygen atoms. In a number of cases the metal ion is also bound to the solvent molecules and/or the anions, i.e. the polyether ring could only partially replace the solvation sphere of the cation. In the 18-crown-6·NaSCN complex, the ether oxygen ring of 18-crown-6 is strongly distorted from its symmetrical conformation to accommodate the smaller cation, i.e. one of the oxygen atoms is drawn out of the mean plane of the other five to give a somewhat irregular pentagonal pyramidal coordination of the Na^+ ion (28). The 2:1 complexes, e.g. potassium ion benzo-15-crown-5 (30) and sodium ion 12-crown-4 complexes (31, 32), were shown to have a "sandwich" structure in which the metal ion lies between two ligand molecules and does not interact with either the solvent molecules or the anions.

The solution structures of some crown ethers and their cation complexes in water, water-acetone, acetone and chloroform were investigated by Live and Chan (33) using proton (^1H) and carbon (^{13}C) nuclear magnetic resonance. The complexes of benzo-18-crown-6 and dibenzo-18-crown-6 (DB18C6) with Na^+ and K^+ ions were shown to have the same structure in the various solvents as do the DB18C6 complexes in the crystalline state. The "sandwich" complex with a Cs^+ ion between two DB18C6 molecules was found to exist in acetone and chloroform solutions.

The formation of complexes between the cyclic polyethers and alkali metal salts has been studied by a number of different techniques: solubility changes, extraction, potentiometry, calorimetric titration, polarographic reduction, conductance measurement, UV, IR and NMR spectroscopy (2). Frensdorff (34) determined the complex stability constants of a variety of crown ethers with several cations in aqueous and methanolic solutions potentiometrically with cation selective electrodes. The stability constants were found to be three to four decades higher in methanol than in water, since methanol is a much weaker solvating medium and thus competes less with the polyether for the cations.

Selectivity toward different cations varies with polyether ring size, the optimum ring size being such that the cation just fits into the hole. Comparison of the stabilities of the Na^+, K^+ and Cs^+ ions each with the crown of optimum ring size in methanol reveals that the K^+ complex is the most stable by at least one order of magnitude. This observation seems to reflect the competition between complex formation and solvation. The largest cation has low stability constant because it has low charge density and thus does not attract the polyether very much, while the smallest cation is too strongly solvated for the polyether to compete successfully for the cation. It was noted that the substitution of nitrogen

or sulfur atoms for oxygen in the polyether ring reduces the stabilities of potassium complexes but greatly strengthens those of the Ag^+ ion complexes which involve covalent bonding. The K^+ ion complex stability constants decrease in the order, O > NR > NH > S.

Izatt et al. (35-38) determined the formation constants and thermodynamic parameters ($\Delta H°$ and $\Delta S°$) for the interaction of the two isomers of dicyclohexano-18-crown-6 with several uni- and divalent cations in water by using a calorimetric titration technique. The stability order for the alkali metal ions with either isomer is essentially the same as the permeability order for these same metal ions with the structurally related antibiotics, valinomycin and monactin, i.e. $K^+ > Rb^+ > Cs^+$, $Na^+ > Li^+$, for the transport of these ions through natural and synthetic membranes. The behavior of these two isomers in terms of log K, $\Delta H°$, $\Delta S°$ and the selectivity toward the alkali and alkaline earth cations for the complexation reaction in aqueous solution is different due to the structural differences of the isomers.

By using electrical conductance measurements, Evans et al. (39) determined the formation constants of dibenzo-18-crown-6 and dicyclohexano-18-crown-6 complexes with sodium, potassium and cesium salts in methanol and acetonitrile solutions. These authors found that the association constants of Na^+·DBC in methanol and acetonitrile and K^+·DBC in acetonitrile are nearly independent of temperature

in the range 10-25°C. The fact that the sodium ion is more strongly complexed in acetonitrile than in methanol was explained by its weaker solvation in the former solvent. Similar results were also obtained by Koryta et al. (40, 41) from polarographic studies of alkali metal cations complexed with crown ethers in methanol and acetronitrile solutions; the stability constants of the sodium complexes with some 18- and 24-membered crown ethers in acetonitrile are comparable or higher than the stability constants of the potassium complexes with the same crowns. This behavior was attributed to the higher surface charge density of the sodium ion and, therefore, a stronger dipole-ion bond of the ion with the ligand. The difference in the solvation energies of Na^+ and K^+ ions in the weaker solvating medium of acetonitrile also becomes less significant. It was noted that the sodium ion forms more stable complexes with 18-membered crowns than with the 15-membered ones.

The complexation constants of sodium, potassium and cesium salts with dicyclohexano-18-crown-6 were measured polarographically in methanol, ethanol and n-propanol by Agostiano et al. (42). For each ion the equilibrium constant of the complex was found to increase in the order of methanol < ethanol < n-propanol. This was attributed to the decrease in the dipole moment of the solvent molecule from methanol to n-propanol by the authors.

Stability constants for complex formation of dibenzo-18-crown-6 with a series of metal ions in aqueous solutions were determined spectrophotometrically by Shchori et al. (43). They noted that the concentration formation constants of the complexes depend on the counter ion and on the ionic strength of the solution. The thermodynamic constants were obtained by extrapolating the experimental values at several ionic strengths to infinite dilution. A similar dependence of the concentration formation constants (Kc) on the ionic strength (I) of the solution was found by Smetana and Popov (44) for the 18-crown-6 sodium salt complex in anhydrous methanol solutions. It was also shown that the Kc values remained reasonably constant for $I \leq 0.05$ mol dm^{-3}.

The effect of substituents in the aromatic ring on the complexation of sodium cation with dibenzo-18-crown-6 (DBC), cis-4, 4'-dinitrodibenzo-18-crown-6 (NDBC) and cis-4, 4'-diaminodibenzo-18-crown-6 (AmDBC) in dimethylformamide solution was investigated conductometrically by Shchori and Grodzinski (45). The order of the equilibrium constant was found to be as follows:

$$K_{NDBC} < K_{DBC} \cong K_{AmDBC}$$

The sodium ion complex of the dinitro derivative NDBC, which contains the electron-withdrawing $-NO_2$ groups, is five times less stable than that of DBC. The AmDBC contains two

strongly electron-donating $-NH_2$ groups and thus is expected to form more stable complex with sodium ion than DBC. The nearly identical complex stabilities of sodium ion with DBC and with AmDBC was attributed to possible conformational changes in the macrocyclic ring due to hydrogen bonding involving the two amino groups.

Substituent effects on the stabilities of sodium and potassium cation complexes with a series of 4'-substituted monobenzo-15-crown-5 and monobenzo-18-crown-6 ethers were also determined conductometrically in acetone solution by Ungaro et al. (46). The substituent effect for the complexes of Na^+ ion with benzo-15-crown-5 is very pronounced, e.g. a nearly 25-fold difference in K between the 4'-amino- and 4'-nitrobenzo-15-crown-5, while the effect on the complexes of Na^+/benzo-18-crown-6 is much smaller, and almost negligible for the electron-withdrawing substituents. The above results were explained by the possible conformational changes in the polyether ring of Na^+/benzo-18-crown-6 complexes on varying the 4'-substituents. The effects are somewhat larger for K^+/benzo-18-crown-6 complexes than for Na^+/benzo-18-crown-6 complexes.

Pannell et al. (47) studied substituent effects on the selectivity of dibenzo-18-crown-6 vis-a-vis sodium and potassium salts by extracting the salts in water with the crown ether in methylene chloride solution. The results

showed: (a) a nearly inverse relationship between the cumulative electron-withdrawing power of the substituents and the ability of the crown ether to extract the sodium and potassium salts due to the decreased basicity of the oxygen crown system, and, (b) crown ethers with cumulatively large electron-withdrawing substituents exhibit a reversal of the "normal" ion extraction selectivity, $K^+ > Na^+$, of 18-crown-6 ethers. The reversal of the $K^+ - Rb^+$ selectivity of 18-crown-6 in methanol was also noted by Curtis et al. (48) for a tetra-O-isopropylidene substituted 18-crown-6.

Recently, Izatt et al. (49, 50, 51) have extended their calorimetric titration studies of the interaction of several mono- and divalent cations with dicyclohexano-18-crown-6 to 15-crown-5, 18-crown-6, thia-18-crown-6 and benzo-15-crown-5 in aqueous, methanol and water-methanol solutions. The marked selectivities toward uni- and bivalent cations shown by 18-crown-6 were not found with 15-crown-5 which shows nearly identical log K values for all the alkali cations in water and shows very little selectivity in methanol solutions. The enthalpy change shows the same order as the change in log K for the complexation of alkali cations with each of these 18-membered crowns in water and with 18-crown-6 in methanol, while the entropy change shows a nearly opposite order of log K values. Thus $\Delta H°$ and $\Delta S°$ compensate each other with

$\Delta H°$ being the dominant quantity in determining the magnitude of log K. A change in the solvent composition from water to water-methanol mixtures results in different cation selectivity patterns for 15-crown-5 and 18-crown-6. It was also shown that the substitution of one sulfur atom for oxygen in 18-crown-6, to give thia-18-crown-6, considerably reduces the stabilities of the Na^+, K^+ and Ba^{2+} complexes in methanol solution due largely to the less favorable $\Delta H°$ values.

With only a few exceptions, both the enthalphy and entropy changes of the above macrocyclic complexation reactions are negative. These data clearly show that the origin of the macrocyclic effect might be different from that of the chelate effect. Cabbiness and Margerum (52) were the first to use the term "macrocyclic effect" to distinguish it from the chelate effect, since there is an additional enhancement in the stabilities of macrocyclic complexes beyond that of chelates. Since that time, the macrocyclic effect has been studied by many authors mostly on the complexation of transition metal ions with the macrocycles and their linear counterparts. Based on a detailed study of the thermodynamic properties of nickel (II)-tetramine complexes in water, Hinz and Margerum (53) concluded that the macrocyclic effect is almost entirely enthalpic in origin. The large negative enthalpy changes were attributed to the decreased

solvation of the macrocyclic ligand which has fewer hydrogen bonds with water molecules to be broken in complex formation. The smaller loss in configurational entropy upon complexation of the macrocyclic ligand tends to be offset by less water being released from the solvated ligand. In solvents with weak or no hydrogen bonding, changes in configurational entropy of the ligand should be more important.

In contrast, Kodama and Kimura (54) reported a polarographic study on the thermodynamics of Cu (II)-tetramine complexes in water and stated that the macrocyclic effect is due solely to the entropy gain. Shchori and Grodziński (45) studied the complexation of dibenzo-18-crown-6 with a sodium salt at various temperatures by electrical conductance measurements and showed that the complexation reaction is both enthalpy and entropy driven in dimethoxyethane solution. On the basis of the results obtained from a microcalorimetric study of copper (II) and zinc (II)-tetramine complexes and the corresponding linear counterparts in aqueous solution, Anichini et al. (55) summarized that the macrocyclic effect is due to a favorable entropy term and to a normally favorable enthalpy term. The magnitude of the latter is critically dependent on matching the size of the metal cation to that of the macrocyclic ligand.

The thermodynamics of complexation reaction between the various cyclic polyethers and cations have been studied

extensively by Izatt et al. (49, 50, 51). However, their data contain no trends in $\Delta H°$ and $\Delta S°$ among the complexes studied which would explain the macrocyclic effect. It is clear from the above discussion that although the chelate effect is definitely of entropic origin, no agreement has been reached as to whether the macrocyclic effect results from a more favorable enthalpy or more favorable entropy term in the complexation free energy.

Mei et al. (56, 57) studied the complexation of the cesium cation with 18-crown-6 (18C6), dibenzo-18-crown-6 (DBC) and dicyclohexano-18-crown-6 (DCC) in various solvents by cesium-133 NMR technique. In all solvents studied, 18-crown-6 forms 1:1 and 2:1 (ligand to metal) complexes. In most solvents the formation of 2:1 complexes by the other two crown ethers was also indicated. The chemical shift of the 2:1 complex of Cs^+ with 18-crown-6 is essentially independent of solvent, indicating that in the "sandwich" complex the cesium ion is effectively shielded from the solvent. In all solvents the one to one complexation constants (K_1) decrease in the order 18C6 $\geq$ DCC >> DBC while the two to one complexation constants (K_2) follow the order DBC $\geq$ 18C6 >> DCC. It was shown that there is no simple relationship between K_1 values and either the dielectric constant or the

donicity* (58, 59) of the solvent, although the solvent plays an important role in the complexation process. The kinetic parameters for the release of Cs^+ ion from some macrocyclic complexes in several solvents were also reported.

The complexing ability of 1,10-diaza-18-crown-6 (DA18C6) with Tl^+ and alkali metal cations in several non-aqueous solvents was recently studied in detail by Shamsipur (23). For the Cs^+·DA18C6 complex in the solvents studied, there is no clear indication of the formation of 2:1 (ligand:metal) complex as found for other crown ethers by Mei et al. (56, 57). The Na^+ and Cs^+ ion complexes of DA18C6 were found to be less stable than those of 18C6 (57, 60). Similar results were reported by Frensdorff for the K^+ ion complexes with these two crowns in methanol solution (34). The formation constants of Li^+·DA18C6 in various solvents are unexpectedly large and greater than those of the Li^+·18C6 complex (61) in the same solvents. This difference was attributed to possible covalent bonding between the Li^+ ion and DA18C6. With the exception of pyridine, the stabilities of the Li^+, Na^+ and

---

*The Gutmann donor number is the positive enthalpy value (in kcal/mole) of 1:1 complex formation between the given solvent molecule and antimony pentachloride in 1,2-dichloroethane solution:

$$S + SbCl_5 \xrightarrow{1,2\text{-DCE}} S\cdot SbCl_5$$

$$-\Delta H_{S\cdot SbCl_5} = \text{donor number}$$

Gutmann used the term "donicity" when referring to the donor ability of a solvent.

Cs^+ ion complexes with DA18C6 increase roughly with decreasing donicity of the solvent.

Kinetic information about the complexation reactions between crown ethers and alkali metal ions is very limited. The kinetics of complexation of sodium ion with dicyclohexano-18-crown-6, dibenzo-18-crown-6 (DBC) and its derivatives in several nonaqueous solvents were investigated by Shchori et al. (62, 63) using sodium-23 NMR. They postulated that the dominant exchange mechanism involves the decomplexation step:

$$Na^+(X^-), \text{crown} \rightleftharpoons Na^+(X^-) + \text{crown}$$

and showed that the rate of decomplexation is very strongly affected by substituents in the aromatic rings of DBC.

It was found that the rate constants of complexation increase with an increase in the stability of the complex, while the rate constants of decomplexation vary in the opposite direction. It was also shown that the effect of solvent on the equilibrium constants for complexation is very pronounced, while the activation energy of the decomplexation of DBC and of its derivatives is independent of solvent (to within $\pm$ 1 kcal). Because of this constant activation energy and the coincidence of this value with the energy of activation of a conformational change of the macrocyclic ring, these authors speculated that the energy barrier for decomplexation may be

determined by the energy required for a conformation rearrangement of the complex. Similarly, the kinetics of complexation of potassium and rubidium ions with dibenzo-18-crown-6 (DBC) in methanol were studied by Shporer and Luz (64) using potassium-39 and rubidium-87 NMR techniques respectively. The rate constant and activation energy of the decomplexation of $K^+ \cdot DBC$ are similar to those of $Na^+ \cdot DBC$ complex (62, 63). But the dissociation rate constant of the $Rb^+ \cdot DBC$ complex is much larger possibly because of the weaker binding between the larger rubidium ion and the DBC molecule.

Kinetics studies of the conformational equilibrium of 18-crown-6, and its complexation with Li^+, Na^+, K^+, Rb^+, Cs^+, Tl^+, Ag^+, NH_4^+, and Ca^{2+} ions as well as of 15-crown-5 and its complexation with Na^+, K^+, Rb^+, Tl^+ and Ag^+ ions in aqueous solution have been carried out using ultrasonic absorption method by Eyring et al. (65-68). According to these authors, the basic reaction scheme for the complexation which best fits their experimental data is the two-step process proposed by Chock (69)

$$CR_1 \underset{k_{21}}{\overset{k_{12}}{\rightleftharpoons}} CR_2 \qquad \text{(i)}$$

$$M^+ + CR_2 \underset{k_{32}}{\overset{k_{23}}{\rightleftharpoons}} MCR_2^+ \qquad \text{(ii)}$$

where CR_1 and CR_2 denote the two different conformations of the polyether. The conformation CR_1 is unreactive, M^+

is a metal ion and MCR_2^+ is the complex ion. The mechanism involves a fast ligand conformational change followed by a stepwise substitution of the coordinated solvent molecules by the ligand.

The equilibrium constant for the rapid conformational rearrangement of the ligand, equation (i), was determined to be $K_{21} = k_{21}/k_{12} = (2 \pm 2) \times 10^{-2}$ for 18-crown-6 and was estimated to be $K_{21} \leq 0.1$ for 15-crown-5. This means that most of the free ligands are in the CR_2 form. The variations of k_{23} for 18-crown-6 complexes suggest that the overall complex stability constants are not solely determined by the changes in the rates of decomplexation. The relative constancy in k_{32} for 15-crown-5 complexes is consistent with the observed nonselectivity of the ligand in complexing with univalent ions. Without exception, k_{32} increases in going from 18-crown-6 to 15-crown-5; that is, decomplexation is facilitated by the smaller ring size and increased rigidity. This, too, is consistent with the observation that the stability constants are greater for the 18-crown-6 complexes. Thermodynamic parameters, $\Delta H°$, $\Delta S°$, $\Delta H^{\ddagger}$, and $\Delta S^{\ddagger}$ for the conformational transition of 18-crown-6 and the volume change for several cations complexed by 18-crown-6 were also reported.

3. Complexation of alkali metal cations with macrobicyclic compounds - Cryptands

Lehn (5) pointed out that the free macrobicyclic cryptands may exist in three forms depending on the orientation of the bridgehead nitrogen atoms lone pairs toward the inside or the outside of the cavity : endo-endo (in-in), endo-exo (in-out), and exo-exo (out-out) (Figure 3). These forms may interconvert rapidly via nitrogen inversion. However, cyrstal structure determinations of a number of cryptates (70-72) show that the cation is located inside the molecular cavity with the ligand in the in-in form and that the ligand may adjust to some extent to the cation size by contraction or expansion of its internal cavity. Although it is not known in which form the free ligand exists in solution (and which also may depend on the nature of the ligand and of the medium) the cryptate is probably in the in-in form since in this form all heteroatoms can participate in the complexation.

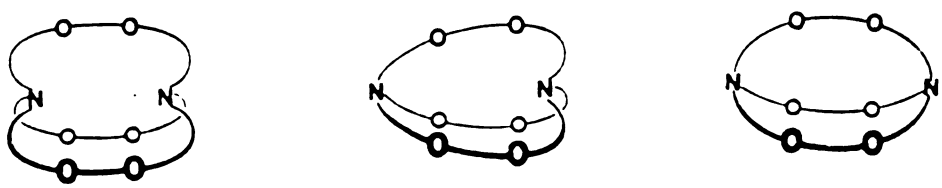

endo-endo exo-endo exo-exo

Figure 3. The three conformations of C222 cryptand.

Lehn et al. (73-76) measured the stability constants of the 2-cryptates for alkali and alkaline earth

cations in water, methanol and methanol-water mixture (95:5 methanol:water) using potentiometric technique. They found that the 2-cryptates display a pronounced macrobicyclic cryptate effect characterized by a high stability and selectivity with respect to the macromonocyclic ligands. For instance, the stability of the (K^+·C222) cryptate in a methanol-water mixture is higher by a factor of about 10^5 than the stability of the K^+ complex of its macrocyclic counterpart (IX) which is equivalent to opening one bridge of the C222 cryptand (73).

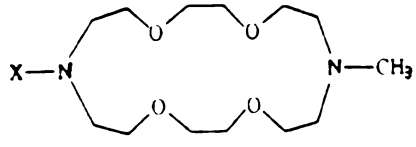

X = $CH_2CH_2OCH_2CH_2OCH_3$
(IX)

The small, rigid ligands whose cavities are delineated by short, relatively nonflexible chains display peak and cavity selectivities, the preferred cation being that one whose size most closely matches the cavity, since distortion of a rigid ligand either by contraction or by expansion of its cavity leads to pronounced destabilization of the complex. Thus cryptands C211, C221 and C222 preferentially complex Li^+, Na^+, and K^+ ions respectively. Plateau selectivity which shows high K^+/Na^+ selectivity but little selectivity among K^+, Rb^+, and Cs^+ ions was observed for the large, more flexible ligands, C322, C332,

and C333. Changing from water to methanol solution generally leads to a marked increase in cryptate stability and selectivity. This was attributed to the lower dielectric constant of methanol.

The stability constants of the alkali and alkaline earth metal cryptates decrease as the number of binding sites decrease, e.g. the stabilities of the Na^+ and K^+ cryptates decrease by a factor of about 10^4 - 10^5 on replacement of two oxygen atoms in C222 by two $-CH_2$ groups ($C22C_8$) (74). The selectivity of M^+/M^{2+} can be controlled by increasing ligand thickness (as in benzo derivatives of C222) or by removing some binding sites (74). Substitution of sulfur or nitrogen atoms for the oxygen atoms of the cryptands results in a drastic decrease of the stabilities and selectivities of the alkali and alkaline earth complexes. However, the complexation is strongly shifted in favor of cations such as Ag^+, Tl^+, Ca^{2+}, and Pb^{2+} (75, 76).

Yee et al. (77) measured the stability constants of alkali and Tl^+ ion complexes with C222 in water, methanol and dimethylsulfoxide solutions using cyclic voltammetry. Cahen et al. (78) investigated the lithium complexes of C211, C221, and C222 cryptands in water and several nonaqueous solvents by lithium-7 NMR and clearly showed that the dielectric constant is not the only solvent property which influences the stabilities of the

complexes. There is little or no complex formation between Li^+ ion and C222 in a strongly solvating solvent such as dimethylsulfoxide, while in a nearly equally polar but much poorer solvating solvent, nitromethane, the complex is quite stable (Log K > 4). The chemical shift of the lithium cation complexed by C211 is essentially independent of the solvent and of the counterion used, indicating that the lithium ion is completely insulated from the external medium, i.e. it forms an inclusive complex.

Hourdakis and Popov (79) studied the complexation of Li^+, Na^+ and Cs^+ ions with cryptand C222-dilactam (X) (which is the product of the penultimate step in the synthesis of cryptand C222) in various solvents by lithium-7, sodium-23, cesium-133 NMR and far infrared measurements. The complexing ability of the dilactam is similar to, but weaker than that of the crytand C222. The formation constants of C222-dilactam complexes with Li^+, Na^+ and Cs^+ ions in several nonaqueous solvents were reported.

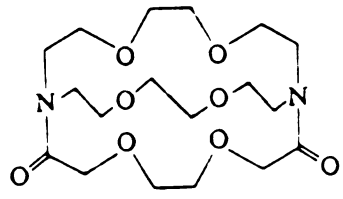

(X)

In order to have a better understanding of the thermodynamics of cryptate formation, Kauffmann et al. (80) obtained the enthaplies (ΔH°_C) and entropies (ΔS°_C) of

complexation of alkali and alkaline earth cryptates from calorimetric measurements of ΔH_c° and the previously determined stability constants. It was found that both enthalpy and entropy changes play an important role in the stability and selectivity of the complex, but the cryptate effect and the selectivity peaks observed in the stability constants of the cryptates are of enthalpic origin. The cavity-radius/cation-radius effect used as an empirical criterion for discussing the selectivity of cryptand complexation (73) was shown to incorporate both enthalpic and entropic effects and is not just a measure of the steric fit. They also reported that the marked increase in stability on transfer from water to methanol/water mixture is entirely due to an increase in enthalpy of complexation in the mixed solvent, which was then explained by them as an increased electrostatic interaction of the cation with the ligand in the medium of lower dielectric constant and the smaller interaction of the cation with the solvent.

Abraham et al. (81), however, report that for both cryptates, $Na^+ \cdot C222$ and $K^+ \cdot C222$, the enthalpically favored complexation in methanol solution is entirely due to the effect of solvent on the free cryptand C222. These authors obtained an extraordinarily large enthalpy of transfer, $\Delta H_t^\circ = +13.9\ kcal \cdot mol^{-1}$, from water to methanol for the ligand. This means that the free cryptand is much more strongly solvated in aqueous solution than in methanol.

On the other hand, the solvent effect on M^+ and $M^+ \cdot C222$ in terms of enthalpy both disfavor complex formation in methanol, i.e. the M^+ ions are more solvated in methanol while the $M^+ \cdot C222$ ions are more solvated in water.

Mei et al. (82, 83) investigated the complexation reaction of cesium cation with 2-cryptands in various solvents by cesium-133 NMR. It was found that both the dielectric constants and the solvating abilities of solvents influence the complexation reactions. The relative stabilities of the complexes were shown to be in the order of $Cs^+ \cdot C221 \geq Cs^+ \cdot C222 > Cs^+ \cdot C222B >> Cs^+ \cdot C211$. The $Cs^+ \cdot C222$ complex was found to be enthalpy stabilized, but entropy destabilized in all the nonaqueous solvents studied. It was noted that there is a temperature- and solvent-dependent equilibrium between "exclusive" and "inclusive" conformations of the $Cs^+ \cdot C222$ complex, with the inclusive complex (in which the Cs^+ ion is located in the center of the cavity) favored at lower temperatures. In the exclusive complex, the cation is not completely within the cavity and so it is only partially insulated from the external medium. Thermodynamic parameters (ΔH_1° and ΔS_1°) for the formation of the exclusive complex and for its conversion to the inclusive complex (ΔH_2° and ΔS_2°) in acetone, propylene carbonate and N, N-dimethylformamide solutions were reported. The possibility of the existence of both exclusive and inclusive $Cs^+ \cdot C222$ complex in water

was shown recently by Desrosiers and Morel (84) from the determination of the standard volumes of complexation of the alkali chlorides with cryptand C222.

The kinetics of cryptate formation was first studied by Lehn et al. (85) by temperature dependent proton NMR in D_2O solutions. The authors assumed that the exchange mechanism proceeds by a dissociation-complexation process rather than a bimolecular process and the exchange becomes slower as the stability of the cryptate increases, as was found for the metal cation-crown ether complexes (63). Cahen et al. (86) investigated the kinetics of the complexation reaction of the lithium cation with cryptand C211 in water and in several nonaqueous solvents by lithium-7 NMR. The energy of activation for the release of Li^+ from the $Li^+ \cdot$C211 complex was found to increase with increasing donicity of the solvent. By contrast, Shchori et al. (63) found that the activation energy for release of Na^+ from the complexes of DBC and its derivatives is independent of the solvents used. However, two of the three solvents used, methanol and dimethylformamide, have the same donicity while that of the third solvent, dimethoxyethane, is not known. Cahen et al. pointed out that the transition state for cryptate formation appears to be on the reagent side, i.e. it involves substantial solvation of the cation. Activation energies (E_a), dissociation rate constants, and values of $\Delta H_o^{\ddagger}$, $\Delta S_o^{\ddagger}$, and $\Delta G_o^{\ddagger}$ for the release of Li^+ from the cryptate were reported.

Sodium-23 NMR kinetics studies on C222-cryptate in four solvents were performed by Ceraso et al. (87, 88). It was shown that the exchange proceeds through a dissociation-association process in ethylenediamine solution. The activation energies were found to depend upon the solvents used. However, the correlation between the activation energy and the donicity of the solvent reported by Cahen et al. for Li^+-cryptate decomplexation (86) was not observed. The rate constants and values of $\Delta G_o^{\ddagger}$, $\Delta H_o^{\ddagger}$ and $\Delta S_o^{\ddagger}$ for the decomplexation reaction of $Na^+ \cdot$C222 cryptate were also reported.

Cox and Schneider (89) measured the dissociation rates of metal cryptates in aqueous solution using a conductance method. It was found that in some cases, e.g. the $Li^+ \cdot$C211 and $Na^+ \cdot$C221 cryptates, the dissociation of the metal-cryptand complex is acid catalyzed, i.e. the observed rate constants increase as the acid concentrations increase. A mechanism was suggested for the dissociation reaction in which there is a preceding conformational change from in-in (M^{n+}) to in-out (M^{n+}) or out-out (M^{n+}) complex that leaves one of the lone pairs on nitrogen free to be trapped by H^+, prior to the dissociation of the metal ion from the cryptate.

Cox et al. (90) have also studied the kinetics and thermodynamics of some alkali metal complexes with three cryptands, C211, C221 and C222, in methanol solutions by electrical conductance measurements and

potentiometric titrations. It was shown that the pronounced selectivity of the ligand is reflected entirely in the dissociation rates, with the formation rates which are about 10^8 larger than the dissociation rates increasing monotonically with increasing cation size. These results strongly suggest that the transition state for the formation reaction lies very close to the reactants as was found in the lithium-7 NMR kinetics studies (86). In the transition stage there is no specific interaction between the cryptands and the cations that strongly differentiates between the various cations. The specific size-dependent interactions between the metal ions and the cryptands must then occur subsequent to the formation of the transition state. The quantitative data currently available on sodium salt complexes of 15-crown-5, benzo-15-crown-5, 18-crown-6, and 2-cryptands are presented in Tables 1-4.

4. Conclusion

From the previous discussions, the parameters which influence the stabilities and selectivities of macrocyclic complexes may be summarized as follows: (a) the relative sizes of cation and ligand cavity, (b) the type and number of donor atoms in the ring, (c) substitution on the macrocyclic ring, (d) type and charge of cation, (e) solvent properties. Most of the investigations in solution were done in water, methanol and methanol-water mixtures, while studies in other nonaqueous solutions are quite sparse.

Table 1. Reported thermodynamic quantities for the complexation of sodium cation with 15-crown-5, monobenzo-15-crown-5, and 18-crown-6 in various solvents at 25°C

Ligend	Solvent	Log K_f	$\Delta H°$ (kcal/mol)	$\Delta S°$ (cal/mol deg)	Method[a]	Ref.
15-crown-5	Water	0.70 ± 0.10	-1.50 ± 0.04	-1.8	cal	49
		0.67 ± 0.03			pot	94
	MeOH	3.48 ± 0.01	-4.99 ± 0.03	-0.80	cal	51
MB15-crown-5	Acetone	3.53 ± 0.06			con	46
	MeCN	4.55[b]			pola	41
	Water	0.4[c]	~ 0		cal	50
	20% MeOH	0.72 ± 0.03	-1.77 ± 0.02	-2.6	cal	50
	40% MeOH	1.17 ± 0.12	-2.63 ± 0.11	-3.5	cal	50
	60% MeOH	1.64 ± 0.04	-3.78 ± 0.08	-5.2	cal	50
	70% MeOH	1.99 ± 0.10	-3.82 ± 0.07	-3.7	cal	50
	80% MeOH	2.26 ± 0.02	-8.32 ± 0.03	-17.6	cal	50
18-crown-6	Water	< 0.3			pot	34
		0.80 ± 0.10	-2.25 ± 0.10	-3.7	cal	49
		0.82 ± 0.02			pot	94

Table 1 (continued)

Ligend	Solvent	Log K_f	$\Delta H°$ (kcal/mol)	$\Delta S°$ (cal/mol deg)	Method[a]	Ref.
	70% MeOH	2.76 ± 0.02	-4.89 ± 0.01	-3.8	cal	50
	90% MeOH	3.66	-6.64	-5.5	cal	2
	MeOH	4.36 ± 0.02	-8.4 ± 0.3	-8.0	cal	51
		4.32 ± 0.04			pot	34

[a]cal is calorimetry, pot is potentiometry, pola is polarography, con is conductance.

[b]at 22°C

[c]estimated

Table 2. Reported thermodynamic quantities for the complexation of sodium cation with 2-cryptands in various solvents at 25°C

Ligand	Solvent	Log K_f^b	ΔH° (kcal/mol)	ΔS° (cal/mol deg)	Method[a]	Ref.
C211	Water	3.2	-5.4 ± 0.2	-3 ± 2	pot & cal	73 & 80
	Methanol	6.1			pot	73
	95% MeOH	6.08			pot	73
C221	Water	5.40	-5.35 ± 0.2	+6.2 ± 2	pot & cal	73 & 80
	Methanol	> 8.0			pot	73
		9.6_5 ± 0.1			pot	90
	95% MeOH	8.84			pot	73
C222	Water	3.9	-7.4 ± 0.2	-7 ± 2	pot & cal	73 & 80
		4.11	-7.4	-6	pot & cal	92
		3.9			cycl vol	77
	Methanol	> 8.0			pot	73
		7.9_8 ± 0.1			pot	90
		7.9			cycl vol	77
		7.8			Arge	93

Table 2 (continued)

Ligand	Solvent	Log K_f	$\Delta H°$ (kcal/mol)	$\Delta S°$ (cal/mol deg)	Method[a]	Ref.
	95% MeOH	7.21	-10.6 ± 0.2	-2.6 ± 2	pot & cal	73 & 80
	DMSO	5.4			cycl vol	77
C222B	Water	4.0			pot	74
	95% MeOH	7.4			pot	74

[a]pot is potentiometry
cal is calorimetry
cycl vol is cyclic voltametry
Arge is Argentometry

[b]The values (from Ref. 73 & 80) are precise to ± 0.2 for $1 < \log K < 5$, and the error becomes larger the more log K is outside the range.

Table 3. Reported kinetic quantities for the complexation of sodium cation with 15-crown-5, monobenzo-15-crown-5 and 18-crown-6 in various solvents at 25°C

Ligand	Solvent	k_f ($M^{-1}s^{-1}$)	k_d (s^{-1})	Method[a]	Ref.
15-crown-5	Water	$\sim 2.4 \times 10^8$	4.8×10^7	ultr. abs.	67
MB15-crown-5	No data available				
18-crown-6	Water	$\sim 2.2 \times 10^8$	3.4×10^7	ultr. abs.	66

[a]Ultr. Abs. is ultrasonic absorption

Table 4. Reported kinetic quantities for the complexation of sodium cation with 2-cryptands in various solvents at 25°C

Ligand	Solvent	k_d (s^{-1})	k_f ($M^{-1}s^{-1}$)	Method[e]	Ref.
C211	Water	$(1.4 \pm 0.1) \times 10^2$	$(9 \pm 1) \times 10^4$	T.J.R.	91
	Methanol	2.50[a]	3.1×10^6[b]	cond	90
C221	Water	14.5	3.6×10^6	cond	89
		18 ± 2	$(6 \pm 2) \times 10^6$	T.J.R.	91
	Methanol	2.35×10^{-2}[a]	1.7×10^8[b]	cond	90
C222	Water	147.4(2.6)[c]	1.2×10^6	NMR	88
	Methanol	2.87[a]	2.7×10^8[b]	cond	90
	Pyridine	1.14(0.09)[c]		NMR	88
	THF[d]	8.03(0.27)[c]		NMR	88
	EDA[d]	165.0(4.9)[c]		NMR	88

[a]These values have an uncertainty of ± 5%.

[b]These values have an uncertainty of ± 25%.

[c]Standard deviation.

[d]THF = Tetrahydrofuran, EDA = Ethylenediamine

[e]cond is conductance, T.J.R. is temperature jump relaxation

Especially for sodium cation complexes with 15-crown-5, monobenzo-15-crown-5, 18-crown-6 and 2-cryptands, very few data exist on the thermodynamics and kinetics of the complexation reaction in nonaqueous solutions as can be seen from Tables 1-4.

The use of macrocyclic compounds in organic synthesis, electrochemistry and analytical separations has been demonstrated. Sam and Simmons (95) showed that the $KMnO_4$ complex of dicyclohexano-18-crown-6 oxidized olefins, alcohols, aldehydes and alkylbenzenes under mild conditions in benzene. In the absence of the crown ether, $KMnO_4$ has no detectable solubility in benzene and no reaction occurs with organic substrates. Valinomycin has been used as a membrane component in a potassium-selective liquid-membrane electrode (96). The above electrode could make measurements of potassium ion activities in the range of 1 M to at least 10^{-6} M in unbuffered aqueous solutions with a selectivity of potassium over sodium cations of more than 4,000. It has been shown that crown ethers and cryptands may serve as model compounds for investigating and understanding the phenomenon of ion transport through cellular membranes (2, 22, 35, 36, 97). Numerous other actual and possible applications of the macrocyclic compounds in synthetic organic, electro-chemistry, separations, biology and drugs have been discussed in references 2, 3, 18, 19, 21, and 22.

Many uses of macrocyclic compounds depend on their marked ion specificities. Consequently, a knowledge of log K values for the interaction between these compounds and ions becomes very important in predicting their behavior and determining their uses. Therefore, this dissertation reports an investigation of the thermodynamic properties of the complexation reaction between sodium cation and several crown ethers and cryptands in aqueous and various nonaqueous solutions by proton, carbon-13, and sodium-23 NMR as well as calorimetric techniques.

CHAPTER II

EXPERIMENTAL PART

1. Salt and Ligand Purification

Sodium salts used in this study were reagent grade quality and not further purified before use except for drying. Sodium tetraphenylborate (J.T. Baker) and sodium thiocyanate (Mallinkrodt) were dried under vacuum at 50°C for 3 days. Sodium perchlorate, iodide (Matheson, Coleman and Bell) and chloride (J.T. Baker) were dried at 110°C for 3 days. Tetrabutylammonium iodide (Aldrich) was recrystallized first from water and then from a 9:1 ethylacetate : 95% ethanol mixture. The purified tetrabutylammonium iodide (TBAI) was dried under vacuum at 50°C for 3 days.

The macrocyclic polyether 18-crown-6 (18C6, Aldrich) was twice recrystallized from acetonitrile, dried under vacuum at $\leq$ 40°C for three hours and then at room temperature for three days. The dried 18C6 melted at 37-38°C (lit. mp 36.5-38.0°C (98), 39-40°C (1)). Macrocyclic 15-crown-5 (15C5, Aldrich) is a liquid and was purified by vacuum distillation and dried under vacuum over Drierite at room temperature for three days. The dried 15C5 in CCl_4 solvent has a large singlet proton NMR peak at δ 3.53 ppm (lit. δ 3.58 ppm (49)). Dibenzo-18C6 (DB18C6, Parish) was recrystallized twice from benzene and dried under vaccum over Drierite at room temperature for

three days; mp 165-166°C (lit. mp 164°C (1)). Monobenzo-15C5 (MB15C5) was synthesized according to Pedersen's method (1) by M. Shamsipur in this laboratory. It was recrystallized from n-heptane twice and dried under vacuum over Drierite at room temperature for three days; mp 79-80°C (lit. mp 79-79.5°C (1)).

Cryptand C222 (E.M. Laboratories, Inc.) was recrystallized twice from Hexane and dried under vacuum over Drierite at room temperature for three days; mp 69°C (lit. mp 68-69°C (99)). C211, C221 and C222B (E.M. Laboratories, Inc.) are liquids and were used without further purification except drying under vacuum over Drierite at room temperature for three days.

Potassium hexafluorophosphate (Pflaltz and Bauer) was recrystallized from water and dried for several days at 110°C under vacuum.

2. Solvent Purification and Sample Preparation

Tetrahydrofuran (THF) was refluxed over metallic potassium and benzophenone for 24 hours and then fractionally distilled using a 30 cm Vigreux column. Acetone (Me_2CO) was refluxed over Drierite for 24 hours and then fractionally distilled. 2-Nitropropane was refluxed over Drierite for 24 hours and then fractionally distilled under reduced pressure. Acetonitrile (MeCN) and 1,3-dioxolane were refluxed over calcium hydride for 24 hours and then fractionally distilled. Tetramethylguanidine (TMG) was

refluxed for 24 hours under reduced pressure and then fractionally distilled. Nitromethane ($MeNO_2$), pyridine (PY), propylene carbonate (PC), dimethylsulfoxide (DMSO) and N,N-dimethylformamide (DMF) were refluxed over calcium hydride for 24 hours under reduced pressure and then fractionally distilled. Before use all the distilled solvents were further dried overnight over freshly activated 4A or 3A molecular sieves. The water content of all solvents, except acetone, was measured with Karl Fischer automatic titrator (Photovolt Aquatest II) and was found to be always less than 100 ppm. The water content of acetone was less than 100 ppm as measured by gas chromatography analysis. Deuterated DMSO-d^6 (Stohler Isotope Chemicals) was used as received. Useful solvent properties are listed in Table 5.

The molecular sieves used were washed with distilled water and dried at 100°C overnight. The dried molecular sieves were further heated at 500°C under nitrogen for 24 hours.

All solutions were prepared in a dry box under nitrogen atmosphere. Ligands were quickly weighed out in the desired amount into a 2 ml volumetric flask and then transferred to the dry box for subsequent manipulation. Each sample solution was prepared by mixing appropriate amounts of stock salt solution, ligand and solvent.

Table 5. Key Solvent Properties and Correction for Magnetic Susceptibility on DA-60

Solvent	Dielectric Constant	Dipole Moment (D)	Gutmann Donor Number*	Volume Susceptibility x 10^6	Correction on DA-60 (ppm)
Pyridine	12.4	2.23	33.1	0.612	-0.226
Water	78.5	1.87	18.0 (33.0)**	0.720	0.000
Dimethylsulfoxide	46.7	3.9	29.8	0.605	-0.241
N,N-dimethylformamide	36.7	3.86	26.6	0.573	-0.308
Methanol	32.7	1.70	25.7**	0.515	-0.429
Tetrahydrofuran	7.6	1.63	20.0	0.613	-0.224
Acetone	20.7	2.88	17.0	0.460	-0.545
Propylene carbonate	65.0	5.2	15.1	0.634	-0.180
Acetonitrile	37.5	3.96	14.1	0.534	-0.390
Nitromethane	35.9	3.44	2.7	0.391	-0.689
2-Nitropropane	25.5	3.73	---	0.509	-0.442
Tetramethylguanidine	11.0	---	---	0.590	-0.272
1,3-Dioxolane	---	1.47	~ 14.7***	---	---

*Ref. (58, 59).

**Predicted by ^{23}Na NMR (100).

***Ref. (129).

3. Recovery of Cryptands from Cryptates

A. Preparation of Resins

Cation-exchange resin Dowex 50Wx8 (100-200 mesh) in the H^+ form was purified by soaking in warm (60°C) 4 M hydrochloric acid with stirring for three hours, followed by several washes with distilled water. The product was further purified by carrying through the same procedure once again. The resin was then washed with distilled water by suction using a dispersion tube until the pH of the filtrate was about 4.

Anion-exchange resin Dowex 1x2 (50-100 or 100-200 mesh) in the Cl^- form was purified by stirring in a beaker with 4 M hydrochloric acid for three hours, and washing several times with distilled water. The same procedure was likewise repeated once again. The resin was then washed with distilled water until the pH of the filtrate was about 7. The purified resin was stirred in a beaker with 50% v/v water and acetonitrile mixture before transferred to the column.

Anion-exchange resin Dowex 1x2 (50-100, or 100-200 mesh) in the Cl^- form was converted into the OH^- from by stirring the chloride form of the resin in a beaker with 3 M NaOH for three hours, followed by several washes with distilled water. The same procedure was likewise repeated once again. Then the resin was washed with deionized water until the pH of the filtrate was 7.

B. Procedure

Shih et al. (101) developed a recovery process for cryptands from used solution mixtures of the complexes. The procedure was followed in this work apart from minor modifications which are given below.

(i) To remove a large quantity of solvent with a regular vacuum pump is quite inconvenient because the trap of the pump is very quickly plugged with frozen solvent. Instead of being dried in vacuo at ~ 10^{-2} torr (101), solutions of metal cryptates in various solvents were dried with a rotavapor to remove the bulk solvent mixtures and then the last traces of solvents were removed in vacuum at ~ 10^{-2} torr.

(ii) Shih et al. (101) pointed out that if the original solution mixtures contained a variety of anions, it was useful to convert the salts to the chloride form by passing the solution through an anion exchange column in the Cl^- form. However, they did not give details of the procedure which is described as follows: After the metal ion cryptates were converted to the diprotonated cryptand salt by addition of excess HCl, the solid (~ 0.5 g) was dissolved in a 50% v/v aqueous acetonitrile mixture (~ 5-10 ml). The solution was then passed through the anion exchange column (1.5 × 25 cm) in the Cl^- form. The chloride salt of the metal cation and the diprotonated cryptand were eluted with about 40 ml of the same aqueous

acetonitrile mixture at a flow rate of about one ml per minute.

4. Instrumental Measurements and Data Handling

A. Nuclear Magnetic Resonance

Most of the sodium-23 NMR measurements were obtained by using a Varian DA-60 spectrometer operating at a field of 1.409 Tesla and a frequency of 15.871 MHz in the pulsed Fourier transform mode. The spectrometer is equipped with a wide-band probe capable of multinuclear operation (102) and with a home-built lock probe (103) which uses the DA-60 console to lock the magnetic field on an external proton resonance. A Fabri 1080 computer was employed to carry out the time averaging of spectra and the Fourier transformation of the data. Some sodium-23 NMR data were obtained with a Bruker HFX-90 spectrometer operating at a field of 2.114 Tesla and a frequency of 23.81 MHz in the pulsed Fourier transform mode. A Nicolet 1080 computer was employed to carry out the time averaging of spectra and the Fourier transformation of the data.

A 3.0 M aqueous sodium chloride solution was used as an external reference and the reported sodium-23 chemical shifts are referred to this 3.0 M aqueous NaCl solution. Ten mm o.d. precision NMR tubes were used. The reported data were also corrected for the differences in bulk diamagnetic susceptibilities between sample and reference solvents according to the following equation

(104) for a cylindrical sample in a spectrometer with a perpendicular magnetic field.

$$\delta_{corr.} = \delta_{obs.} - 2\Pi/3\ (x_v^{ref.} - x_v^{sample}) \qquad (2.1)$$

where $x_v^{ref.}$ and x_v^{sample} are the volume susceptibility (105) of the reference and sample solvents respectively and $\delta_{obs.}$ and $\delta_{corr.}$ are the observed and corrected chemical shifts respectively. It was assumed that the contribution of the added salt to the susceptibility of the solution was negligible as shown by Templeman and Van Geet (106). The magnitude of the correction for various solvents is given in Table 5. The paramagnetic shift from the reference (downfield) is designated as a positive value.

Carbon-13 NMR measurements were performed on a Varian CFT-20 spectrometer operating at a field of 1.868 Tesla and a frequency of 20.0 MHz in the pulsed Fourier transform mode. The sample solution was in an 8 mm o.d. NMR tube which was coaxially centered in the 10 mm o.d. NMR tube containing the mixture of reference and lock solvents (50% v/v acetone:D_2O). The methyl carbon NMR peak of acetone was used as the external reference. All carbon-13 chemical shifts were corrected for the differences in bulk diamagnetic susceptibilities of solvents according to equation (2.1) and referred to the internal TMS resonance in acetone. The paramagnetic shifts (downfield) are designated as positive.

Proton (^1H) NMR measurements were obtained by using a Bruker WH-180 superconducting spectrometer operating at a field of 4.228 Tesla and a frequency of 180.05 MHz in the pulsed Fourier transform mode. A Bruker BNC-80 computer was used to perform the Fourier transformation. Deuterated solvents were used to lock the magnetic field. All the proton chemical shifts reported are referenced to the internal TMS resonance.

B. Calorimetry

Enthalpies of Na^+ ion-macrocyclic complexation reactions were determined with a Guild Model 401 isoperibol solution calorimeter (107, 108) under nitrogen atmosphere. The calorimeter cell, calorimeter insert (including thermister, calibration heater, stirrer and stainless steel cooling coil) and stirrer motor were contained in a glove bag (I^2R, Model X-27-27) which was continuously purged with a flow of nitrogen during the entire experimental process. A Beaker containing some fresh P_2O_5 was placed inside the glove bag to absorb any traces of moisture. A Sargent-Welch Model SRG millivolt strip chart recorder was used to record the temperature changes. The voltage applied to the calibration heater was measured with a Keithley Model 169 digital multimeter and an 8.5:1 voltage divider fabricated with 1% precision resistors. Potentials could be read in a range of $\pm$ 2.000 V with $\pm$ 0.5 mV accuracy.

About 50 ml of the sodium salt solution was allowed to equilibrate for ~ 1.5 hours in a calorimeter cell which is the smaller one of the two silvered glass dewars fabricated in the Michigan State University glass shop (61). When the temperature of the solution inside the calorimeter cell was higher than the ambient temperature, the horizontal baseline was kept as close as possible to the ambient temperature by adjusting the flow rate of cooling nitrogen gas which came from an external cooling coil immersed in an ice bath and went into an internal cooling coil immersed in the solution. If the temperature of the solution inside the calorimeter cell was lower than the ambient temperature, the baseline was obtained by heating the solution to slightly above the ambient temperature with the calibration heater and then adjusting the flow rate of cooling nitrogen gas to compensate for the heat of stirring.

The system was then calibrated by electrically adding a definite quantity of energy into the calorimeter cell and measuring the recorder response. Because it requires a finite time period to generate the calibration energy electrically, and there is a change in the rate of heat loss as the solution temperature changes due to the imperfect insulation, the final solution temperature is not reached instantaneously. A typical recorder response curve for calibration is shown in Figure 4. The recorder deflection corresponding to the energy of

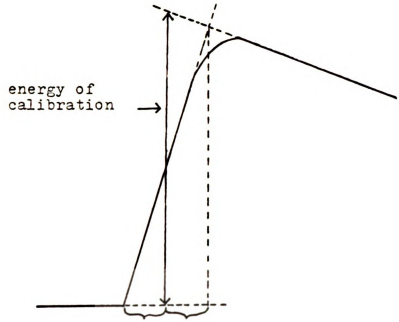

Figure 4. Calorimeter calibration response curve.

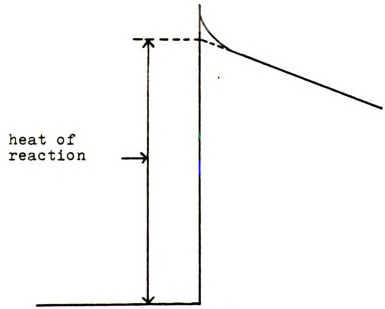

Figure 5. Calorimeter response curve for fast exothermic reaction.

calibration was obtained by using a temperature extrapolation and time averaging procedure as shown in Figure 4. The energy (Q, calories) generated was calculated by using equation (2.2) (108)

$$Q = \frac{V^2 t}{4.184\ R} \tag{2.2}$$

where R(ohms), the resistance of the calibration heater, V(volts), the voltage across the calibration heater and t(sec), the time of heating, were all known and the factor 4.184 converts joules to calories. The recorder deflection was then calibrated in units of calories per division on the chart paper.

After this first calibration run, the system was cooled down to the initial temperature by increasing the flow rate of the cooling gas and re-equilibrated. The entire calibration procedure was repeated. Generally, the precision of the calibration procedure was found to be better than $\pm$ 1%. Then, the heat of dilution of the salt solution (as the ligand solution was added) was determined by adding a known volume (1 ml or less) of pure solvent to the calorimeter cell with a syringe and measuring the recorder response. The system was brought back to the initial temperature as previously described, and the same volume of a ligand solution was added to the calorimeter cell with a syringe. After the complexation reaction was complete, the system was brought back to the initial

temperature, re-equilibrated, re-calibrated twice. A typical response curve for an exothermic reaction is shown in Figure 5. For a rapid reaction, the linear portion of the temperature decay was extrapolated back to the initial time of reaction to determine the heat released. For a slower reaction, the response curve resembled a calibration curve and was analyzed similarly.

A separate experiment was performed to determine the heat of dilution of the ligand solution by adding the same volume and concentration of the ligand solution as in the previous complexation reaction run into about 50 ml pure solvent in the calorimeter cell. The heat of reaction was calculated by comparing the recorder deflection with the post-reaction calibration data and was corrected for any heat of dilution of the salt and ligand solutions.

Since the system is calibrated directly in calories per division on the recorder chart paper, solution heat capacity measurements may be omitted. For reactions which go virtually to completion, the enthalpy of complexation is obtained by dividing the heat of reaction by the number of moles of complex formed. For incomplete reactions, the complex formation constants must be known in order to calculate the number of moles of complex formed or else a large enough excess of one of the reaction components must be used to drive the reaction completely to the right.

C. Data Handling

The stability constants of complexes were calculated by fitting the NMR chemical shift-mole ratio (ligand to metal ion) data to appropriate equations using a weighted nonlinear least squares program KINFIT (109) on a CDC-6500 computer. Details on the use of this program are given in the appendices.

CHAPTER III

NMR STUDIES OF SODIUM CATION COMPLEXES WITH SOME CROWN ETHERS IN VARIOUS SOLVENTS

1. Introduction

The importance of nuclear magnetic resonance spectroscopy, especially proton and carbon-13 NMR, as applied to the elucidation of the structures of organic molecules and electrolyte solutions is well established. In recent years, an increasing number of investigators are utilizing magnetic resonance of other nuclei, particularly the alkali metal cations and the halide ions, to study the behavior of ions in aqueous and various nonaqueous solutions (110-114). Alkali metal and halide NMR studies allow a more direct observation of ionic interactions. Moreover, the sensitivity (to the immediate chemical environments) of alkali metal NMR is considerably larger than that of ^{13}C NMR which in turn is larger than that of PMR. Hence, weak ion-ion, ion-solvent and ion-ligand interactions can be observed more easily by alkali metal NMR methods with the aid of computerized Fourier transform instrumentation.

By monitoring the chemical shifts and linewidths of the resonances and the relaxation times of various nuclei, one may obtain information about ionic solvation, association and complexation. Thus, ^{7}Li, ^{23}Na, ^{39}K and ^{133}Cs NMR have been shown to be very sensitive and powerful probes of the immediate chemical environments of the

individual cations (2, 115-118). The physical properties of the ^{23}Na, ^{13}C, and proton nuclei are shown in Table 6 (119).

As indicated previously in the historical review, with the exception of methanol, very few studies on sodium cation complexes with crown ethers have been done in non-aqueous solvents. This chapter reports studies by sodium-23, carbon-13 and hydrogen-1 NMR techniques of Na^+ ion complexes with three crown ethers; 15C5, MB15C5 and 18C6, in several solvents.

2. Results and Discussion

The variation of the sodium-23 chemical shift as a function of ligand/Na^+ mole ratio in various solvents at ambient temperatures is shown in Tables 7-9 and Figures 6-9. In all cases, except 18C6 and sodium tetraphenylborate in THF solutions, (which will be discussed in detail in part 3), only one population-averaged resonance was observed indicating that the exchange of the Na^+ ion between the bulk solution and the complex is fast on the NMR time scale. From Figures 6-9, it is obvious that the solvent plays an important role in the complexation reaction. Generally, in solvents of poor solvating ability the chemical shifts begin to level off at mole ratio of about one indicating the formation of a stable 1:1 complex. However, in stronger solvating solvents the chemical shifts change gradually and do not reach the limiting values as

Table 6. The Physical Properties of the ^{23}Na, ^{13}C and Proton Nuclei

	^{23}Na	^{13}C	^{1}H
Resonance frequency in MHz for			
a 1.409 Tesla field	15.87	15.08	60.00
a 2.114 Tesla field	23.81	22.63	90.00
Natural abundance, %	100	1.108	99.985
Relative sensitivity (vs. ^{1}H) for equal number of nuclei at constant field	9.25×10^{-2}	1.59×10^{-2}	1.00
Magnetic moment μ, in multiples of the nuclear magneton ($eh/4\pi M_c$)	2.2161	0.702199	2.79268
Spin I, in multiples of $h/2\pi$	3/2	1/2	1/2
Electric quadrupole moment Q, in multiples of $e \times 10^{-24}$ cm^2	0.14-0.15	-	-

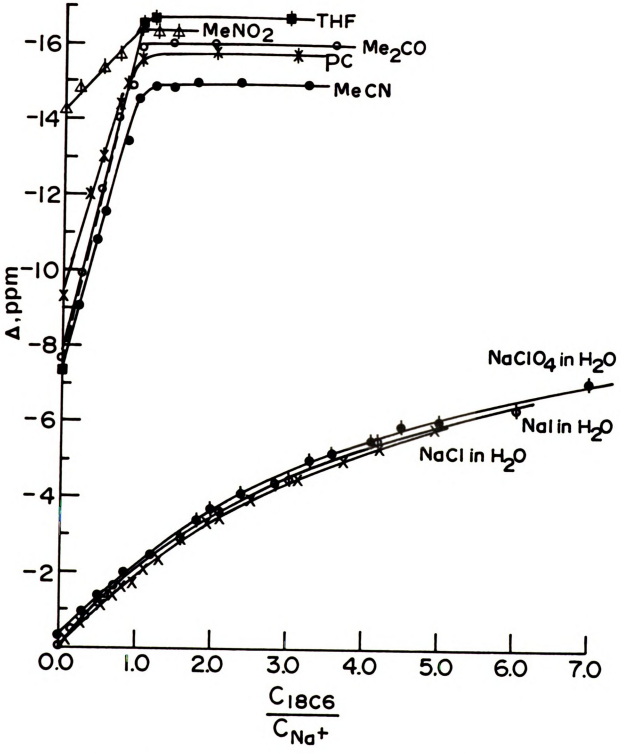

Figure 6. Sodium-23 chemical shift vs 18C6/Na^+ mole ratio in various solvents. The solutions, except H_2O, were 0.05 M in $NaBPh_4$.

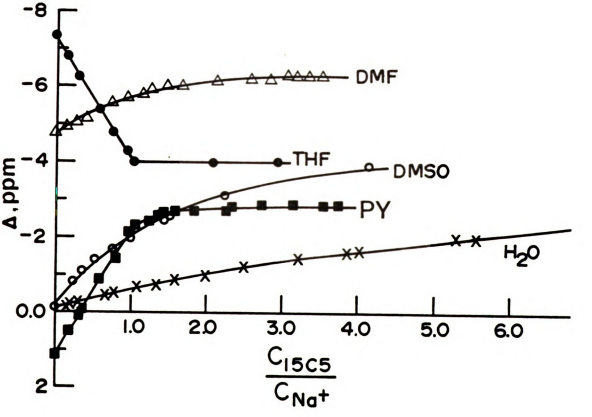

Figure 7. Sodium-23 chemical shift vs. 15C5/Na^+ mole ratio in various solvents. The solutions were 0.05 M in $NaBPh_4$ except in H_2O where the salt was NaI.

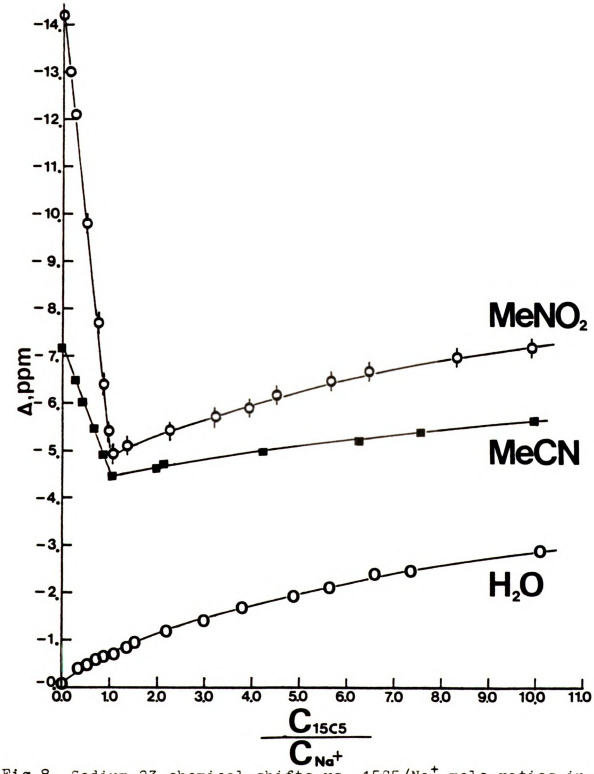

Fig 8. Sodium-23 chemical shifts vs. 15C5/Na^+ mole ratios in various solvents. The solutions were 0.05 M in $NaBPh_4$ except in H_2O where the salt was NaCl.

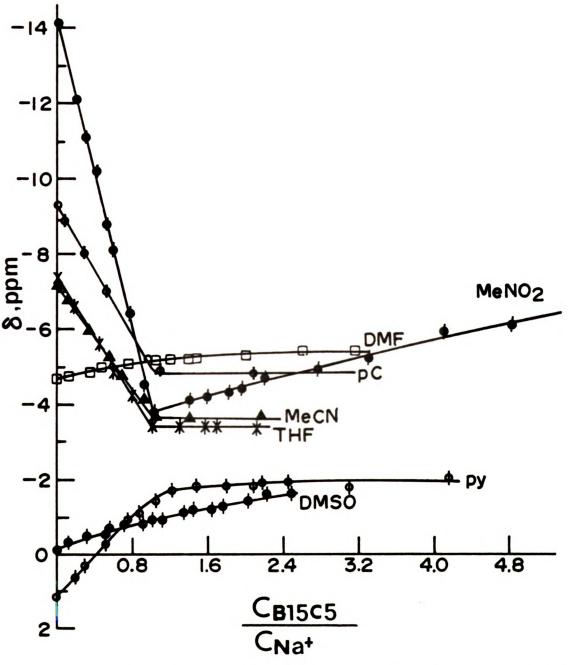

Figure 9. Sodium-23 chemical shift vs. B15C5/Na^+ mole ratio in various solvents. The solutions were 0.05 M in $NaBPh_4$.

Table 7. Sodium-23 NMR Chemical Shift-Mole Ratio Data for Na^+ ion Complex with 18C6 in Various Solvents at Ambient Temperatures[a]

Water		Water		Water	
$\frac{[18C6]}{[NaCl]}$[b]	δ_{ppm}	$\frac{[18C6]}{[NaI]}$[b]	δ_{ppm}	$\frac{[18C6]}{[NaClO_4]}$[b]	δ_{ppm}
0	-0.46	0	-0.45	0	-0.65
0.12	-0.54	0.17	-0.88	0.30	-1.32
0.32	-1.00	0.35	-1.23	0.53	-1.73
0.42	-1.23	0.52	-1.58	0.58	-1.69
0.56	-1.46	0.58	-1.73	0.86	-2.4
0.72	-1.77	0.72	-2.04	1.06	-2.6
0.83	-2.0	1.23	-2.9	1.23	-2.9
0.97	-2.1	1.60	-3.3	1.83	-3.8
1.12	-2.5	1.65	-3.4	2.01	-4.1
1.32	-2.7	2.13	-4.0	2.39	-4.5
1.63	-3.3	2.55	-4.4	2.87	-5.1
1.95	-3.7	2.84	-4.8	3.30	-5.4
2.13	-3.8	3.03	-4.9	3.60	-5.6
2.56	-4.3	4.20	-5.8	4.13	-5.9
3.17	-4.9	6.06	-6.8	4.53	-6.3
3.77	-5.4			5.03	-6.4
4.24	-5.7			7.00	-7.5
4.97	-6.3				

Table 7 (continued)

MeCN		Me_2CO		PC	
$\frac{[18C6]}{[Na^+]^c}$	δ_{ppm}	$\frac{[18C6]}{[Na^+]^c}$	δ_{ppm}	$\frac{[18C6]}{[Na^+]^c}$	δ_{ppm}
0	-7.56	0	-8.08	0	-9.7
0.23	-9.48	0.24	-10.30	0.36	-12.4
0.45	-11.12	0.51	-12.53	0.52	-13.4
0.55	-11.91	0.73	-14.41	0.74	-14.8
0.83	-13.80	1.04	-16.3	0.84	-15.3
1.00	-14.94	1.46	-16.4	1.02	-16.0
1.22	-15.22	2.00	-16.4	2.02	-16.2
1.46	-15.22	3.58	-16.4	3.12	-16.1
1.78	-15.32				
2.34	-15.35				
3.25	-15.30				
$MeNO_2$[c]		DMSO[c]		Pyridine[c]	
0	-14.68	0	-0.5	0	+0.75
0.20	-15.11	0.51	-4.0	0.50	~ -0.3
0.52	-15.7	1.00	~ -6	0.99	~ -13
0.74	-16.1				
1.06	-16.8				
1.26	-16.7				
1.51	-16.7				
2.12[d]					

Table 7 (continued)

DMF		TMG	
$\frac{[18C6]}{[Na^+]}$ [e]	δ_{ppm}	$\frac{[18C6]}{[Na^+]}$ [c]	δ_{ppm}
0	-5.0	0	-10.2
0.98	~-13	0.60	~ 4
		1.07	~ 9
		2.12	~12

[a]The temperature was either 27 ± 1°C or 28 ± 1°C.

[b]The solutions were 0.05 M in sodium salt.

[c]The solutions were 0.05 M in $NaBph_4$.

[d]Insoluble.

[e]The solutions were 0.10 M in $NaClO_4$.

Table 8. Sodium-23 NMR Chemical Shift-Mole Ratio Data for Na^+ ion Complex with 15C5 in Various Solvents at Ambient Temperatures

Water		Water		DMF	
$\frac{[15C5]}{[NaCl]}$ [a]	δ_{ppm}	$\frac{[15C5]}{[NaI]}$ [a]	δ_{ppm}	$\frac{[15C5]}{[Na^+]}$ [b]	δ_{ppm}
0	-0.46	0	-0.44	0	-5.06
0.30	-0.78	0.14	-0.54	0.14	-5.31
0.46	-0.84	0.19	-0.58	0.27	-5.42
0.67	-0.97	0.32	-0.64	0.38	-5.52
0.79	-1.02	0.65	-0.81	0.52	-5.77
1.04	-1.10	0.77	-0.85	0.76	-5.96
1.30	-1.21	1.08	-1.04	0.94	-6.08
1.47	-1.30	1.35	-1.08	1.13	-6.15
2.13	-1.56	1.62	-1.19	1.18	-6.23
2.93	-1.77	2.00	-1.35	1.25	-6.31
3.73	-2.05	2.49	-1.54	1.47	-6.38
4.84	-2.28	3.23	-1.77	1.67	-6.38
5.60	-2.48	3.88	-2.00	2.16	-6.50
6.63	-2.74	4.02	-2.04	2.59	-6.58
7.30	-2.79	5.31	-2.38	2.83	-6.56
10.44	-3.21	5.58	-2.35	3.07	-6.62
		7.14	-2.69	3.19	-6.60
				3.36	-6.65
				3.53	-6.64

Table 8 (continued)

DMSO		Pyridine		$MeNO_2$	
$\frac{[15C5]}{[Na^+]^b}$	δ_{ppm}	$\frac{[15C5]}{[Na^+]^b}$	δ_{ppm}	$\frac{[15C5]}{[Na^+]^b}$	δ_{ppm}
0	-0.5	0	+0.75	0	-14.55
0.23	-1.2	0.18	+0.07	0.14	-13.4
0.36	-1.5	0.31	-0.31	0.24	-12.5
0.52	-1.8	0.34	-0.41	0.51	-10.2
0.74	-2.1	0.57	-1.27	0.73	- 8.1
1.01	-2.4	0.80	-1.85	0.85	- 6.8
1.17	-2.5	0.97	-2.49	0.97	- 5.8
1.44	-2.9	1.03	-2.72	1.04	- 5.3
1.52	-3.0	1.24	-2.81	1.34	- 5.5
2.24	-3.5	1.34	-2.93	2.26	- 5.8
2.35	-3.5	1.45	-2.97	3.22	- 6.1
4.14	-4.3	1.57	-3.04	3.94	- 6.3
		1.87	-3.03	4.52	- 6.5
		2.27	-3.08	5.65	- 6.8
		2.31	-3.16	6.45	- 7.1
		2.72	-3.18	8.32	- 7.4
		3.16	-3.20	9.90	- 7.6
		3.56	-3.20		
		3.75	-3.20		

Table 8 (continued)

MeCN		THF		PC	
$\frac{[15C5]}{[Na^+]}$ [b]	δ_{ppm}	$\frac{[15C5]}{[Na^+]}$ [b]	δ_{ppm}	$\frac{[15C5]}{[Na^+]}$ [b]	δ_{ppm}
0	-7.56	0	-7.72	0	-9.7
0.24	-6.89	0.15	-7.18	0.11	-9.1
0.41	-6.43	0.31	-6.65	0.37	-8.0
0.64	-5.86	0.58	-5.8	0.52	-7.7
0.87	-5.33	0.75	-5.2	0.70	-6.9
1.04	-4.89	0.94	-4.7	0.90	-6.3
1.99	-4.93	1.05	-4.4	1.19	-5.9
2.11	-5.54	2.10	-4.4	1.48	-5.9
4.20	-5.77	2.93	-4.4	2.01	-5.8
6.27	-6.00			2.70	-6.0
7.56	-6.19			3.12	-5.9
9.95	-6.46				

[a]The solutions were 0.05 M in sodium salt.

[b]The solutions were 0.05 M in $NaBph_4$.

Table 9. Sodium-23 NMR Chemical Shift-Mole Ratio Data for Na^+ ion Complex with MB15C5 in Various Solvents at Ambient Temperatures

Pyridine		DMSO		$MeNO_2$	
$\frac{[MB15C5]}{[Na^+]^a}$	δ_{ppm}	$\frac{[MB15C5]}{[Na^+]^a}$	δ_{ppm}	$\frac{[MB15C5]}{[Na^+]^a}$	δ_{ppm}
0	+0.75	0	-0.5	0	-14.55
0.19	+0.25	0.13	-0.7	0.21	-12.5
0.30	-0.08	0.33	-0.9	0.30	-11.5
0.52	-0.7	0.55	-1.1		
0.76	-1.3	0.71	-1.2	0.42	-10.6
0.89	-1.5	0.92	-1.2	0.52	- 9.2
1.03	-1.8	1.00	-1.3	0.60	- 8.5
1.22	-2.1	1.13	-1.3	0.78	- 6.8
1.49	-2.2	1.34	-1.5	0.92	- 4.9
1.81	-2.2	1.45	-1.6	1.02	- 4.2
2.08	-2.2	1.63	-1.6	1.40	- 4.5
2.16	-2.3	1.72	-1.7	1.58	- 4.6
2.43	-2.3	2.02	-1.8	1.83	- 4.7
3.10	-2.2	2.22	-2.0	1.95	- 4.8
4.15	-2.4	2.49	-2.0	2.20	- 5.1
				2.77	- 5.3
				3.30	- 5.6

Table 9 (continued)

$MeNO_2$		MeCN		THF	
$\frac{[MB15C5]}{[Na^+]^a}$	δ_{ppm}	$\frac{[MB15C5]}{[Na^+]^a}$	δ_{ppm}	$\frac{[MB15C5]}{[Na^+]^a}$	δ_{ppm}
4.10	-6.3	0	-7.56	0	-7.76
4.82	-6.5	0.11	-7.14	0.19	-7.00
6.01	-7.2	0.34	-6.30	0.43	-6.0
8.33	-8.2	0.56	-5.61	0.55	-5.5
		0.68	-5.10	0.61	-5.3
		0.91	-4.5	0.79	-4.6
		1.04	-4.1	1.01	-3.8
		1.40	-4.0	1.29	-3.8
		2.16	-4.1	1.56	-3.8
				1.70	-3.8
				2.11	-3.7

DMF[a]		PC[a]	
0	-5.05	0	-9.7
0.14	-5.15	0.09	-9.3
0.36	-5.23	0.30	-8.4
0.48	-5.31	0.53	-7.4
0.77	-5.46	0.74	-6.7
1.03	-5.54	0.95	-5.6

Table 9 (continued)

DMF		PC	
$\frac{[MB15C5]}{[Na^+]}$	δ_{ppm}	$\frac{[MB15C5]}{[Na^+]}$	δ_{ppm}
1.20	-5.6	1.09	-5.3
1.40	-5.6	2.08	-5.2
1.48	-5.6	3.33[b]	
2.00	-5.7		
2.61	-5.8		
3.16	-5.8		

[a]The solutions were 0.05 M in $NaBph_4$.

[b]Insoluble.

ligand is added to the Na^+ ion solution. The addition of 15C5 crown ether to a nitromethane solution of sodium tetraphenylborate results in a paramagnetic shift with a sharp break at mole ratio of one followed by a diamagnetic shift which is changed gradually as the concentration of the ligand is increased. This behavior clearly indicates the successive formation of a 1:1 and 2:1 (ligand : cation) complex. Both 1:1 and 2:1 complexes are also formed with 15C5 crown ether in acetonitirle and MB15C5 in nitromethane solutions. Similar behavior was observed in the complexation of 12C4 with Li^+ ion in nitromethane and PC solutions (61) as well as 18C6 with Cs^+ ion in several nonaqueous solvents (57). In all the above cases where two complexes are formed the cavity size of the ligand is smaller than the cation size.

The successive formation of the 1:1 and 2:1 complexes is also shown in the variation of the half-height linewidth which is plotted versus the ligand/cation mole ratio in Figure 10 for the complexation of 15C5 and MB15C5 with the Na^+ ion in nitromethane solutions. The linewidth increases rapidly to mole ratio of one and then decreases as more and more ligand is added to the Na^+ ion solution. This variation strongly indicates that the electronic environment of the Na^+ ion in the 2:1 "sandwich" complex is much more symmetrical than that in the 1:1 complex.

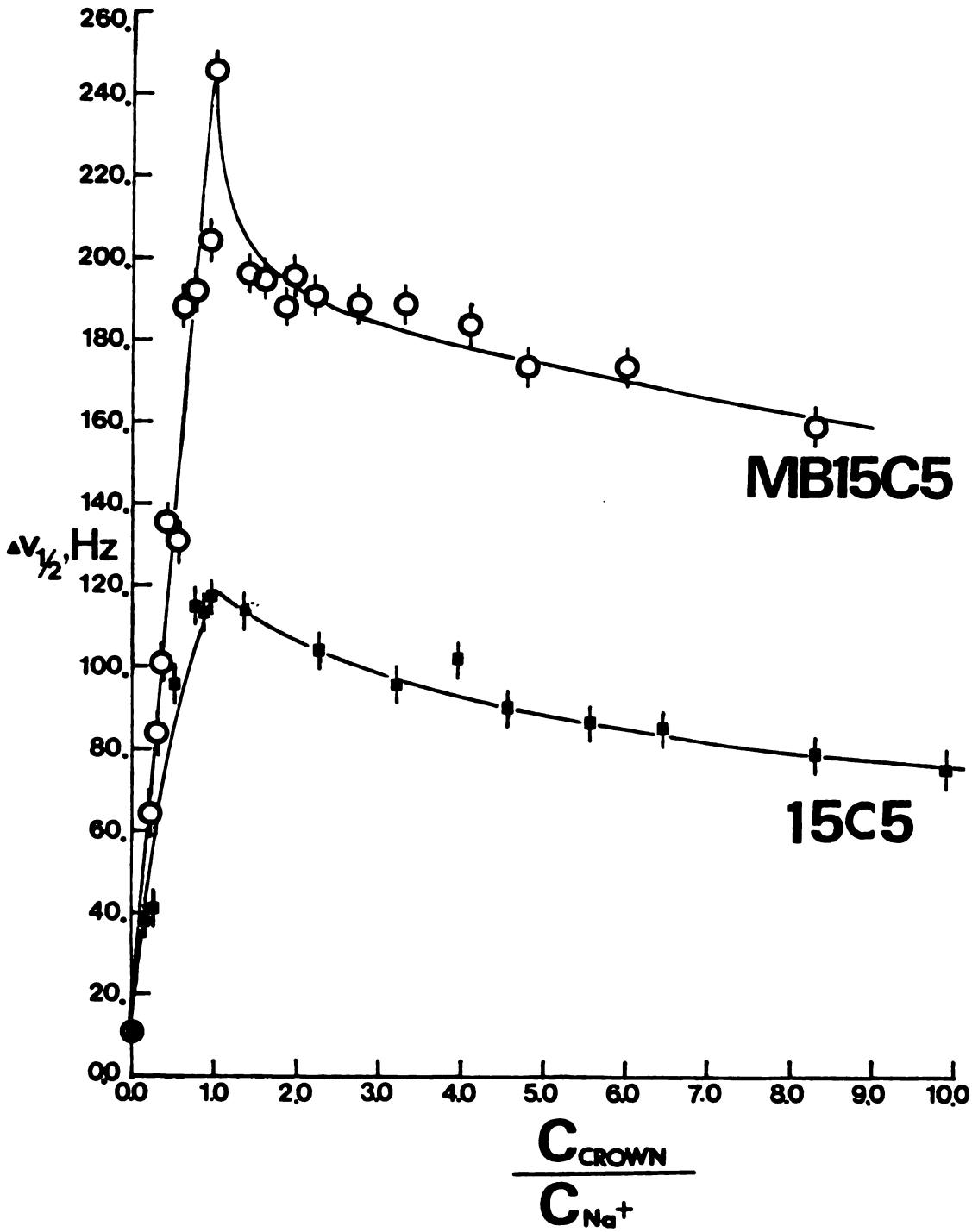

Fig 10. The half-height linewidth vs. ligand/Na^+ mole ratio in $MeNO_2$ solutions. The solutions were 0.05 M in $NaBPh_4$.

The formation constants of the 1:1 $Na^+\cdot$ crown complexes were obtained by analyzing the chemical shift vs. mole ratio data with a weighted nonlinear least-squares curvefitting program, KINFIT (109), according to the equilibrium (3.1)

$$M^+ + L \rightleftharpoons ML^+ \qquad (3.1)$$

where M^+, L and ML^+ represent the metal ion, the ligand and the complex respectively. The concentration equilibrium constant (K) is given by the equation (3.2)

$$K = \frac{C_{ML^+}}{C_{M^+} \cdot C_L} \qquad (3.2)$$

where C_{ML^+}, C_{M^+} and C_L denote the equilibrium molar concentration of the complex, the metal ion and the ligand respectively. If only the formation of 1:1 complex is important and the exchange between the free and the complexed cation is fast on the NMR time scale, a population-averaged chemical shift is observed.

$$\delta_{obs} = X_M\delta_M + X_{ML}\delta_{ML} \qquad (3.3)$$

where the δ_{obs}, δ_M and δ_{ML} are the observed, solvated and complexed cation chemical shifts, X_M and X_{ML} are the relative mole fractions of solvated and complexed cation respectively. From equations 3.2-3.3 and the mass balance equations it can be easily shown that,

$$\delta_{obs} = [(KC_M^t - KC_L^t - 1) + (K^2C_L^{t2} + K^2C_M^{t2} - 2K^2C_L^tC_M^t + 2KC_L^t + 2KC_M^t + 1)^{\frac{1}{2}}](\frac{\delta_M - \delta_{ML}}{2KC_M^t}) + \delta_{ML} \quad (3.4)$$

In equation (3.4), the total concentration of the cation and the ligand (C_M^t and C_L^t respectively) are known, δ_M is determined by measuring the cation chemical shift in the absence of the ligand. The equation, therefore, has two unknown quantities, K and δ_{ML}, which are obtained by an iteration method using the program, KINFIT, starting with reasonable estimates of K and δ_{ML}. The results of the above analysis, the formation constants (K) and limiting chemical shifts (δ_{ML}) of the Na^+·crown complexes in various solvents, are shown in Tables 10-12. When both 1:1 and 2:1 complexes are formed, an upper limit for the 2:1 complexation constant (K_2) was calculated by assuming the formation constant of the 1:1 complex (K_1) is so large that in solutions with ligand/Na^+ ion mole ratios greater than one, the concentration of the free Na^+ ion is negligible, that is, only the data above mole ratio of one were used to evaluate K_2. For very stable Na^+·crown complexes, only the lower limit of $K = 10^4$ could be obtained by our technique.

In the cases of the Na^+ ion complexed with 18C6 in PY, DMF and DMSO solutions, the ^{23}Na resonance peak is so broad (about 220 to 400 Hz) that precise measurements of the chemical shifts are impossible with either the

Table 10. Formation Constants and Limiting Chemical Shifts of $Na^+ \cdot 18C6$ Complex in Various Solvents at Ambient Temperature

Solvent	Salt	Log K_f	Limiting Chemical Shift of Complex, ppm
H_2O	$NaClO_4$	0.70 ± 0.05	-11.8 ± 0.4
	NaI	0.82 ± 0.05	-10.2 ± 0.3
	NaCl	0.57 ± 0.05	-13.2 ± 0.8
Pyridine	$NaBPh_4$	-[a]	69.99 ± 0.05
DMSO	$NaBPh_4$	1.41 ± 0.07[b]	70.43 ± 0.05
DMF	$NaBPh_4$	2.31 ± 0.05[b]	70.36 ± 0.05
THF	$NaBPh_4$	> 4	-17.0 ± 0.2
Me_2CO	$NaBPh_4$	> 4	-16.4 ± 0.2
PC	$NaBPh_4$	> 4	-16.1 ± 0.2
$MeNO_2$	$NaBPh_4$	> 4	-16.7 ± 0.2
MeCN	$NaBPh_4$	3.8 ± 0.2	-15.3 ± 0.1

[a] Beyond the upper limit of the technique used.

[b] From ^{13}C NMR.

Table 11. Formation Constants and Limiting Chemical Shifts of Na^+ ion Complexes with 15C5 in Various Solvents at Ambient Temperature

Solvent	Salt	Log K_f	Limiting Chemical Shift of Complex, ppm
H_2O	NaI	0.41 ± 0.05	-5.3 ± 0.2
	NaCl	0.44 ± 0.05	-5.1 ± 0.2
Pyridine	$NaBPh_4$	2.68 ± 0.08	-3.2 ± 0.1
DMSO	$NaBPh_4$	1.31 ± 0.06	-5.3 ± 0.2
DMF	$NaBPh_4$	1.97 ± 0.05	-6.8 ± 0.1
THF	$NaBPh_4$	> 4	-4.4 ± 0.1
PC	$NaBPh_4$	-[c]	-5.9 ± 0.2
MeCN	$NaBPh_4$	> 4[a]	
$MeNO_2$	$NaBPh_4$	$K_{f1} > 10^4$ $K_{f2} = 1.6 \pm 0.2$	-11.1 ± 0.6[b]

[a]The K_{f2} of the 2:1 complex (ligand:sodium ion) is too small to be calculated.

[b]Limiting chemical of the 2:1 complex.

[c]It cannot be determined by the techniques used because of the very braod linewidth.

Table 12. Formation Constants and Limiting Chemical Shifts of Na^+ ion Complexes with MB15C5 in Various Solvents at Ambient Temperature

Solvent	Salt	Log K_f	Limiting Chemical Shift of Complex, ppm
Pyridine	$NaBPh_4$	2.6 ± 0.1	-2.4 ± 0.2
DMSO	$NaBPh_4$	1.1 ± 0.2	-3.2 ± 0.5
DMF	$NaBPh_4$	1.6 ± 0.1	-6.0 ± 0.2
THF	$NaBPh_4$	> 4	-3.8 ± 0.2
PC	$NaBPh_4$	-[b]	-5.2 ± 0.5
MeCN	$NaBPh_4$	> 4	-4.1 ± 0.1
$MeNO_2$	$NaBPh_4$	$K_{f1} > 10^4$	
		$K_{f2} = 0.8 \pm 0.2$	-22 ± 3[a]

[a]Limiting chemical shift of the 2:1 complex.

[b]It cannot be determined by the techniques used because of the very broad linewidth.

DA-60 or the Bruker-90 spectrometer. Therefore, carbon-13 NMR was used to study the complexation reaction of 18C6 with Na^+ ion in these three solvents. The variation of the carbon-13 chemical shift as a function of Na^+/18C6 mole ratio at 31 $\pm$ 1°C is shown in Table 13 and Figure 11. The data were also analyzed with the program, KINFIT, and the results are shown in Table 10. The formation constant of the Na^+·18C6 complex in pyridine is beyond the upper limit of our technique. It has been shown that the carbon-13 NMR determination with a 100 MHz NMR spectrometer is accurate for the equilibrium constants within the range $100 \geq K \geq 0.01$ (120). It has also been shown that the complex formation constants, within the range $200 \geq K > 5$, obtained from the carbon-13 NMR (using an 80 MHz NMR spectrometer) agree very well with those from the alkali metal NMR for the complexation of potassium ion with 12C4 in several nonaqueous solvents (118). The same agreement was also found for the complexation of the Na^+ ion with 15C5 in DMF and DMSO solutions as shown in Tables 14-15 and Figure 12. The upper limit of the complexation constant which can be obtained by ^{13}C NMR is lower than that obtained by ^{23}Na NMR because of the smaller range of the ^{13}C NMR chemical shift. Thus the experimental error in the determination of the chemical shift is relatively larger with ^{13}C NMR.

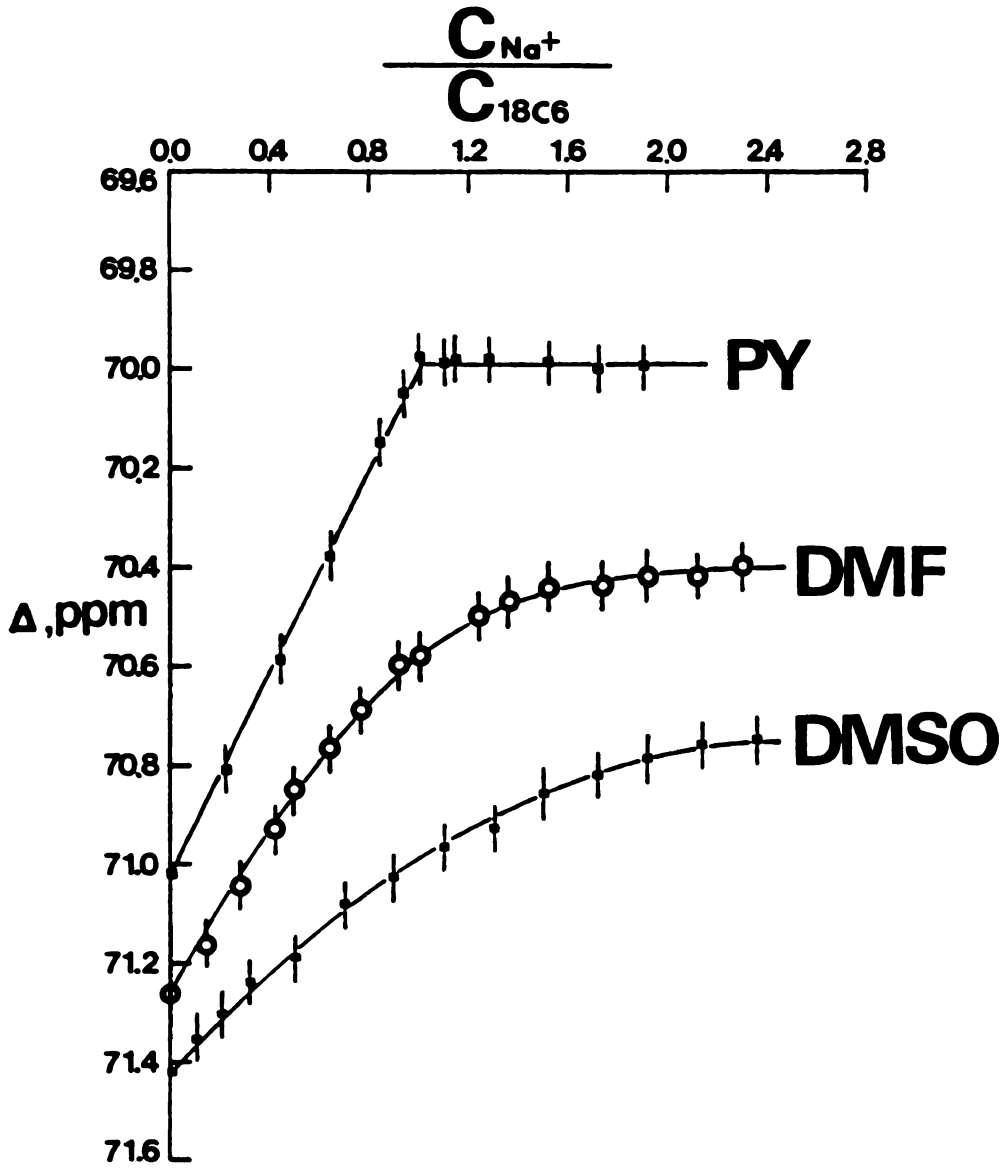

Fig 11. Carbon-13 chemical shifts vs. Na^+/18C6 mole ratios in various solvents. The solutions were 0.05 M in 18-Crown-6 except in DMF where the concentration was 0.06 M.

Table 13. Carbon-13 NMR Chemical Shift-Mole Ratio Data for Na^+ Ion Complex with 18C6 in Various Solvents at 31 ± 1°C

PY		DMSO		DMF	
$\frac{[NaBph_4]}{[18C6]}$ [a]	δ^c_{ppm}	$\frac{[NaBPh_4]}{[18C6]}$ [a]	δ^c_{ppm}	$\frac{[NaBph_4]}{[18C6]}$ [b]	δ^c_{ppm}
0	71.02	0	71.42	0	71.26
0.22	70.81	0.10	71.35	0.14	71.16
0.43	70.59	0.21	71.31	0.27	71.04
0.64	70.38	0.31	71.24	0.42	70.93
0.84	70.15	0.50	71.19	0.51	70.85
0.93	70.05	0.70	71.08	0.65	70.77
1.01	69.98	0.90	71.03	0.77	70.69
1.10	69.99	1.10	70.97	0.92	70.60
1.14	69.98	1.30	70.93	1.00	70.58
1.29	69.98	1.51	70.86	1.24	70.50
1.52	69.99	1.72	70.82	1.37	70.47
1.73	70.00	1.93	70.79	1.52	70.44
1.90	70.00	2.14	70.76	1.74	70.44
		2.35	70.75	1.93	70.42
				2.12	70.42
				2.31	70.40

[a]The solutions were 0.05M in 18C6.

[b]The solutions were 0.065M in 18C6.

[c]Values are precise to ±0.05 ppm.

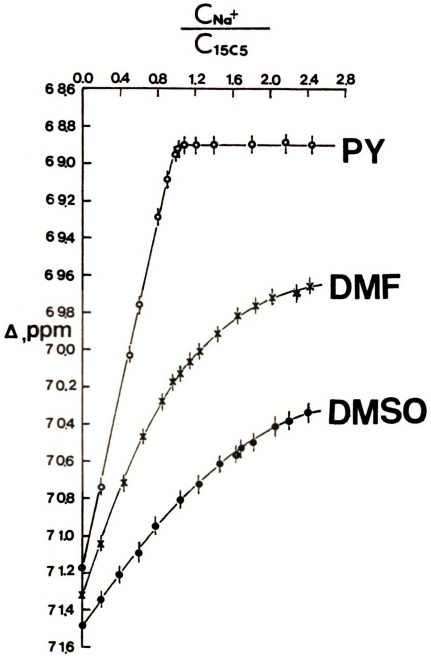

Figure 12. Carbon-13 chemical shifts vs. Na^+/15C5 mole ratios in various solvents. C^T_{15C5}= 0.05 M.

Table 14. Carbon-13 NMR Chemical Shift-Mole Ratio Data for Na^+ Ion Complex with 15C5 in Various Solvents at 31 ± 1°C

PY		DMSO		DMF	
$\frac{[NaBph_4]}{[15C5]^a}$	δ^b_{ppm}	$\frac{[NaBph_4]}{[15C5]^a}$	δ^b_{ppm}	$\frac{[NaBph_4]}{[15C5]^a}$	δ^b_{ppm}
0	71.18	0	71.50	0	71.33
0.20	70.74	0.20	71.35	0.20	71.05
0.50	70.03	0.39	71.21	0.44	70.72
0.60	69.76	0.59	71.10	0.64	70.47
0.79	69.29	0.78	70.95	0.84	70.28
0.90	69.09	1.04	70.81	0.94	70.18
0.99	68.94	1.24	70.73	1.04	70.14
1.02	68.92	1.43	70.62	1.14	70.06
1.09	68.90	1.63	70.56	1.23	70.02
1.20	68.90	1.67	70.53	1.43	69.92
1.39	68.90	1.82	70.50	1.63	69.82
1.79	68.90	2.06	70.41	1.83	69.77
2.17	68.90	2.21	70.39	2.02	69.72
2.43	68.90	2.41	70.34	2.27	69.70
				2.42	69.66

[a]The solutions were 0.05M in 15C5.

[b]Values are precise to ± 0.05 ppm.

Table 15. The Comparison of Complexation Constants Obtained from Alkali Metal NMR and Carbon-13 NMR

Solvent	Salt	Crown	Log K_f Na-23 NMR	Log K_f K-39 NMR[a]	Log K_f C-13 NMR
DMSO	$NaBPh_4$	15C5	1.31 ± 0.06		1.12 ± 0.04
DMF	$NaBPh_4$	15C5	1.97 ± 0.05		1.88 ± 0.04
Pyridine	NaBPh	15C5	2.68 ± 0.08		-[b]
DMSO	KPF_6	12C4		0.31 ± 0.04	0.7 ± 0.1[a]
Me_2CO	KPF_6	12C4		1.8 ± 0.2	1.87 ± 0.07[a]
MeCN	KPF_6	12C4		2.2 ± 0.2	2.26 ± 0.07[a]
DMF	KPF_6	18C6		2.70 ± 0.04	-[b]

[a]Data from Ref. (117).

[b]Beyond the upper limit of the technique used.

Since 15C5 and MB15C5 crown ethers form both 1:1 and 2:1 complexes with Na^+ ion in nitromethane solution, the possibility of the formation of both complexes in other solvents could not be ruled out although our ^{23}Na NMR measurements did not seem to show the existence of 2:1 complexes. The possibility of 2:1 complex formation was examined by using proton NMR of MB15C5 and its complex with Na^+ ion. The variation of the proton chemical shift as a function of Na^+ ion/MB15C5 mole ratio in d^6-DMSO solutions is shown in Table 16 and Figure 13. The results seem to show that there is a very small amount of 2:1 complex in the solution as indicated by the fairly slight curvature at mole ratio of 0.5 (Figure 13) for proton number 2 as well as numbers 3 and 4, which cannot be separated by the limited resolution of the instrument used. However, the quantity of 2:1 complex is so small that it is negligible compared with the 1:1 complex.

In fact, as shown in Tables 11 and 12, the stability constants of the 2:1 complexes are quite small even in nitromethane solutions. It is expected that the formation of the 2:1 complex is more favorable in nitromethane solution because of its poor solvating ability. By contrast, in solvents of higher donicity, the 2:1 complex may be quite unstable due to the solvation of the 1:1 complex so that the second ligand molecule cannot readily attach to the 1:1 complex.

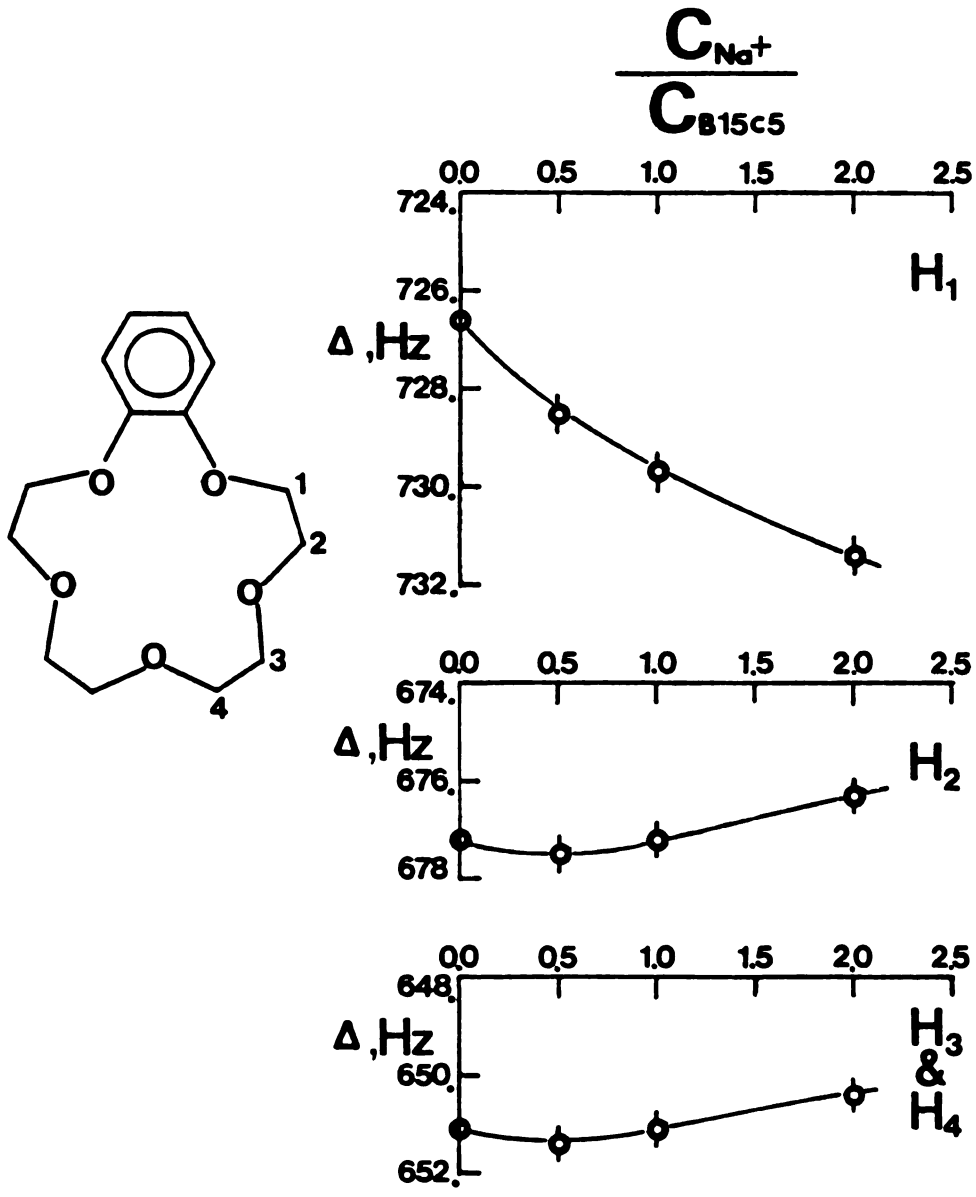

Figure 13. Proton(H^1) chemical shifts vs. Na^+/ B15C5 mole ratios in DMSO-$_d$6 solutions. C^T_{B15C5}= 0.05 M.

Table 16. Proton Chemical Shifts of Na^+/MB15C5 Complex in DMSO-d^6 at Ambient Temperature[a]

$[NaBph_4]$ / $[MB15C5]$[b]	H_1		H_2		H_3 and H_4	
	δ_{Hz}	δ_{ppm}	δ_{Hz}	δ_{ppm}	δ_{Hz}	δ_{ppm}
0.00	726.6	4.036	677.2	3.762	651.1	3.617
0.50	728.5	4.046	677.5	3.763	651.4	3.618
1.00	729.7	4.053	677.2	3.762	651.1	3.617
2.00	731.4	4.063	676.3	3.756	650.4	3.612

[a]Protons are designated by the number of the carbon to which they are attached (see Figure 13).

[b]The solutions were 0.05M in MB15C5.

The possibility of the formation of two complexes in solutions was also checked by the following method. Equation (3.3) (see page 68) can be rearranged to give equation (3.5) because $X_M + X_{ML} = 1$.

$$\delta_{obs} = X_M\delta_M + X_{ML}\delta_{ML} \tag{3.3}$$

$$\delta_{obs} = (\delta_M - \delta_{ML})X_M + \delta_{ML} \tag{3.5}$$

The relative mole fraction of solvated Na^+ ion, X_M, was calculated from the formation constant obtained using equation (3.4) (see page 69) and then δ_{obs} was plotted versus X_M. Some typical plots are shown in Figure 14. The data points fall on a straight line with the predicted slope ($\delta_M - \delta_{ML}$) and intercept (δ_{ML}), indicating that the data fit very well the 1:1 complex model. If a 2:1 complex is also formed, its concentration is negligible as compared with the concentrations of other species in the solution.

From the data in Tables 10-12, it seems that in the complexation reactions the donor ability of the solvent plays a more important role than the dielectric constant. In general, the stability of the complex increases as the Gutmann donor number (see page 15) of the solvent decreases. It is obvious that in strongly solvating solvents the competition between the solvent molecules and the ligand for the coordination sites of the cation should decrease the stability of the complex. However, in

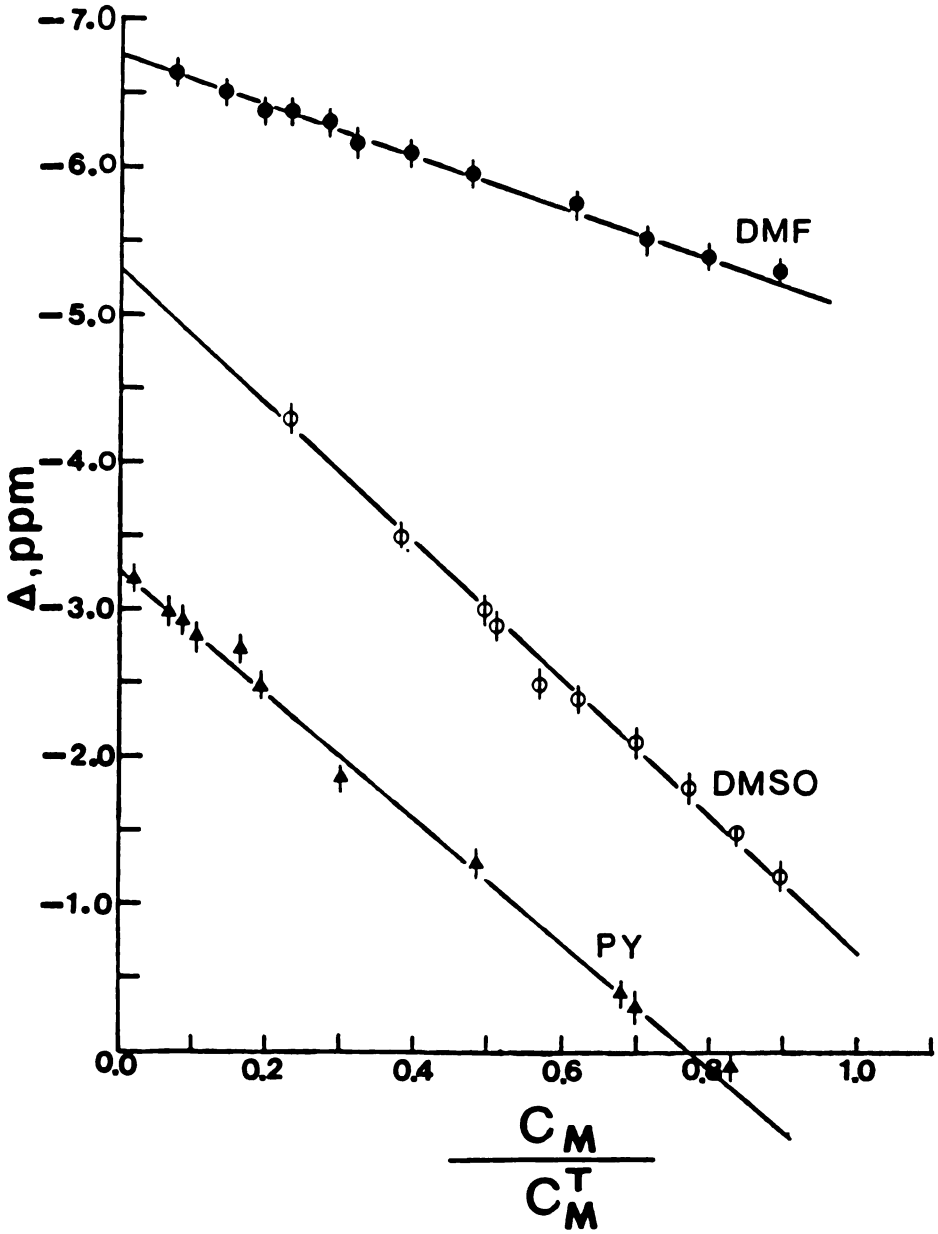

Figure 14. Observed chemical shift vs relative mole fraction of solvated sodium ion for Na^+/15C5 system in PY, DMSO and DMF solutions.

pyridine solution which has the highest donicity among the solvents used, the complex formation constants are quite large. Similar results have been shown in the complexation of the Li^+ ion with 15C5 (61), the Na^+ and Cs^+ ions with 1,10-dithia-18C6 (23) and the Cs^+ ion with (2)-cryptands (82) in various nonaqueous solvents. A possible reason for the behavior in pyridine is that this solvent, being a nitrogen donor or a "soft" base, does not solvate strongly a "hard" acid such as an alkali ion (121). There is another exception in the complexation of Na^+ ion with 18C6 that the stability constant of this complex in MeCN solution is smaller than in PC, THF and acetone which have higher donor numbers than MeCN. Similar behavior has been found in the complexation of Li^+ ion with 18C6 in PC and acetonitrile solutions (61). The above exception in MeCN solution could be due to the strong interaction between the ligand and solvent molecules which decreases the stability of the complex. It has been shown that 18C6 forms a stable complex with acetonitrile (98).

In the calculation of the complex stability constants possible cation-anion interactions were not taken into account since sodium tetraphenylborate was used in all the nonaqueous solvents studied. It was shown from conductance studies that sodium tetraphenylborate is completely dissociated in acetonitrile (122) and sodium perchlorate is essentially completely dissociated in DMF

and DMSO solutions (115, 123). It has also been shown that the behavior of sodium tetraphenylborate is quite similar to that of sodium perchlorate in these solvents (115). Therefore, it is reasonable to assume that at the concentrations studied the competition from the ion pairing is negligible in these three nonaqueous solvents and in nitromethane solution which has a comparable dielectric constant (35.9) to that of DMF (36.7). In solvents of low dielectric constant such as pyridine ion pairing should be more important. Unfortunately, there are no data available in literature about the ion pair formation constants of sodium perchlorate or sodium tetraphenylborate in pyridine. Therefore, the formation constants given in Tables 10-12 for the 1:1 complexes in pyridine are lower limits which represent the relative complexing abilities of the three ligands in this solvent. It is difficult to understand the small but noticeable variation in the formation constants of $Na^+ \cdot 18C6$ complex in water with three anions, Cl^-, I^- and ClO_4^-, as shown in Table 10. However, it may be due to the formation of ion pairs to different extent with various anions.

In the solvents studied the stability constants decrease in the order $Na^+ \cdot 18C6 > Na^+ \cdot 15C5 > Na^+ \cdot B15C5$. It has been shown that one of the major factors affecting the stabilities of macrocyclic complexes is the relative sizes of the cation and of the hole in the polyether ring.

As far as the cavity size is concerned (Table 17), the Na^+ ion seems to fit better into the 15C5 crown ether which is slightly smaller than the Na^+ ion based on molecular models while 18C6 is too large. The formation constants currently available, together with those obtained in this study, for the Na^+ ion complexes with 18C6, B18C6 and DB18C6 in several solvents are shown in Table 18. It is known (1, 5) that the aromatic groups in B18C6 and DB18C6 decrease the basicity of the oxygen atoms. The O···O distance also decreases, which causes a decrease in the cavity size. Finally there is an increase in the rigidity of the polyether ring. When the basicity of the oxygen atoms and the rigidity of the ring are concerned, the stability constants should be in the order DB18C6 $\leq$ B18C6 < 18C6. Since the order was found to be DB18C6 $\geq$ B18C6 > 18C6, it seems that the cavity size factor is much more important, i.e. the DB18C6 fits Na^+ ion much better than 18C6. Therefore, the greater stability of Na^+·18C6 than Na^+·15C5 complex in the solvents studied may be due to the larger number of oxygen atoms in the polyether ring. As expected, (57, 82) 15C5 crown ether forms more stable sodium complexes than MB15C5 in which the decreased basicity of the oxygen atoms, flexibility of the ring and cavity size disfavor the complex formation.

Table 17. Ionic Diameters of Alkali Cations and Ring Sizes of Some Crown Ethers

Cation	Ionic Diameter (Å)[a]	Crown Ether	Ring Size (Å)[b]
Li^+	1.72	12C4	1.2 - 1.5
Na^+	2.24	15C5	1.7 - 2.2
K^+	2.88	18C6	2.6 - 3.2
Rb^+	3.16		
Cs^+	3.68		

[a]Reference 125.

[b]Reference 24.

Table 18. Comparison of the Formation Constants Currently Available for the Na^+ Ion Complexes with 18C6, B18C6 and DB18C6 in Several Solvents

	Log K			
Solvent	18C6	B18C6	DB18C6	Reference
H_2O	0.8			50
			1.16	43
DMF	2.31			60
			2.69	62
MeOH	4.32			34
			4.36,4.16,4.5	34,39,2
MeCN	3.8			60
		4.90		41
			5.04	39

3. Anion effects on the complexation of Na^+ ion with 18C6 in THF and 1,3-dioxolane solutions

It was previously indicated in part 2 that the exchange rate of the sodium cation between the bulk solution and the complex in the system $NaBPh_4$/18C6 in THF solutions is slow on the NMR time scale since two resonances of ^{23}Na nucleus were observed when free Na^+ ion was present in excess. The complexation reaction of Na^+ ion with 18C6 in THF was studied with three salts, $NaBPh_4$, $NaClO_4$ and NaI, and the results are presented in Table 19. The data show that anions play an extremely important role in the complexation process. With sodium iodide or sodium perchlorate only one population-averaged ^{23}Na NMR signal was observed under the same experimental conditions. As shown in Table 20 and Figure 15, when a small amount of tetrabutylammonium iodide was added to a solution, which was 0.05 M in $NaBPh_4$ and 0.025 M in 18C6, the two sodium resonance peaks collapsed to give one broad peak. As the concentration of tetrabutylammonium iodide was increased, the linewidth of the peak decreased and the frequency of the peak moved downfield toward the value of 18C6/NaI in THF at mole ratio of 0.5.

In order to understand the behavior of the Na^+/18C6 system in THF solutions, an attempt was made to study the complexation reaction of dibenzo-18C6 with three sodium salts, $NaBPh_4$, $NaClO_4$ and NaI, in THF. Unfortunately, in

Table 19. Sodium-23 NMR Chemical Shift-Mole Ratio Data for Na^+ ion Complex with 18C6 in THF Solutions with Various Anions at Ambient Temperatures

$NaBph_4$		$NaClO_4$		NaI	
$\frac{[18C6]}{[Na^+]}$ [a]	δ ppm	$\frac{[18C6]}{[Na^+]}$ [a]	δ ppm	$\frac{[18C6]}{[Na^+]}$ [a]	δ ppm
0	-7.72	0	- 8.3	0	6.50
0.20	-7.9	0.51	-12.8	0.51	-2.1
	c	1.02[b]		1.01	-11.4
0.59	-7.8			2.19	-12.6
	-17.1			2.98	-12.5
1.04	-16.9				
1.21	-17.1				
3.00	-17.1				

[a]The solutions were 0.05 M in sodium salt.

[b]The complex is not soluble.

[c]The chemical shift could not be measured precisely because the peak was very broad and noisy.

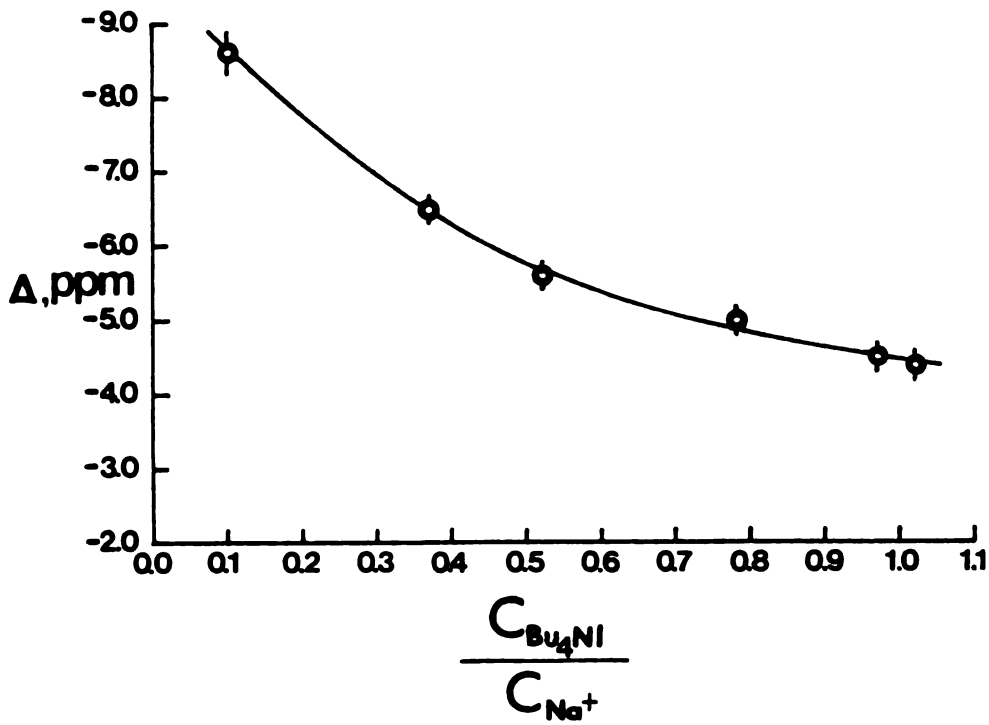

Figure 15. Sodium-23 chemical shift vs. Bu_4NI/Na^+ mole ratio in THF solutions. The solutions were 0.05 M in $NaBPh_4$ and 0.025 M in 18-Crown-6.

Table 20. Sodium-23 NMR Chemical Shifts for Na^+ ion Complex with 18C6 in THF Solutions as a Function of Added Bu_4NI at 28 ± 1°C

$\frac{[Bu_4NI]}{[Na^+]}$ [a]	δ_{ppm}	$\Delta\nu_{1/2}$ (Hz)
0.10	9	218
0.37	6.9	182
0.52	6.0	161
0.78	5.4	155
0.97	4.9	160
1.02	4.8	150
2.04[b]	-	-

[a]The solutions were 0.050 M in $NaBPh_4$ and 0.025 M in 18C6.

[b]Insoluble.

all three cases either the free crown ether or the complex is not soluble in the solvent at total salt concentration of 0.05 M. Then the complexation reaction of the Na^+ ion with 18C6 was studied in 1,3-dioxolane solutions. The results are presented in Table 21. The same phenomena as those in THF were observed, i.e. at 18C6/Na^+ mole ratio of 0.5 two ^{23}Na NMR signals were observed with the tetraphenylborate anion, while only one signal was observed with the perchlorate anion.

Two typical spectra for the cation exchange between the two sites as a function of temperature are shown in Figures 16-17 and the corresponding NMR data are presented in Table 22. In Figure 17 at -14 and -21°C there is another peak coming out at higher field, corresponding to the complexed sodium ion, and the frequency of the peak at lower field is equal to that of the solvated Na^+ ion and the linewidth of this peak is smaller than those at -6 and 3 °C. As the temperature of the solution is lower than -21 °C, the peak at higher field is smeared out by viscosity broadening and, therefore, two distinct peaks are not observed in this case. The coalescence temperature and approximate exchange rate at coalescence calculated from equation (3.6) for the Na^+·18C6 complex in THF and 1,3-dioxolane solutions are shown in Table 23.

$$k = \frac{\pi}{\sqrt{2}} (\nu_f - \nu_c) \qquad (3.6)$$

Table 21. Sodium-23 NMR Chemical Shift-Mole Ratio Data for Na^+ ion Complex with 18C6 in 1,3-dioxolane Solutions with Various Anions at 28 ± 1°C

$NaBPh_4$		$NaClO_4$		NaI^b
$\frac{[18C6]}{[Na^+]^a}$	$\delta^{obs.}_{ppm}$	$\frac{[18C6]}{[Na^+]^a}$	$\delta^{obs.}_{ppm}$	
0	-9.90	0	-9.40	
0.57	-9.8	0.54	-13.6	
	-16.8	1.04	-16.9	
1.11	-17.0	2.16	-17.0	
2.01	-17.0			

[a]The solutions were 0.05 M in sodium salt.

[b]NaI is not soluble enough in 1,3-dioxolane to perform ^{23}Na NMR measurements.

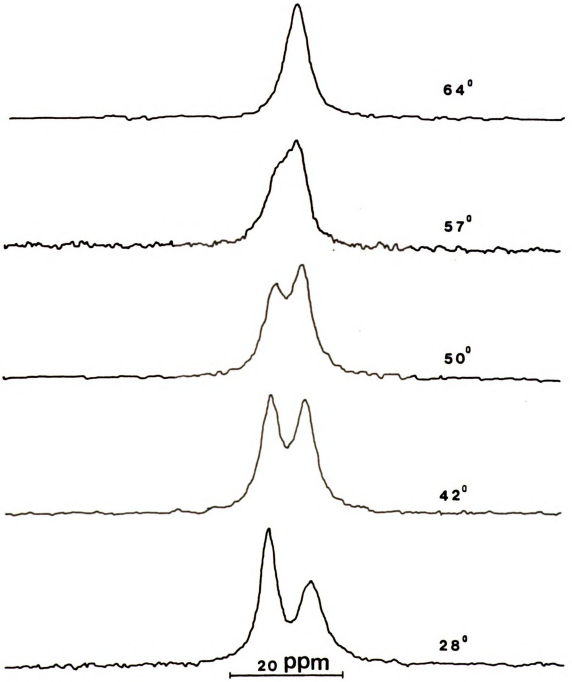

Figure 16. Sodium-23 NMR spectra at various temperatures for a solution containing 0.05 M $NaBPh_4$ and 0.026 M 18-Crown-6 in 1,3-Dioxolane.

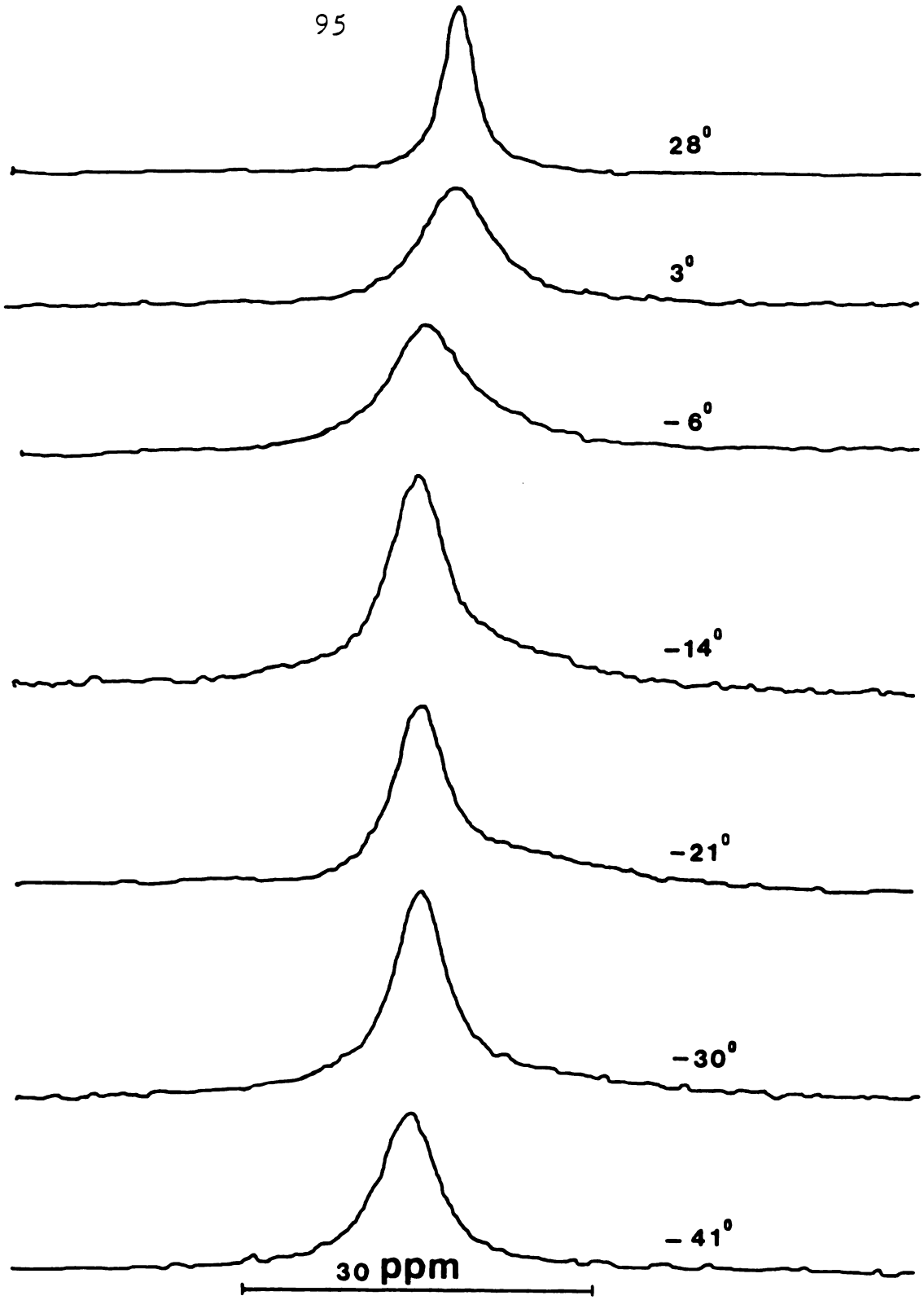

Figure 17. Sodium-23 NMR spectra at various temperatures for a solution containing 0.05 M $NaClO_4$ and 0.025 M 18-Crown-6 in 1,3-Dioxolane.

Table 22. Sodium-23 NMR Chemical Shifts at [18C6]/[Na^+] Mole Ratio of 0.5 in 1,3-dioxolane Solutions at Various Temperatures[a]

$NaBPh_4$			$NaClO_4$		
Temp (°C)	δ^{obs}_{ppm}	$\Delta V_{1/2}$ (Hz)	Temp (°C)	δ^{obs}_{ppm}	$\Delta V_{1/2}$ (Hz)
28	- 9.7	54	28	-13.1	45
	-17.1	93	3	-12.8	114
42	-10.7	-[b]	-6	-10.5	123
	-16.8	-[b]	-14	- 9.7	92
50	-11.8	-[b]	-21	- 9.6	82
	-16.3	-[b]	-30	- 9.8	84
57	-15.5	118	-41	- 9.5	89
64	-14.8	74	-59	-9.4	133

[a]The solutions were 0.05 M in sodium salts.

[b]The two peaks were so close to each other that the $\Delta V_{1/2}$ could not be measured.

Table 23. The Coalescence Temperature and Approximate Exchange Rate of Na^+ ion Complex with 18C6 in THF and 1,3-dioxolane Solutions

Solvent	Salt	$\frac{[18C6]}{[Na^+]}$ [a]	Coalescence Temperature (°C) [b]	Exchange Rate at Coalescence (s^{-1})
THF	$NaBPh_4$	0.59	41	3.3×10^2
	$NaClO_4$	0.54	-20	- [c]
	NaI	0.50	-30	6.7×10^2
1,3-dioxolane	$NaBPh_4$	0.52	54	2.5×10^2
	$NaClO_4$	0.50	-5	2.7×10^2

[a] The solutions were 0.05 M in salt.

[b] Values are precise to ± 3°C.

[c] It can not be calculated because the resonance frequency of the complexed Na^+ ion is unknown due to the limited solubility of the complex.

where ν_f and ν_c are the resonance frequencies of free and complexed Na^+ ion respectively at total salt concentration of 0.05 M and k is the exchange rate.

It was shown previously that the ion pair dissociation constant of $NaBPh_4$ is 8.8×10^{-5} at 25°C and that NaI forms a much more stable ion pair than $NaBPh_4$ in THF (125, 115). It has also been shown that the dissociation constant of the DB18C6 complexed $NaBPh_4$ ion pair i.e. $Na^+ \cdot DBC \cdot BPh_4^-$ is 6.0×10^{-5} at 20 °C in dimethoxyethane which has dielectric constant (7.2) as low as that of THF (7.6) (45). Therefore, the observed variation in the cation exchange rate may be due to ion pair or even triple ion formation of the solvated salts and the ion pair formation of the complexed salts to different extent with different anion.

4. Sodium-23 NMR study of the exchange kinetics for sodium tetraphenylborate complex with 18C6 crown ether in 1,3-dioxolane solutions

It was previously shown in part 3 that the apparent exchange rate of the sodium cation between the bulk solution and the complex in the system $NaBPh_4$/18C6 in THF and 1,3-dioxolane solutions is slow on the NMR time scale at ambient temperatures. Therefore, an attempt was made to study the kinetics of the complexation reaction between the Na^+ ion and the 18C6 crown ether in 1,3-dioxolane by ^{23}Na NMR technique from changes of the resonance lineshape as a

function of temperature (116, 117).

In order to determine the linewidths of the two sites (free and complexed Na^+ ion) at various temperatures in the absence of exchange, separate lineshape analyses were made of the salt and the completely complexed Na^+ ion at various temperatures. The results (chemical shifts and linewidths) are listed in Table 23(b). It is immediately seen that the linewidth of the free Na^+ ion increases as the solution temperature increases and the chemical shifts of the free Na^+ ion and the complex change with temperature. As far as the viscosity is concerned, the linewidth of a resonance in the absence of exchange should decrease as the solution temperature increases because the viscosity of the solution decreases. Therefore, the variation of the linewidth of the free Na^+ ion with temperature seems to indicate that there is an exchange between the free Na^+ ion and the ion pair in the salt solution. Similarly, it may have an exchange between the complexed Na^+ ion and the ion pair of the complexed salt in the solution containing stoichiometric amount of the salt and the ligand.

It is not surprising that there is substantial ion pairing between the free (and the complexed) Na^+ ion and the tetraphenylborate anion in this solvent of low dielectric constant (see part 3). Therefore, the complexation

Table 23(b). The Observed ^{23}Na Chemical Shifts and Half-Height Linewidths of Solvated and 18C6 Complexed Na^+ ion in 1,3-Dioxolane at Four Temperatures

Temp (°C)	$\delta_{ppm}^{Na^+}$ [a]	$\Delta\nu_{1/2}^{Na^+}$ Hz	$\delta_{ppm}^{Na^+\cdot 18C6}$ [b]	$\Delta\nu_{1/2}^{Na^+\cdot 18C6}$ Hz
28.3 ± 0.1	-9.8 [c]	31.3 [d]	-16.9 ± 0.2	88.9 ± 0.5
37.6	-10.7	35.6	-16.5	75.5
46.4	-11.2	39,0	-16.2	60.8
54.9	-11.9	43.8	-15.7	49.8

a. The solution was 0.051 M in $NaBPh_4$.

b. The solution was 0.051 M in $NaBPh_4$ and 0.055 M in 18C6.

c. The values are precise to ± 0.1.

d. The values are precise to ± 0.5.

reaction in solutions containing free Na^+ ion in excess involves exchanges of more than two sites (free and complexed Na^+ ion). As seen in Table 23(c), however, the chemical shifts of the free and of the complexed Na^+ ion are independent of concentrations. Both salts are preferentially ion-paired in the measurable (by ^{23}Na NMR) concentration ranges. Since the chemical shifts and the linewidths of the free Na^+ ion, the complex and the ion pairs of the free and the complexed salt cannot be obtained, the kinetics of the complexation reaction in 1,3-dioxolane (and likewise in THF) solution cannot be studied by ^{23}Na NMR method. Thus, the observed variation in the apparent cation exchange rate with the anion (part 3, Table 23) in these two solvents may attribute to the different exchange rates between the various species in the solutions.

Table 23(c). The Observed ^{23}Na Chemical Shifts of Solvated and 18C6 Complexed Na^+ ion in 1,3-Dioxolane as A Function of Concentration at 28 ± 1 °C

Conc.[a] (M)	$\delta^{Na^+}_{ppm}$	$\delta^{Na^+\cdot 18C6}_{ppm}$
0.010	-10.0 ± 0.1	-17.0 ± 0.2
0.030	-9.9	-17.0
0.050	-9.9	-17.0
0.10		-16.9

a. The salt was $NaBPh_4$.

1. Introduction

It has been shown previously that the stabilities and selectivities of the cryptand complexes with suitable alkali cations are several orders of magnitude larger than those of crown ethers (5). Cahen et al. (78) found that the chemical shift of the lithium cation complexed by cryptand C211, which has a cavity radius nearly equal to that of the unsolvated lithium ion, is essentially independent of the solvent and the counterion used. Mei et al. (83) showed that the limiting chemical shift of the $Cs^+ \cdot$ C222 complex is dependent on both the solvent and the temperature but converges to a solvent-independent value at low temperature. Since the cavity size of cryptand C221 is nearly equal to that of the unsolvated sodium cation and the radius ratio of Na^+/C211 (=1.4) is close to that of Cs^+/C222 (=1.3), it would be interesting to study the complexation reaction of Na^+ ion with the cryptands. This chapter reports the studies of sodium cation complexes with four cryptands; C211, C221, C222 and C222B in several solvents using sodium-23 NMR technique.

2. Results and Discussion

The variations of the sodium-23 chemical shifts as a function of cryptand/Na^+ mole ratio in various solvents at ambient temperatures are shown in Tables 24-27. In most of the cases studied, the cation exchange between the bulk solution and the complex is slow on the NMR scale since

CHAPTER IV

NMR STUDIES OF SODIUM CATION COMPLEXES WITH SOME 2-CRYPTANDS IN VARIOUS SOLVENTS

Table 24. Sodium-23 NMR Chemical Shift-Mole Ratio Data for Na^+ ion Complex with C211 in Various Solvents at Ambient Temperature

Solvent	Salt	$[Na^+]$ (M)	$\frac{[C211]}{[Na^+]}$	δ_{ppm}	$\Delta V_{1/2}$ (Hz)
Water	NaI	0.0502	0	-0.45	7
			0.56	-0.23	31
				12.6	262
			1.11	11.8	329
			2.17	12.3	264
			2.95	12.4	272
	NaCl	0.0501	0	-0.46	8
			2.02	12.7	268
Pyridine	$NaBPh_4$	0.100	0	0.84	18
			0.65	-[a]	-
			0.99	10.7	251
			2.00	10.8	208
			3.35	10.9	297
	$NaClO_4$	0.0508	0	-0.7	39
			0.43	-1.0	39
				~11.5	-[b]
			1.03	10.9	217
			2.18	10.8	219
	NaI	0.0500	0	7.3	40
			0.61	7.5	77[c]
			1.00	11.5	230
			1.79	11.5	242

Table 24 (continued)

Solvent	Salt	$[Na^+]$ (M)	$\frac{[C211]}{[Na^+]}$	δ_{ppm}	$\Delta V_{1/2}$ (Hz)
DMSO	$NaBPh_4$	0.0501	0	- 0.5	51
			0.88	- 0.5	95
				11.8	-[b]
			1.09	10.0	294
			2.26	9.7	289
DMF	$NaBPh_4$	0.0502	0	- 5.04	28
			2.30	10.1	194
	$NaClO_4$	0.0501	0	- 5.13	27
			0.56	- 4.8	46
				-[d]	~195
			1.15	10.1	177
			2.21	10.0	187
	NaI	0.0502	0	- 4.95	28
			0.59	- 4.6	56
				10.2	192
			1.15	10.0	174
			2.48	10.0	171
THF	$NaBPh_4$	0.0502	0	- 7.72	25
			0.62	- 7.4	60
				10.5	~198
			1.40	10.7	252
			2.00	10.6	264

Table 24 (continued)

Solvent	Salt	$[Na^+]$ (M)	$\frac{[C211]}{[Na^+]}$	δ_{ppm}	$\Delta V_{1/2}$ (Hz)
	$NaClO_4$	0.0500	0	-8.29	16
			0.66	-8.06	27
				8.8	198
			1.02	8.1	203
			2.25	8.1	232
		0.0251	6.54	8.1	203
		0.100	1.03[e]	-	-
	NaI	0.0503	0	6.55	22
			0.65	9.4	162[c]
			1.14[e]	-	-
Me_2CO	$NaBPh_4$	0.100	0	-7.94	17
			0.53	-7.74	20
				~11.5	~176
			2.54	10.5	200
			3.35	10.2	193
		0.0501	0	-8.08	15
			1.07	10.5	161
			2.10	10.6	151
			2.22	10.5	164
	NaI	0.0249	0	-4.99	19
			2.03	10.8	142
			4.25	10.9	142

Table 24 (continued)

Solvent	Salt	$[Na^+]$ (M)	$\frac{[C211]}{[Na^+]}$	δ_{ppm}	$\Delta V_{1/2}$ (Hz)
MeCN	$NaBPh_4$	0.0502	0	-7.56	10
			0.55	-7.56	20
				~12.1	~156
			1.00	11.2	182
			2.38	11.2	183
	$NaClO_4$	0.0506	0	-7.8	8
			0.52	-7.5	12
				11.5	145
			2.54	11.2	168
	NaI	0.0536	0	-6.51	8
			0.62	-6.53	13
				11.5	172
			1.02	11.4	164
			2.06	11.5	168
$MeNO_2$	$NaBPh_4$	0.0502	0	-14.55	10
			0.51	-13.90	37
				-[d]	-
			1.06	~11	~471
PC	$NaBPh_4$	0.100	0	-9.7	62
			1.06	-[d]	-
MeOH	$NaBPh_4$	0.0502	0	-3.71	17
			0.50[e]	-	-

Tal

[a] Th

[b] Th
cou

[c] An

[d] Th
mea

[e] In

Table 24 (continued)

[a]The two peaks were not well-separated.

[b]The two peaks were so close to each other that $\Delta V_{1/2}$ could not be measured precisely.

[c]An unsymmetrical peak.

[d]The peak was so noisy that the chemical shift could not be measured precisely.

[e]Insoluble.

Table 25. Sodium-23 NMR Chemical Shift-Mole Ratio Data for Na^+ ion Complex with C221 in Various Solvents at Ambient Temperature

Solvent	Salt	$[Na^+]$ (M)	$\frac{[C221]}{[Na^+]}$	δ_{ppm}	$\Delta V_{1/2}$ (Hz)
Water	NaI	0.0502	0	-0.45	8
			0.52	-0.69	16
				-[a]	-
			1.08	-4.8	102
			2.18	-4.9	106
			3.31	-4.8	108
	NaCl	0.0506	0	-0.46	9
			0.99	-4.8	99
			2.59	-4.9	107
	$NaClO_4$	0.201	0.14[b]		
Pyridine	$NaBPh_4$	0.0501	0	0.76	15
			1.07	-5.0	67
			1.71	-5.0	69
	$NaClO_4$	0.0509	0	-0.8	43
			1.32	-5.0	67
		0.100	0	-0.7	53
			1.13	-5.1	69
			3.26	-5.1	76
	NaI	0.0510	0	7.3	42
			0.61	7.4	53
				-6.1	75
			3.01	-5.2	73

Table 25 (continued)

Solvent	Salt	$[Na^+]$ (M)	$\frac{[C221]}{[Na^+]}$	δ_{ppm}	$\Delta\nu_{1/2}$ (Hz)
Pyridine	NaSCN	0.0504	0	2.6	61
			0.46	2.6	85
				-5.1	-[c]
			1.38	-5.2	66
			2.15	-5.1	70
	NaI	0.103[b]			
DMF	$NaBPh_4$	0.100	0	-5.1	31
			0.55	-5.4	41
			1.15	-5.2	75
			2.05	-5.2	76
			3.25	-5.1	77
		0.0501	0	-5.1	27
			1.04	-5.3	67
			2.17	-5.3	68
	NaI	0.0506	0	-4.89	26
			1.16	-5.2	65
	NaBr	0.0501	0	-3.7	29
			1.16	-5.3	66
			3.19	-5.2	70
	NaF	0.0500[b]			
Me_2CO	$NaBPh_4$	0.0500	1.07	-4.1	44
			1.40	-4.2	45

Table 25 (continued)

Solvent	Salt	$[Na^+]$ (M)	$\frac{[C221]}{[Na^+]}$	δ_{ppm}	$\Delta V_{1/2}$ (Hz)
	$NaClO_4$	0.0501	0	-7.96	14
			1.47	-4.0	43
	NaSCN	0.0507	0	-6.1	42
			1.10	-4.2	46
			2.32	-4.2	43
THF	$NaBPh_4$	0.0500	0	-7.85	19
			1.05	-4.2	64
			1.52	-4.2	67
	NaSCN	0.0508	0	-3.2	60
			1.38	-4.6	74
			2.03	-4.8	72
	$NaClO_4$	0.0501	1.11[b]		
	NaI	0.0509	0.56[b]		
PC	$NaBPh_4$	0.100	0	-9.6	68
			0.52	-[d]	
			1.05	-4.3	190
			2.11	-4.4	198
		0.0501	0	-9.7	66
			1.01	-4.6	180
			2.14	-4.5	181
	NaI	0.0503	0	-9.4	64
			1.24	-4.6	170
			2.02	-4.6	171
			3.22	-4.6	171

Table 25 (continued)

Solvent	Salt	$[Na^+]$ (M)	$\frac{[C221]}{[Na^+]}$	δ_{ppm}	$\Delta\nu_{1/2}$ (Hz)
MeCN	$NaBPh_4$	0.100	0	-7.53	10
			0.53	-7.76	13
				-4.0	-[c]
			1.08	-4.0	47
			2.05	-4.0	52
		0.0500	1.26	-4.0	48
	$NaClO_4$	0.0500	0	-7.86	9
			1.32	-4.2	43
			3.10	-4.1	44
	NaI	0.0507	0	-6.68	7
			1.09	-4.0	41
			2.15	-4.0	43
			3.30	-4.0	46
2-Nitro-propane	$NaBPh_4$	0.0501	0	-13.25	18
			0.63	-12.9	48
				-4.1	79
			1.04	-3.9	83
			1.24	-3.9	78
			3.27	-3.7	80
$MeNO_2$	$NaBPh_4$	0.0501	0	-14.58	14
			1.05	-3.7	71
			1.87	-3.7	74

Table 25 (continued)

Solvent	Salt	$[Na^+]$ (M)	$\frac{[C221]}{[Na^+]}$	δ_{ppm}	$\Delta V_{1/2}$ (Hz)
DMSO	NaI	0.0506	0	-0.7	35
			3.05	-4.7	133

[a]The peak was so noisy and weak that the chemical shift could not be measured precisely.

[b]Insoluble.

[c]The two peaks were so close to each other that $\Delta V_{1/2}$ could not be measured precisely.

[d]The two peaks were not well-separated.

Table 26. Sodium-23 NMR Chemical Shift-Mole Ratio Data for Na^+ ion Complex with C222 in Various Solvents at Ambient Temperature

Solvent	Salt	$[Na^+]$ (M)	$\frac{[C222]}{[Na^+]}$	δ_{ppm}	$\Delta V_{1/2}$ (Hz)
Pyridine	$NaBPh_4$	0.100	0	0.84	20
			0.50	0.84	25
				-12.4	42
			0.74	0.84	20
				-12.4	35
			1.00	-12.5	40
			2.00	-12.5	45
			3.06	-12.4	42
	NaI	0.0506	0	7.3	42
			0.52	8.3	43
				-12.2	34
			1.36	-12.4	37
DMF	$NaBPh_4$	0.100	0	-5.10	29
			0.23	-5.4	38
				-12.0	-[a]
			0.50	-5.5	56
				-11.6	75
			0.70	-6.0	58
				-11.7	-[a]
			0.82	-11.5	56[b]
			1.00	-11.5	38
			1.92	-11.5	43
			2.90	-11.5	43

Table 26 (continued)

Solvent	Salt	$[Na^+]$ (M)	$\frac{[C222]}{[Na^+]}$	δ_{ppm}	$\Delta V_{1/2}$ (Hz)
PC	$NaBPh_4$	0.100	0	-9.8	73
			0.33	-10.4	76
			0.50	-10.9	77
			0.71	-11.0	87
			0.83	-10.9	90
			1.02	-11.4	90
			2.51	-11.4	114
MeCN	$NaBPh_4$	0.0501	0	-7.76	12
			0.50	-9.2	50
			1.01	-11.18	23
			1.39	-11.22	23
THF	$NaBPh_4$	0.0503	0	-7.71	20
			0.50	-7.80	22
				-11.93	33
			1.00	-11.93	29
			1.62	-12.10	31
	$NaClO_4$	0.0502	0.51[c]		
	NaI	0.0500	0.51[c]		
2-Nitro-propane	$NaBPh_4$	0.0502	0	-13.5	21
			0.60	-12.5	33
			1.01	-11.9	37
			1.56	-11.8	37

Table 26 (continued)

Solvent	Salt	$[Na^+]$ (M)	$\frac{[C222]}{[Na^+]}$	δ_{ppm}	$\Delta V_{1/2}$ (Hz)
$MeNO_2$	$NaBPh_4$	0.0500	0	-14.50	11
			0.25	-13.62	17
			0.41	-13.00	22
			0.56	-12.54	24
			0.80	-11.58	28
			0.96	-11.06	32
			1.01	-10.82	32
			1.17	-10.90	31
			1.53	-10.90	31
			2.21	-10.81	33

[a]The two peaks were so close to each other that $\Delta V_{1/2}$ could not be measured precisely.

[b]An unsymmetric peak.

[c]Insoluble.

Table 27. Sodium-23 NMR Chemical Shift-Mole Ratio Data for Na^+ ion Complex with C222B in Various Solvents at Ambient Temperature

Solvent	Salt	$[Na^+]$ (M)	$\frac{[C222B]}{[Na^+]}$	δ_{ppm}	$\Delta V_{1/2}$ (Hz)
Pyridine	$NaBPh_4$	0.0502	0.55	0.69	18
				-10.1	67
			1.05	-[a]	-
				-9.9	69
			1.49	-9.9	69
			2.07	-9.9	69
	NaI	0.0504	0	7.2	40
			0.47	7.4	42
				-9.9	62
			1.06	5.7	67
				-9.9	62
			1.56	-9.7	63
			2.18	-9.9	64
	NaSCN	0.0504	0	2.6	61
			0.57	2.4	93
				-10.2	66
			1.08	-10.0	64
			1.46	-10.0	66
DMSO	$NaBPh_4$	0.0501	0	-0.6	46
			0.50	-0.6	58
				-7.6	-[b]

Table 27 (continued)

Solvent	Salt	$[Na^+]$ (M)	$\frac{[C222B]}{[Na^+]}$	δ_{ppm}	$\Delta V_{1/2}$ (Hz)
DMSO	$NaBPh_4$	0.0501	1.05	-1.1	-[b]
				-8.2	-[b]
			1.13	~-8,4	202[d]
			1.88	-8.4	132
DMF	$NaBPh_4$	0.0500	0.48	-5.2	-[b]
				-[a]	-
			1.06	-8.8	62
			2.05	-8.8	62
MeCN	$NaBPh_4$	0.0501	0.55	-7.7	16
				-[a]	-
			1.03	-8.9	31
			1.36	-9.0	32
			1.89	-8.9	42
			2.11[c]		
$MeNO_2$	$NaBPh_4$	0.0500	0.38	-14.2	32
				-9.7	-[b]
			1.03	-8.7	47
			1.62	-8.6	47
2-Nitro-propane	$NaBPh_4$	0.0501	0.51	-13.0	54
				-[a]	-
			1.00	-9.3	60
			1.35	-9.1	64
			2.01	-9.3	64

Table 27 (continued)

Solvent	Salt	$[Na^+]$ (M)	$\frac{[C222B]}{[Na^+]}$	δ_{ppm}	$\Delta V_{1/2}$ (Hz)
Me_2CO	$NaBPh_4$	0.0519	0.43	-8.4	24[d]
			1.02[c]		
	$NaClO_4$	0.100	0	-8.4	10
			0.12	-8.5	12
			0.33	-8.6	16
			0.52[c]		
THF	$NaBPh_4$	0.0502	0.59[c]		
	NaI	0.0500	0.52[c]		

[a]The peak was so weak and noisy that the chemical shift could not be measured precisely.

[b]The two peaks were so close to each other that the $\Delta V_{1/2}$ could not be measured precisely.

[c]Insoluble.

[d]An unsymmetrical peak.

two resonances of the ^{23}Na nucleus were observed when the Na^+ ion was present in excess. The results shown in Table 24 indicate that in all solvents used in this study, the three cryptands, C221, C222 and C222B form very stable 1:1 complexes (log $K \geq 4$) with the sodium cation, since the limiting chemical shifts of the complexes are already reached at 1:1 ligand/Na^+ mole ratio. The resonance linewidth of the $Na^+ \cdot$C211 complex is so broad that no definite conclusion about the stability of the complex can be made. The formation constants of the above cryptates cannot be obtained accurately by our techniques (see previous chapter) which depends on the variation of population averaged resonance with the ligand/metal ion mole ratio.

As the data in Table 25 indicate that the addition of cryptand C221 to a DMF solution of $NaBPh_4$ results in a very small change in the ^{23}Na chemical shift, although the half-height linewidth of the resonance broadens. This observation suggests that either a very unstable complex is formed or the electronic environment of the Na^+ ion in the complex is very similar to that of the solvated Na^+ ion in the DMF solution.

In order to find out the reason for the above observation, the system Na^+/C221 in DMF solution was studied with two other salts, NaCl and NaBr. The results (Table 25) show that stable $Na^+ \cdot$C221 cryptate is indeed formed in the solution as indicated by the variation of

chemical shift (in the case of NaBr salt), the large broadenirg of the linewidth (in all three cases) upon addition of cryptand C221, and the same chemical shift of the complex in all three cases.

The data shown in Table 24 seem to indicate that the cryptand C211 forms an exclusive complex with Na^+ ion since the limiting chemical shifts of the complexed sodium ion are both solvent- and anion-dependent. The broad half-height linewidth of the complexed sodium resonance peak indicates that in the Na^+·C211 cryptate, the electronic environment of the Na^+ ion is quite unsymmetrical. The possibility of equilibrium between the inclusive and exclusive Na^+·C211 cryptates, such as in the case of Cs^+·C222 cryptates (83), was studied by the ^{23}Na NMR at low temperatures. Unfortunately, the chemical shift of the complexed Na^+ ion cannot be measured precisely by the instrument used because of the very broad linewidth of the resonance at low temperatures. Therefore, no conclusion about the equilibrium can be made.

Although x-ray studies of the Na^+·C221 cryptate show that in the solid state the sodium ion is located in the center of the cryptand cavity (71), the limiting chemical shift of the Na^+·C221 cryptate is solvent-dependent (Table 28). It has been pointed out previously (78) that the chemical shift of the Li^+·C211 cryptate is independent of the solvent and the counter-ion used and the limiting

Table 28. ^{23}Na NMR Chemical Shifts of Solvated Na^+ Ion and $Na^+ \cdot C221$ Cryptate in Various Solvents at Ambient Temperature

Solvent	Salt	$[Na^+]$ (M)	$\delta^{Na^+}_{ppm}$	$\delta^{Na^+ \cdot C221}_{ppm}$
Water	NaCl	0.051	-0.46	-4.8
	NaI	0.050	-0.45	-4.8
Pyridine	$NaBPh_4$	0.050	0.76	-5.0
	$NaClO_4$	0.100	-0.7	-5.1
	$NaClO_4$	0.051	-0.8	-5.0
	NaI	0.051	7.3	-5.2
	NaSCN	0.050	2.6	-5.1
DMF	$NaBPh_4$	0.100	-5.1	-5.2
	$NaBPh_4$	0.050	-5.1	-5.3
	NaI	0.051	-4.89	-5.2
	NaBr	0.050	-3.7	-5.3
THF	$NaBPh_4$	0.050	-7.85	-4.2
	NaSCN	0.051	-3.2	-4.7
MeCN	$NaBPh_4$	0.100	-7.53	-4.0
	$NaClO_4$	0.050	-7.86	-4.1
	NaI	0.051	-6.68	-4.0
$MeNO_2$	$NaBPh_4$	0.050	-14.58	-3.7
Me_2CO	$NaBPh_4$	0.050	-8.1	-4.1
	$NaClO_4$	0.050	-7.96	-4.0
	NaSCN	0.050	-6.1	-4.2

Table 28 (continued)

Solvent	Salt	$[Na^+]$ (M)	$\delta^{Na^+}_{ppm}$	$\delta^{Na^+\cdot C221}_{ppm}$
PC	$NaBPh_4$	0.100	-9.6	-4.4
	$NaBPh_4$	0.050	-9.7	-4.5
	NaI	0.050	-9.4	-4.6
DMSO	NaI	0.051	-0.7	-4.7
2-Nitro-propane	$NaBPh_4$	0.050	-13.25	-3.8

chemical shift of the inclusive $Cs^+ \cdot C222$ cryptate is solvent independent at low temperature. Thus, the ^{23}Na chemical shifts of $Na^+ \cdot C221$ cryptate at high $C221/Na^+$ mole ratio (>1.4) in pyridine, Me_2CO, THF and 2-nitropropane solutions were mearsured at various temperatures and the results are shown in Table 29 and Figure 18. When the temperature of the solution decreases, the chemical shift of the $Na^+ \cdot$ C221 cryptate moves upfield instead of converging to a solvent independent value as in the case of $Cs^+ \cdot C222$ cryptates. This behavior suggests that the sodium ion is not completely shielded by C221 from the external medium at all temperatures studied. For comparison, the variation of the sodium-23 chemical shift at high $C222/Na^+$ mole ratio (>1.3) as a function of temperature was determined in THF, DMF, MeCN and 2-nitropropane solutions. The results are presented in Table 30 and Figure 19. The changing behavior of the chemical shift of the $Na^+ \cdot C222$ cryptate is quite different from that of the $Na^+ \cdot C221$, i.e. when the solution temperature decreases, the limiting chemical shift moves slightly upfield and then downfield in THF, DMF and 2-nitropropane solutions and it moves downfield gradually in MeCN solution. The reasons for the changing behavior of the limiting chemical shifts of the $Na^+ \cdot C221$ and $Na^+ \cdot C222$ cryptates as a function of temperature are not clear. However, one possible reason is a conformational change of the complex at various temperatures.

Table 29. The ^{23}Na Limiting Chemical Shifts of $Na^+ \cdot C221$ Cryptate as a Function of Temperature in Pyridine, Acetone, THF and 2-nitropropane Solutions.

Solvent	$\frac{[C221]}{[Na^+]}$ [a]	Temp. (°C) [b]	δ_{ppm}	$\Delta V_{1/2}$ (Hz)
Pyridine	1.55	80	-3.5	40
		62	-4.0	54
		28	-5.0	69
		10	-5.7	96
		-4	-6.2	128
		-22	-7.3	198
		-28	-7.6	231
THF	1.83	51	-3.4	50
		28	-4.2	67
		-3	-5.3	107
		-18	-6.2	138
		-30	-6.6	183
		-48	-8.0	305
Me_2CO	1.41	41	-3.8	39
		28	-4.1	45
		12	-4.8	58
		-4	-5.1	72
		-16	-5.5	93
		-22	-5.6	99
		-30	-6.0	118
		-48	-7.0	190

Table 29 (continued)

Solvent	$\frac{[C221]}{[Na^+]}$ [a]	Temp. (°C) [b]	δ_{ppm}	$\Delta V_{1/2}$ (Hz)
2-nitro-propane	1.54	47	-3.4	66
		28	-3.8	86
		11	-4.2	108
		-12	-4.8	167
		-22	-5.4	218
		-34	-6.3	300

[a]The solutions were 0.050 M in $NaBPh_4$.

[b]Values are accurate to ± 1°C.

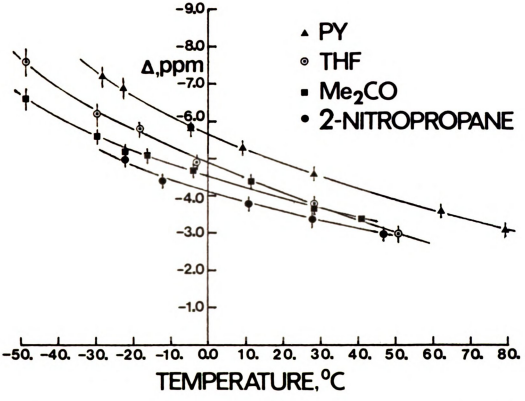

Figure 18. Limiting sodium-23 chemical shift at high C221/Na^+ mole ratio *vs.* temperature in various solvents. The solutions were 0.05 *M* in $NaBPh_4$.

Table 30. The ^{23}Na Limiting Chemical Shifts of $Na^+ \cdot C222$ Cryptate as a Function of Temperature in DMF, THF, MeCN and 2- Nitropropane Solutions

Solvent	$\frac{[C222]}{[Na^+]}$ [a]	Temp. (°C) [b]	δ_{ppm}	$\Delta V_{1/2}$ (Hz)
DMF	1.49	28	-11.4	42
		12	-11.8	51
		-5	-11.6	68
		-13	-11.4	78
		-18	-11.1	88
		-21	-10.9	95
		-34	-10.5	124
		-47	-10.1	195
THF	2.07	28	-12.1	34
		12	-12.6	45
		8	-12.6	60
		-12	-12.4	62
		-28	-12.2	79
		-42	-11.7	106
		-44	-11.4	108
		-60	-11.1	147
		-64	-11.0	165
		-75	-10.2	213
MeCN	1.39	28	-11.2	23
		13	-11.0	29
		11	-10.9	26
		2	-10.8	32
		-9	-10.5	36

Table 30 (continued)

Solvent	$\frac{[C222]}{[Na^+]}$	Temp. (°C)	δ_{ppm}	$\Delta V_{1/2}$ (Hz)
MeCN	1.39	-20	-10.1	42
		-29	-10.1	46
		-39	- 9.6	56
2-Nitro-propane	1.56	28	-11.8	37
		15	-12.2	47
		8	-12.3	52
		-9	-12.0	69
		-24	-11.7	91
		-50	-10.9	174

[a]The solutions were 0.050 M in $NaBPh_4$.

[b]Values are accurate to ± 1°C.

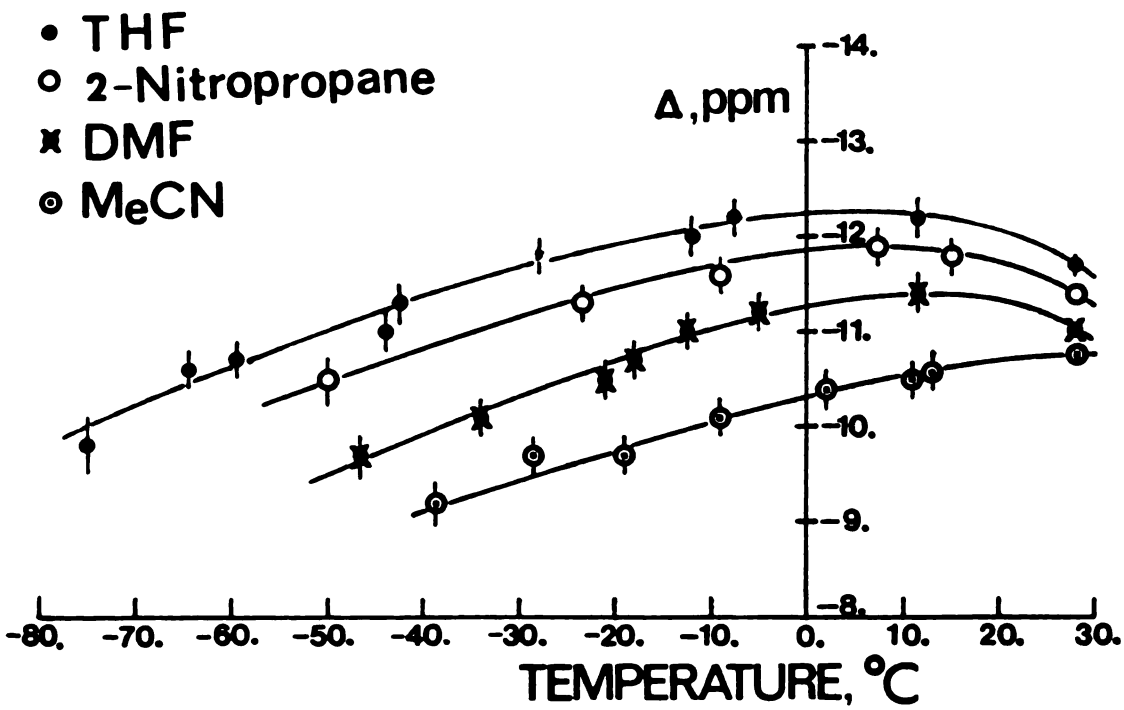

Fig. 19. Limiting Sodium-23 chemical shift at high mole ratio, C222/Na^+, vs. temperature in various solvents. The solutions were 0.05 M in $NaBPh_4$.

As expected (78), the limiting chemical shifts of Na^+·C222 and Na^+.C222B cryptates are solvent-dependent (Table 31) because the cavity sizes of these two cryptands are larger than the size of sodium cation. For the complexation reaction of Na^+ ion with cryptand C222B in pyridine and DMSO solutions, two ^{23}Na resonance peaks (free and complexed Na^+ ion) were observed at ligand/Na^+ mole ratio of one (Table 27 and Figure 20). For the system NaI/C222B in pyridine solution, the separation of these two peaks is large enough to allow a semiquantitative determination of the areas under the peaks. The ratio of the areas was estimated to be 10:1 (complex:free). Hence, the formation constant of the Na^+·C222B complex in pyridine was estimated to be log K $\cong$ 5 by integrating the peak areas, taking the ion pair formation constant of the NaI salt in pyridine as K_{ip}= 2200 (126) and assuming that the extent of ion pair formation of the complex is negligible.

When the chemical shifts of these four cryptates (Na^+.C211, Na^+·C221, Na^+·C222 and Na^+·C222B) in various solvents are compared, the following features are obtained. The similarity of the large paramagnetic chemical shifts (around +11 ppm) of the Na^+·C211 cryptate in the various solvents studied indicates that the Na^+ ion is fored very much into the C211 cavity and thus the short range repulsive interaction leads to the large downfield shift.

The chemical shifts (around -9 ppm) of the Na^+·C222B cryptate are slightly downfield from those (around -11 ppm)

Table 31. The Limiting ^{23}Na NMR Chemical Shifts of $Na^+ \cdot C211$, $Na^+ \cdot C222$ and $Na^+ \cdot C222B$ Cryptates in Various Solvents at Ambient Temperature

Solvent	Salt[a]	δ_{ppm} $Na^+ \cdot C211$	δ_{ppm} $Na^+ \cdot C222$	δ_{ppm} $Na^+ \cdot C222B$
H_2O	NaI	12.3		
	NaCl	12.7		
PY	$NaBPh_4$	10.8[b]	-12.5[b]	-9.9
	$NaClO_4$	10.8		
	NaI	11.5	-12.4	-9.8
	NaSCN			-10.0
DMSO	$NaBPh_4$	9.8		-8.4
DMF	$NaBPh_4$	10.1	-11.5[b]	-8.8
	$NaClO_4$	10.1		
	NaI	10.0		
THF	$NaBPh_4$	10.7	-12.1	
	$NaClO_4$	8.1		
	$NaClO_4$[c]	8.1		
Me_2CO	$NaBPh_4$	10.5		
	NaI[c]	10.8		
MeCN	$NaBPh_4$	11.2	-11.2	-8.9
	$NaClO_4$	11.2		
	NaI	11.4		
$MeNO_2$	$NaBPh_4$	~11	-10.86	-8.7
PC	$NaBPh_4$		-11.4	
2-Nitro-propane	$NaBPh_4$		-11.8	-9.2

[a]The solutions were 0.05 M in sodium salt unless otherwise noted.

[b]The solutions were 0.10 M in $NaBPh_4$.

[c]The solutions were 0.025 M in $NaCLO_4$.

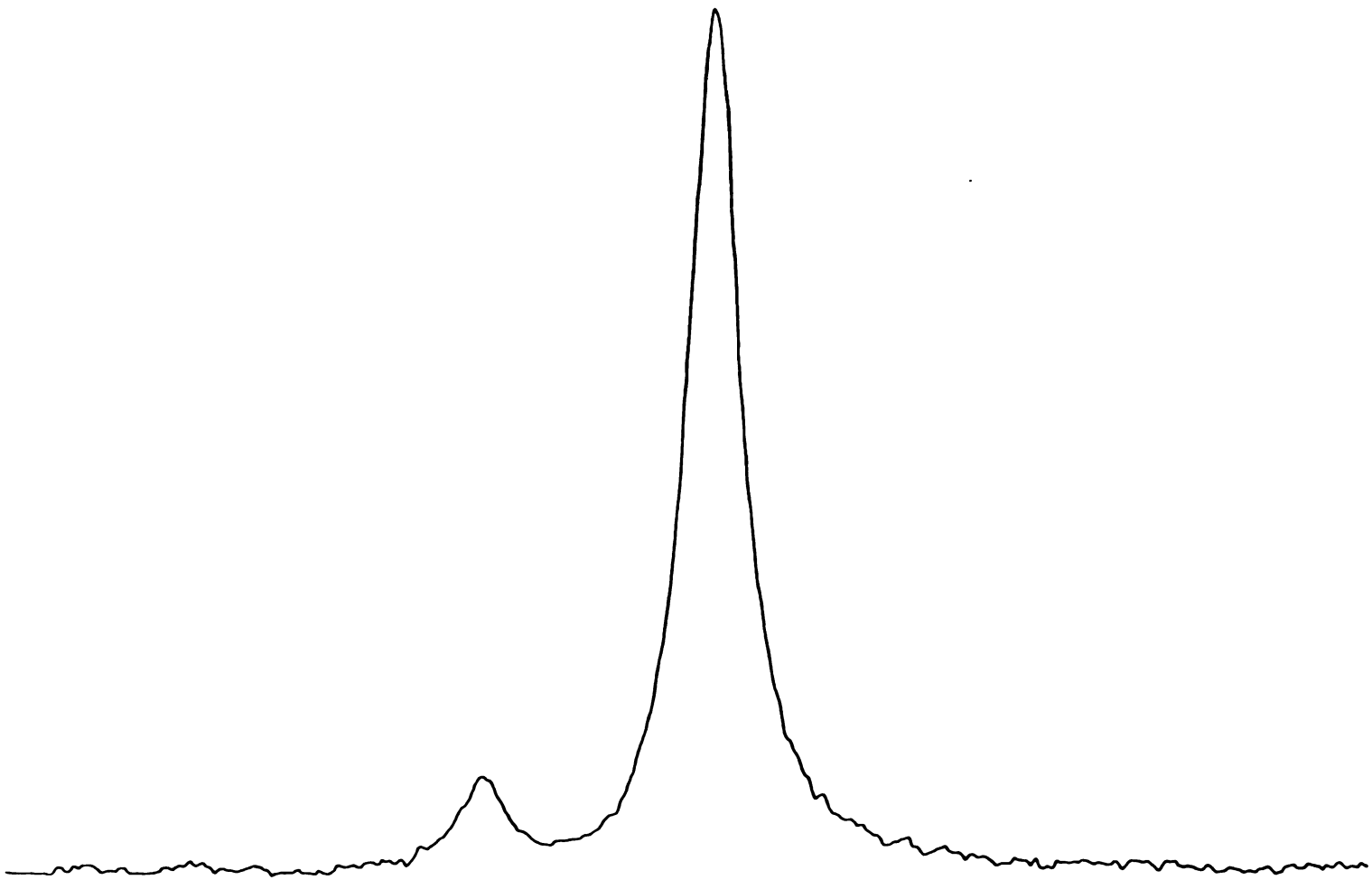

Figure 20. (a) Sodium-23 NMR spectrum of 0.050 M NaI and 0.053 M C222B in pyridine solution.

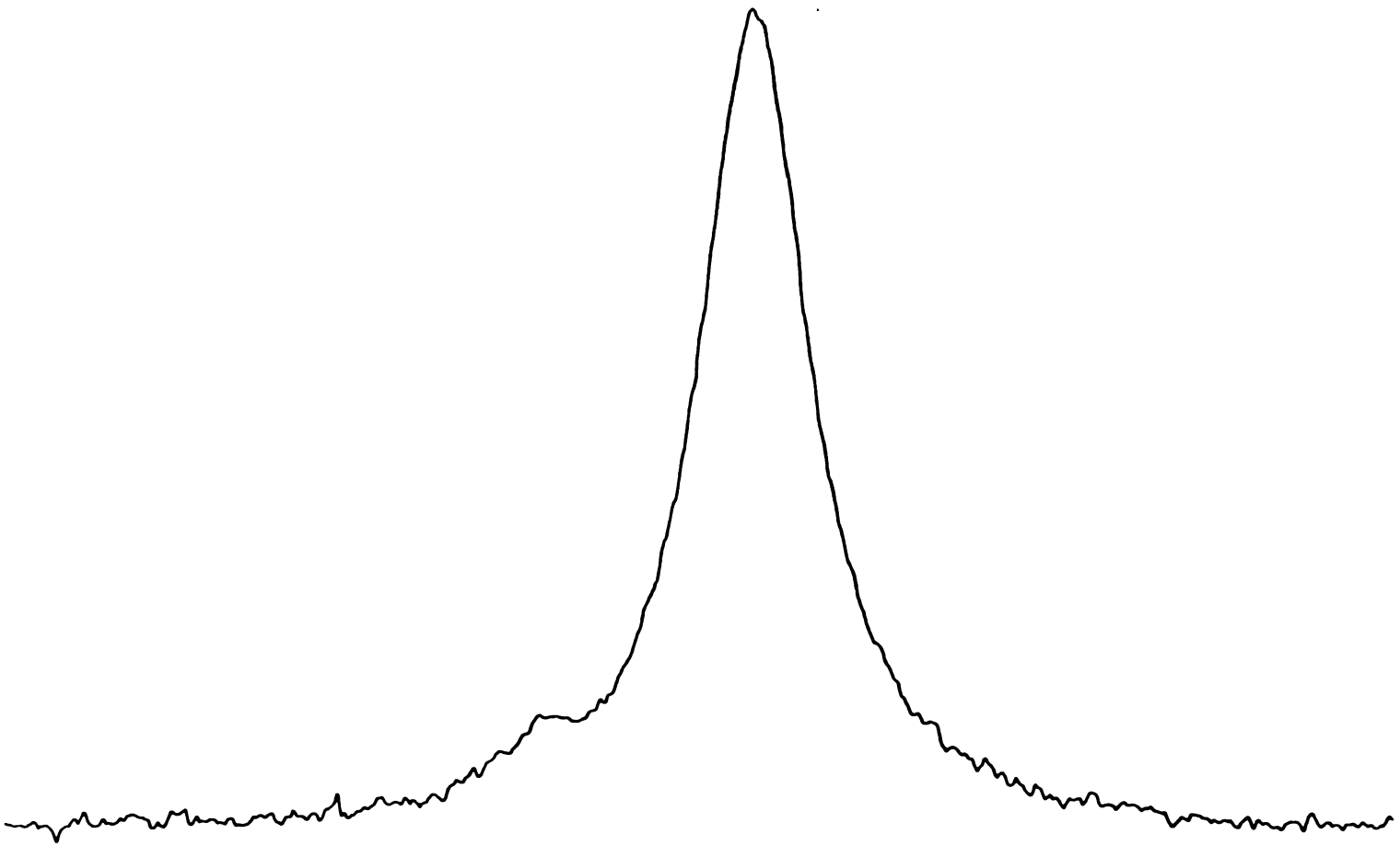

Figure 20. (b) Sodium-23 NMR spectrum of 0.050 M $NaBPh_4$ and 0.052 M C222B in pyridine solution.

of the Na^+·C222. It shows clearly that the orbital overlap between the Na^+ ion and the lone electron pairs of C222B is greater than that in the Na^+·C222 cryptate. This suggests that either the attractive interaction between the Na^+ ion and the lone electron pairs of the ligand is stronger in Na^+·C222B complex or the slightly smaller cavity size of C222B, because of the attachment of a benzo group (74), causes a short range repulsive interaction between the Na^+ ion and the ligand. As far as the decreased basicity of the oxygen atoms in C222B is concerned, Na^+.C222B cryptate is expected to be less stable than Na^+·C222 cryptate. However, Na^+·C222B was found to be slightly more stable than Na^+·C222 in 95% MeOH solution and they are about equally stable in water (Table 2). Therefore, the greater stability of Na^+· C222B than Na^+·C222 may be due to the better fit of the Na^+ ion into the C222B cavity. Thus, the attractive interaction between the Na^+ ion and the lone electron pairs of the ligand is stronger in Na^+·C222B than that in Na^+·C222, and that causes the slightly downfield shift of the Na^+· C222B resonance.

CHAPTER V

THERMODYNAMICS OF THE COMPLEXATION REACTION OF THE SODIUM CATION WITH SOME CROWN ETHERS IN SEVERAL NONAQUEOUS SOLVENTS

1. Introduction

The free energy change (ΔG^o) of a complexation reaction can be separated into two components: the enthalpy change, ΔH^o, and the entropy change, ΔS^o, i.e. $\Delta G^o = \Delta H^o - T\Delta S^o$. The enthalpy change is determined by the bonding interaction between the metal ion and the ligand as well as between the solute species and the solvent molecules. The entropy change depends on the overall change in the order of the system. The thermodynamic parameters of a complexation reaction can be evaluated based on a determination of the formation constant as a function of temperature. The formation constants are related to the relevant thermodynamic parameters by the following relationships:

$$\Delta G^o = -RT \ln K \qquad (5.1)$$

$$\Delta G^o = \Delta H^o - T\Delta S^o \qquad (5.2)$$

$$\ln K = \frac{-\Delta H^o}{RT} + \frac{\Delta S^o}{R} \qquad (5.3)$$

Thus, if ΔH^o is independent of temperature, a plot of ln K vs 1/T (van't Hoff plot (127)) should give a straight line with a slope of $-\Delta H^o/R$ and an intercept of $\Delta S^o/R$.

Another method for evaluating the thermodynamic parameters is to obtain the enthalpy value calorimetrically

at a given temperature and then, knowing ΔG^{o} at the same temperature, ΔS^{o} can be easily calculated.

This chapter reports thermodynamic studies of the complexation reactions between the Na^{+} ion and three crown ethers; 18-crown-6, 15-crown-5, and MB15-crown-5, in several nonaqueous solvents by ^{23}Na NMR and calorimetry.

2. Results and Discussion

It was shown in chapter III that at ambient temperatures most of the stability constants of the complexes in poorly solvating solvents, such as MeCN, $MeNO_2$, THF, Me_2CO and PC, are beyond the upper limit of the ^{23}Na NMR method. Thus, if the complexation reaction is exothermic (which is true for most Na^{+}·crown complexes), the stability constants at higher temperatures should be smaller and may be determined by the NMR techniques. However, with the exception of solutions in PC, the range of temperatures in which the stability constants can be determined is limited by the low boiling points of the solvents. On the other hand, in better solvating solvents such as DMSO, DMF and H_2O, the techniques are limited by the broadening of the ^{23}Na resonance at low temperatures and/or the small range of chemical shifts between the free Na^{+} ion and at high ligand/Na^{+} mole ratio. The broad linewidth makes the chemical shift measurements less accurate, and the small range of chemical shifts makes the error in the chemical

shift measurements relatively larger. Considering all of the above factors, the few systems, which seem to be more favorable for such studies, were investigated by the ^{23}Na NMR method. The data are presented in Figures 21-24 and Tables 32-33.

The complexation constants were calculated by the KINFIT program as described in chapter III, and the results are listed in Table 34. It can be seen that for the systems Na^+/18C6 in PC and in MeCN, and Na^+/15C5 in PC, the variations of the formation constants with temperatures are so small that the ^{23}Na NMR method may be ineffective.

For the system Na^+/15C5 in DMF and in PY solutions, the plots of ln K vs 1/T are shown in Figure 25. The slopes and intercepts of the straight lines were calculated by KINFIT and the corresponding thermodynamic quantities are presented in Table 36. Indeed, for the systems Na^+/18C6 in MeCN and Na^+/15C5 in PC, which have small changes in formation constants with temperatures and for which only three data points are available in the calculations, the standard deviations of the values are very large. These results, together with the data obtained from the calorimetric method, will be discussed later.

It is readily seen from the above results that the thermodynamics of the sodium-crown complexation reaction can be studied by the ^{23}Na NMR technique only in a few

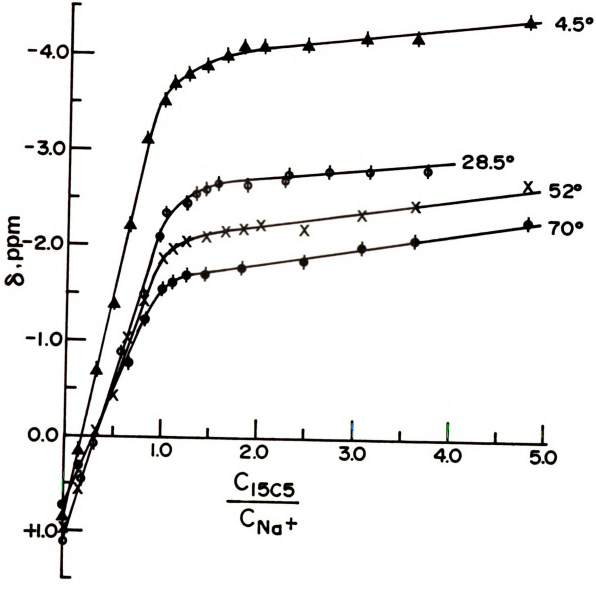

Figure 21. Sodium-23 chemical shift vs. 15C5/Na^+ mole ratio in pyridine solutions at various temperatures. The solutions were 0.05 M in $NaBPh_4$.

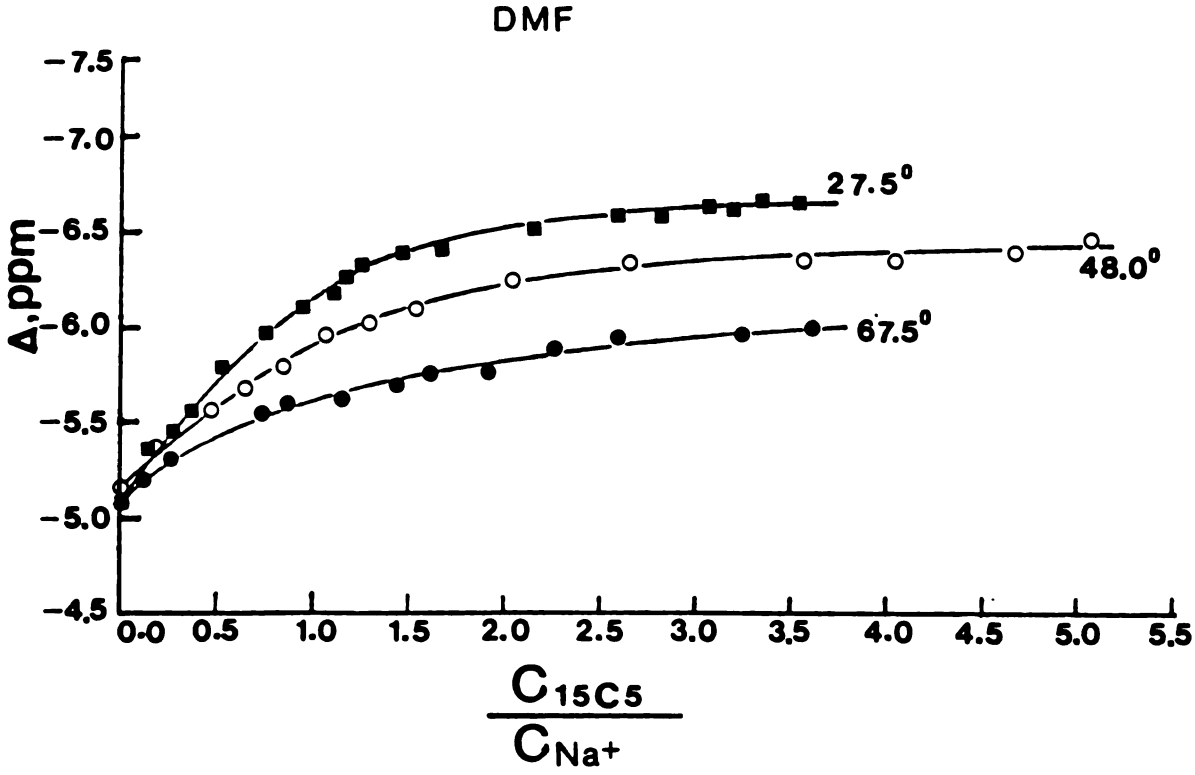

Figure 22. Sodium-23 chemical shift vs. 15C5/Na^+ mole ratio in DMF solutions at various temperatures. The solutions were 0.05 M in $NaBPh_4$.

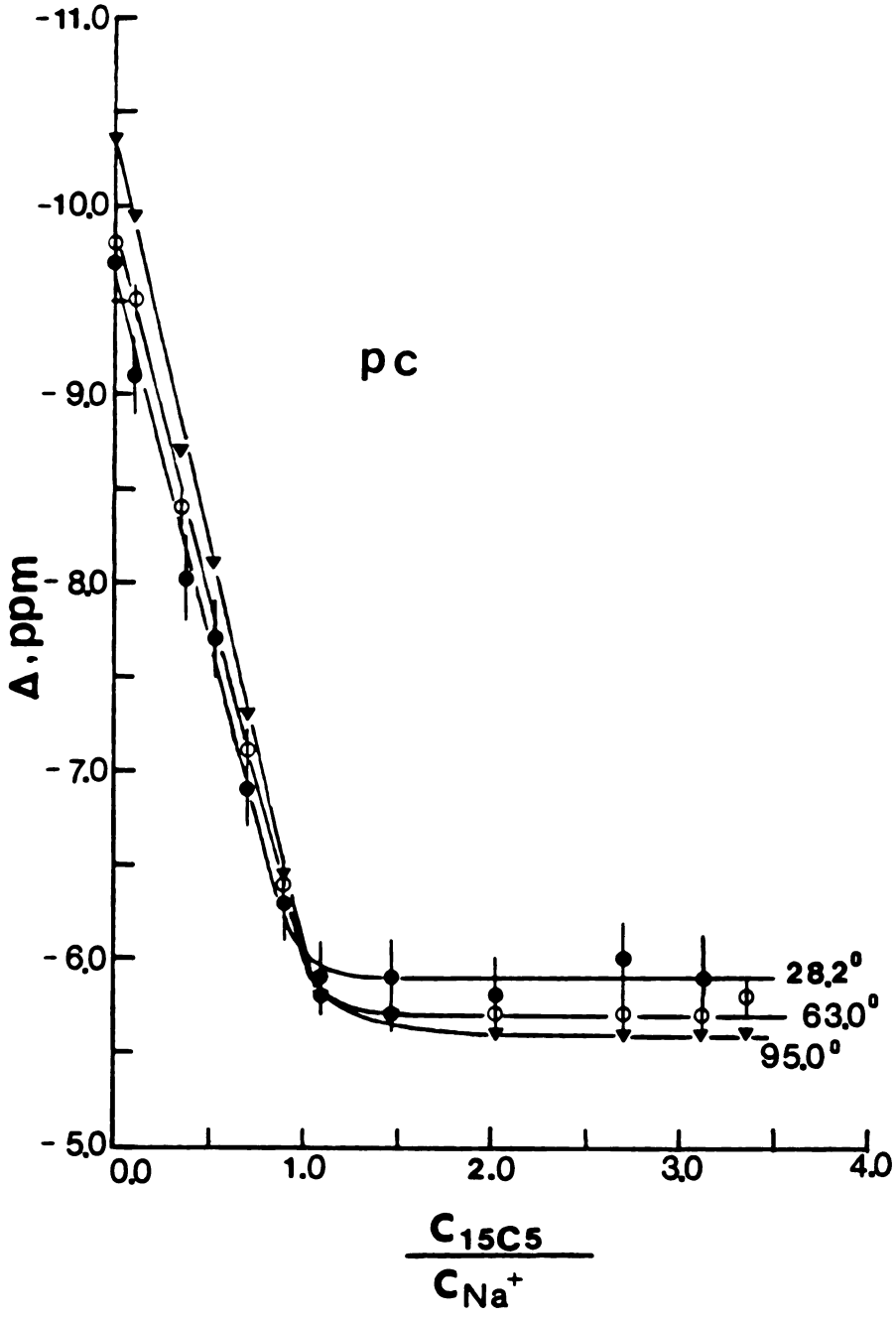

Figure 23. Sodium-23 chemical shift vs. 15C5/Na^+ mole ratio in PC solutions at various temperatures. The solutions were 0.05 M in $NaBPh_4$.

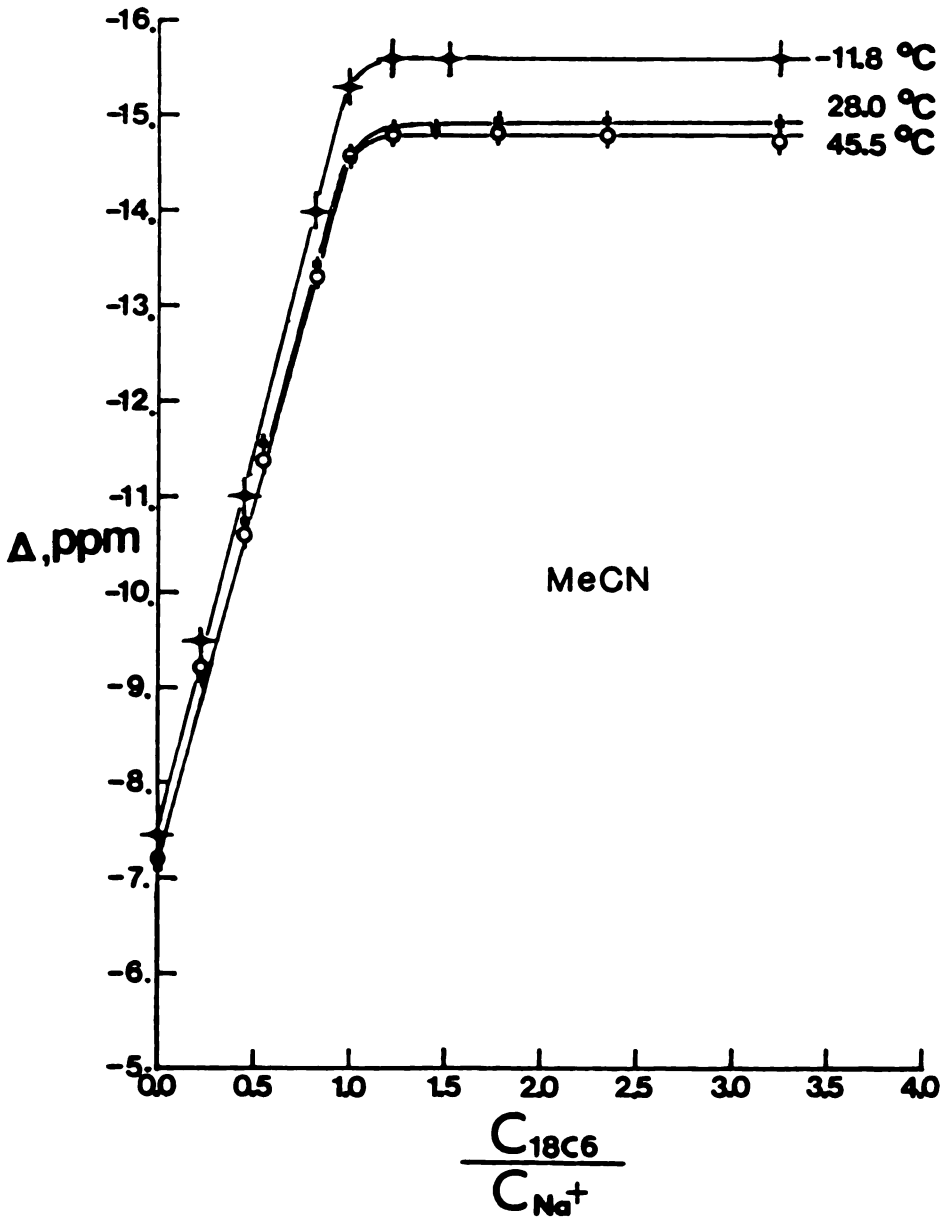

Figure 24. Sodium-23 chemical shifts vs. 15C5/Na^+ mole ratios in MeCN solutions at various temperatures. The solutions were 0.05 M in $NaBPh_4$.

Table 32. ^{23}Na NMR Chemical Shift-Mole Ratio Data for Na^+ ion Complex with 15C5 in DMF, Pyridine and PC Solutions at Various Temperatures[a]

DMF

67.5°C		48.0°C		1.5°C	
[15C5]/[Na^+]	δ_{ppm}	[15C5]/[Na^+]	δ_{ppm}	[15C5]/[Na^+]	δ_{ppm}
0	-5.08	0	-5.15	0	-6.1
0.12	-5.19	0.17	-5.31	0.27	-6.7
0.26	-5.31	0.47	-5.54	0.50	-7.0
0.57	-5.43	0.64	-5.65	0.74	-7.4
0.74	-5.54	0.83	-5.77		
0.87	-5.58	1.07	-5.92	1.04	-7.7
1.16	-5.62	1.30	-6.00	1.27	-7.9
1.45	-5.69	1.53	-6.08	1.50	-8.1
1.62	-5.77	2.05	-6.23	1.66	-8.0
1.93	-5.77	2.67	-6.31	1.88	-8.2
2.26	-5.89	3.58	-6.34	2.32	-8.3
2.60	-5.96	4.06	-6.34	2.59	-8.2
3.24	-5.93	4.68	-6.38	3.30	-8.3
3.63	-6.00	5.08	-6.46	4.03	-8.3
				5.35	-8.3

Table 32 (continued)

Pyridine

$\frac{[15C5]}{[Na^+]}$	δ_{ppm} 70.0°C	52.0°C	4.5°C
0	+0.38	0.57	+0.46
0.15	-0.08	0.15	-0.24
0.33	-0.39	-0.43	-1.1
0.50	-0.90	-0.81	-1.8
0.64	-1.16	-1.39	-2.5
0.82	-1.62	-1.81	-3.5
0.99	-1.93	-2.24	-3.8
1.10	-2.00	-2.35	-4.0
1.26	-2.08	-2.43	-4.2
1.46	-2.08	-2.46	-4.2
1.65	-	-2.52	-4.4
1.83	-2.16	-2.58	-4.5
2.02	-	-2.62	-4.5
2.48	-2.24	-2.58	-4.5
3.08	-2.39	-2.74	-4.6
3.63	-2.47	-2.85	-4.6
4.79	-2.70	-3.08	-4.8

Table 32 (continued)

PC

[15C5]/[Na^+]	δ_{ppm} 141.0°C	95.0°C	63.0°C
0	-9.36	-10.36	-9.8
0.11	-8.74	- 9.95	-9.5
0.37	-7.59	- 8.72	-8.4
0.52	-7.05	- 8.10	-7.7
0.70	-6.18	- 7.33	-7.1
0.90	-5.23	- 6.45	-6.4
1.19	-4.51	- 5.82	-5.8
1.48	-4.36	- 5.72	-5.7
2.01	-4.36	- 5.59	-5.7
2.70	-4.43	- 5.57	-5.7
3.12	-4.36	- 5.59	-5.7
3.36	-4.36	- 5.64	-5.8

[a]The solutions were 0.05 M in $NaBPh_4$ and the data at ambient temperatures are given in Table 8.

Table 33. ^{23}Na NMR Chemical Shift-Mole Ratio Data for Na^+ ion Complex with 18C6 in MeCN and PC Solutions at Various Temperatures

MeCN

[18C6]/[Na^+]	69.0°C	45.5°C	Temperature -11.8°C
0	- 7.86	- 7.60	- 7.85
0.23	- 9.71	- 9.58	- 9.86
0.45	-11.01	-10.96	-11.4
0.55	-11.83	-11.76	-
0.83	-13.63	-13.70	-14.4
1.00	-14.76	-14.96	-15.7
1.22	-14.91	-15.17	-16.0
1.52		-	-16.0
1.78		-15.19	-
2.34		-15.17	-
3.25		-15.09	-16.0

PC

	47.0°C
0	-10.0
0.16	-11.2
0.50	-13.0
0.71	-14.2
1.05	-15.8
1.53	-15.8
2.12	-15.9
3.04	-15.8

[a]The solutions were 0.05 M in $NaBPh_4$ and the data at ambient temperatures are given in Table 7.

Table 34. Formation Constants and Limiting Chemical Shifts of $Na^+ \cdot 15C5$ and $Na^+ \cdot 18C6$ Complexes in Several Solvents at Various Temperatures

Crown	Solvent	Temp(°C)	Log K_f	$\delta^{Na^+ \cdot crown}_{ppm}$
15C5	Pyridine	70.0 ± 0.5	2.4 ± 1	-2.54
		52.0	2.5 ± 1	-2.88
		28.5	2.68 ± 0.08	-3.25
		4.5	2.71 ± 0.08	-4.7
	DMF	67.5	1.5 ± 0.1	-6.16
		48.0	1.64 ± 0.05	-6.56
		27.5	1.97 ± 0.05	-6.85
		1.5	2.17 ± 0.08	-8.4
	PC	141.0	3.2 ± 0.2	-4.33
		95.0	3.0 ± 0.1	-5.55
		63.0	3.3 ± 0.2	-5.7
		28.2	-[a]	-5.8
18C6	MeCN	45.5	4.2 ± 0.6	-15.16
		28.0	3.8 ± 0.2	-15.3
		-11.8	3.9 ± 0.4	-16.0
	PC	47.0	> 4.0	-15.8
		28.0	> 4.0	-16.1

[a]It cannot be determined by the techniques used because of the broad linewidth.

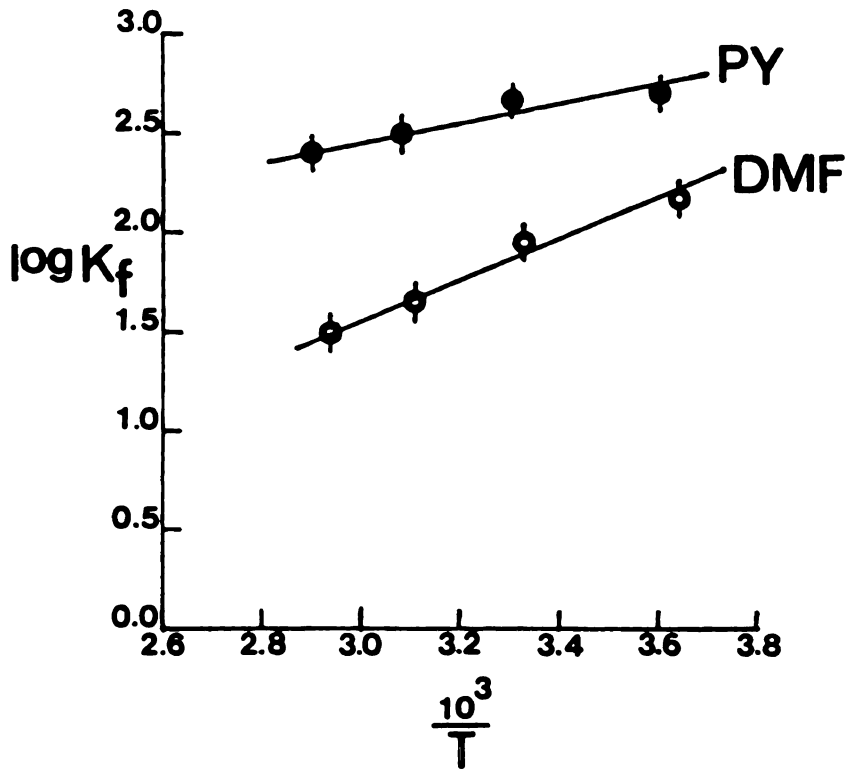

Figure 25. The formation constant vs. $10^3/T$ for Sodium•15C5 complex in pyridine and DMF solutions.

systems. Therefore, we determined the enthalpy of the complexation reaction for some Na^+·crown complexes by a calorimetric method and the data are presented in Table 35.

It is very difficult to get the horizontal baseline, espectially in viscous solutions such as DMSO and PC, possibly because of the inefficient stirring due to the poor design of the stirrer and the fluctuation of ambient temperatures (the calorimeter cell was not immersed in a constant temperature bath). An attempt was made to determine the enthalpy of Na^+·18C6 complex in MeCN solution by the calorimetric method. Unfortunately, after the necessary ~ 2 hours of stirring for equilibration, the thermister lead was above the solution level due to the evaporation of the solvent. At least 45 ml of solution is needed to cover the thermister lead and the maximum volume of the calorimeter cell is about 50 ml. In the actual experiment, less than 1 ml of a concentrated solution of the ligand (~ 0.4 M) in a given solvent was added to about 50 ml of 0.05 M salt solution. Thus, with the design of the calorimeter cell and insert which was used in this study, we cannot measure the heat of reaction in solvents of low boiling points.

Since in most of our cases the complex stability constants are small, the complexation reactions were incomplete under the experimental conditions used and thus

Table 35. Calorimetric Data for Some Sodium-Crown Complexes in DMF and DMSO Solutions at Ambient Temperatures[a]

Ligand	Solvent[b]	C_L ($\underline{M} \times 10^3$)	Heat of Complexation (cal.)[c]
MB15C5	DMF	7.66	-0.9
	DMSO	6.11	-0.7
15C5	DMF	5.90	-1.0
	DMSO	5.86	-0.9
18C6	DMF	7.73	-1.6
	DMSO	10.34	-1.3

a. The temperature was either 24 ± 1 °C or 25 ± 1 °C.

b. The solutions were 0.05 $\underline{M}$ in $NaBPh_4$.

c. The values are precise to ± 0.1 calories.

Table 36. Thermodynamic Quantities for Some Sodium-Crown Complexes in Several Nonaqueous Solvents at Ambient Temperatures

^{23}Na NMR Method

Ligand	Solvent	$\Delta G^{o}_{298\ ^{o}K}$ (kcal/mole)	ΔH^{o} (kcal/mole)	ΔS^{o} (cal/mole deg)
MB15C5	DMF	-2.2 ± 0.1		
	DMSO	-1.5 ± 0.2		
15C5	DMF	-2.69 ± 0.07	-4.7 ± 0.8	-7 ± 3
	DMSO	-1.8 ± 0.1		
	PY	-3.7 ± 0.1	-2.1 ± 0.7	+5 ± 2
	PC	-4.4[a]	-1 ± 3	+12 ± 9
18C6	DMF	-3.17 ± 0.06		
	DMSO	-1.9 ± 0.1		
	MeCN	-5.2 ± 0.2	0 ± 5	+18 ± 17

Calorimetry

MB15C5	DMF		-3.7 ± 0.4	-5 ± 1
	DMSO		-5.5 ± 0.8	-13 ± 3
15C5	DMF		-4.2 ± 0.4	-5 ± 1
	DMSO		-5.9 ± 0.6	-14 ± 2
18C6	DMF		-4.4 ± 0.3	-4 ± 1
	DMSO		-4.2 ± 0.3	-8 ± 1

a. Estimated from the values of ΔH^{o} and ΔS^{o}.

the quantity of the complex formed was calculated from the stability constant obtained by ^{23}Na NMR. The enthalpy change for the complexation reaction was obtained by dividing the heat of reaction by the number of moles of complex formed. The results are shown in Table 36, together with the calculated entropy changes. The values (Table 36) for the complexation reaction of the Na^+ ion with MB15C5 in DMSO solution are less precise than others, because the formation constant is very small and thus less complex is formed and less energy is released upon complexation.

It is immediately seen that for the $Na^+ \cdot 15C5$ complex in DMF solution the values obtained from both methods agree within experimental error. For the $Na^+ \cdot 15C5$ complex in pyridine solution only approximate values are obtained because of the possible ion pair formation in this solvent of low dielectric constant.

In the solvents studied, most of the $Na^+ \cdot$crown complexes are enthalpy stabilized but entropy destabilized. The $Na^+ \cdot 15C5$ complex in PC and $Na^+ \cdot 18C6$ complex in MeCN are entirely entropy stabilized. However, no $Na^+ \cdot$crown complex is entropy stabilized but enthalpy destabilized. Similar results have also been shown previously for the complexation reactions of alkali metal cations with crown ethers in various solvents (23, 45, 49, 50, 51); with only a few exceptions, both the enthalpy and entropy changes are negative.

In DMF and DMSO solutions, all complexes are enthalpy stabilized but entropy destabilized. The enthalpy change follows the same trend as the complex stability in DMF solution while this trend is not followed in DMSO solution. The negative entropy changes for the complexes in these two solvents may be attributed to the increased ligand rigidity upon complex formation because the free crown ether is more flexible than the complex. The possible contributions to overall entropy changes include the different solvation entropies of the metal ion, the ligand and the complex as well as the changes in the ligand configurational entropy, in the translational entropy and in the total number of particles. Thus, other factors may also contribute to the above entropy changes.

The more negative entropy changes for the complexes in DMSO than in DMF solutions may be due to the rearrangement of DMSO structure upon complexation. It is known that DMSO is a structured solvent due to dipolar interactions through the S - O bond (128), and the sodium ion (a small inorganic cation) acts as a structure breaker because the solvation of the cation disturbs the organization of the bulk solvent, but the complexed ion (a large organic cation) acts as a structure maker. The complexation reaction transforms a small inorganic cation into a large organic cation and the effect is a loss in entropy.

As the data shown in Table 36, the higher stability of the $Na^+ \cdot 18C6$ complex in DMF than in DMSO is due to both the more favorable enthalpy and entropy changes in DMF solution. The more stable $Na^+ \cdot 15C5$ and $Na^+ \cdot MB15C5$ complexes in DMF than in DMSO are both due to the more favorable entropy change in DMF, while the enthalpy change disfavors the complex formation in DMF. In DMSO solution, the lower stability of the $Na^+ \cdot 15C5$ than $Na^+ \cdot 18C6$ complex is because of the unfavorable entropy change for $Na^+ \cdot 15C5$, while the enthalpy change actually favors the $Na^+ \cdot 15C5$ complex. On the other hand, the less stable $Na^+ \cdot MB15C5$ than $Na^+ \cdot 15C5$ complex in DMSO is due to the less favorable enthalpy change of $Na^+ \cdot MB15C5$ while the entropy change slightly favors the $Na^+ \cdot MB15C5$ complex.

In acetonitrile solution, the considerable interaction between the solvent molecules and the 18C6 molecules (98) may account for the large entropy gain in the complexation reaction of Na^+ ion with 18C6.

3. Summary

It was shown in chapter III that in general, the stability of the Na^+·crown complex varies inversely with the solvating ability of the solvent as expressed by the Gutmann donor number, and the relative stabilities of the complexes are in the order Na^+·18C6 > Na^+·15C5 > Na^+·MB15C5. The above differences in the stabilities of the complexes were explained by the differences in the solvating ability of the solvent, the flexibility of the macrocyclic ring, the steric fit between the cation and the ligand cavity, and the number and basicity of the donor atoms in the macrocyclic ring.

The thermodynamic quantities shown in this chapter indicate that the contributions of enthalpy and entropy changes to the complex stability are quite different in different system. Thus, in the various solvents the more stable Na^+·18C6 than Na^+·15C5 complex is not simply due to the larger number of donor atoms in the polyether ring as explained in chapter III. Similarly, the higher stabilities of the complexes in DMF than in DMSO is not simply because of the lower solvating ability of DMF.

For the thermodynamics of the Na^+·crown complexes, this chapter reports only some preliminary work from calorimetric method. More work is necessary for a better understanding of the thermodynamic behavior of the Na^+ ion complexes with macrocyclic ligands in nonaqueous solvents.

APPENDICES

APPENDICES

1. Application of computer program KINFIT to the calculation of complex formation constants from NMR data.

The KINFIT computer program was used to fit the sodium-23 and carbon-13 NMR chemical shift vs. mole ratio data to equation (3.4) which was inserted by the user into the SUBROUTINE EQN.

$$\delta_{obs} = [(KC_M^t - KC_L^t - 1) + (K^2C_L^{t2} + K^2C_M^{t2} - 2K^2C_L^tC_M^t + 2KC_L^t + 2KC_M^t + 1)^{\frac{1}{2}}](\frac{\delta_M - \delta_{ML}}{2KC_M^t}) + \delta_{ML} \qquad (3.4)$$

Equation (3.4) has two unknown quantities, δ_{ML} and K, designated as U(1) and U(2) respectively in the FORTRAN code. The two input variables are the analytical concentration of the ligand (C_L^t, M) and the observed chemical shift (δ_{obs}, ppm) which are denoted as XX(1) and XX(2) respectively in the FORTRAN code. Starting with a reasonably estimated value of K and δ_{ML}, the program fit the calculated chemical shifts (the right hand side of equation (3.4)) to the observed ones by iteration method.

The first control card contains the number of data points (columns 1-5 (Format I5)), the maximum number of iterations allowed (columns 11-15 (F I5)), the number of

constants (columns 36-40 (F I5)) and the convergence tolerance (0.0001 work well) in columns 41-50 (F 10.6). The second control card contains any title the user desires. The third control card contains the values of CONST(1) (C_M^t, $\underline{M}$) in columns 1-10 (F 10.6) and CONST(2) (δ_M, ppm) in columns 11-20 (F 10.6) and other constants can be listed in columns 21-30, 31-40, etc. The fourth and final control card contains the initial estimates of the unknowns U(1) = δ_{ML} and U(2) = K, in columns 1-10 and 11-20 (F 10.6) respectively. The fifth through N cards are the data cards which contain XX(1) = C_L^t in columns 1-10 (F 10.6), the variance on XX(1) in columns 11-20, XX(2) = the chemical shift at XX(1) in columns 21-30 (F 10.6) and the variance on XX(2) in columns 31-40 (F 10.6) followed by the same parameters for the next data point. Each card may contain two data points. The SUBROUTINE EQN and a sample data listing are given below.

2. SUBROUTINE EQN

```
      SUBROUTINE EQN
      COMMON A,JNT,ITAPE,JTAPE,I,T,LSP,VINCR,NOPT,NDVAR,NOUNK,X,U,THAN,  EQN
     1TX,TEST,I,K,RIDIO,IAR,EPS,ITYPE,YY,AKTYP,DYII,FOP,FO,FU,P,ZL,TC,E  EQN
     2IGVAL,KST,T,T,L,M,JJJ,Y,DY,VECT,NCST,CONST,NDAT,JDAT,MOPT,LOPT,    EQN
     3YYY,EQN TE
      COMMON/E/IDT/IMETH
      COMMON/E I,I/MOPT,JD-T,XXY
      DIMENSION X(4,300),U(20),TX(4,100),XX(4),FTF(300),FO(300),FU(300) EQ
     1,P(20,21),VECT(20,21),ZL(100),TC(20),EIGVAL(20),XST(300),Y(10),
     2YY(10),JST(50,15),NCST(50),IKIN(50),AKTYP(40),DYII(50),IAK(50)
     3,MOPT(50),LOPT(50),YYY(50),CONST(15),XXY(15)
      GO TO (2,3,4,5,1,7,8,9,10,11,12)  ITYP
    1 CONTINUE
      ITAPE=41
      JTAPE=51
      NOUNK=2
      NDVAR=2
      RETURN
    7 CONTINUE
      RETURN
    8 CONTINUE
      RETURN
    2 CONTINUE
      IF(IMETH.NE.-1) GO TO 35
      RETURN
   35 CONTINUE
      A=(U(2)**2)*(XX(1)**2)
      B=(U(2)**2)*(CONST(1)**2)
      C=-2.0*(U(2)**2)*(XX(1))*CONST(1)
      D=2.0*(U(2))*(XX(1))
      E=2.0*(U(2))*(CONST(1))
      AA=(U(2))*(CONST(1))
      BB=-(U(1))*XX(1)
      CC=(CONST(2)-U(1))/(2.*(CONST(1))*(U(2)))
      F=(((AA+BB-1.)*SQRT(ABS(A+B+C+D+E+1.)))*CC)+U(1)
      RESID=F-XX(2)
      RETURN
    3 CONTINUE
      RETURN
    4 CONTINUE
      RETURN
    5 CONTINUE
      IF(IMETH.NE.-1) GO TO 20
      RETURN
   20 CONTINUE
      RETURN
    9 CONTINUE
      RETURN
   10 CONTINUE
      RETURN
   11 CONTINUE
      RETURN
   12 CONTINUE
      RETURN
      END
```

LITERATURE CITED

1. C.J. Pedersen, J. Amer. Chem. Soc., 89, 2495 and 7017 (1967).

2. G.A. Melson, ed., Chemistry of Macrocyclic Compounds, Plenum, New York, NY (1979).

3. C.J. Pedersen and H.K. Frensdorff, Angew. Chem. Intern. Ed., 11, 16 (1972).

4. B. Dietrich, J.M. Lehn and J.P. Sauvage, Tetrahedron Lett. 34, 2885 and 2889 (1969).

5. J.M. Lehn, Structure and Bonding, 16, 1 (1973).

6. J.L. Dye, M.G. DeBacker, V.A. Nicely, J. Amer. Chem. Soc., 92, 5226 (1970).

7. J.L. Dye in "Electrons in Fluids", J. Jortner and L.R. Kestner, Ed., Springer-Verlag, West Berlin, 1973, p. 77.

8. J.L. Dye, J.M. Ceraso, M.T. Lok, B.L. Barnett, F.J. Tehan, J. Amer. Chem. Soc., 96, 608 (1974).

9. J.M. Ceraso and J.L. Dye, J. Chem. Phys., 61, 1585 (1974).

10. F.J. Tehan, B.L. Barnett, J.L. Dye, J. Amer. Chem. Soc., 96, 7203 (1974).

11. M.G. Dague, J.S. Landers, H.L. Lewis and J.L. Dye, Chem. Phys. Lett., 66, 169 (1979).

12. J.L. Dye, Angew. Chem. Int. Ed. Engl., 18, 587 (1979).

13. J. Cheney, J.M. Lehn, J.P. Sauvage and M.E. Stubbs, J.C.S. Chem. Comm., 1100 (1972).

14. E. Graf and J.M. Lehn, J. Amer. Chem. Soc., 97, 5022 (1975).

15. J.M. Lehn and J. Simon, Helv. Chim. Acta, 60, 141 (1977).

16. J.M. Lehn, Pure and Appl. Chem., 49, 857 (1977).

17. J.M. Lehn, Acc. Chem. Res., 11, 49 (1978).

18. "Structure and Bondong", Vol. 16, Springer-Verlag, New York, NY, 1973.

19. (a) "Synthetic multidentate macrocyclic compounds," R.M. Izatt and J.J. Christensen, Ed., Academic Press, New York, 1978. (b) "Progress in macrocyclic chemistry", R.M. Izatt and J.J. Christensen, Ed., Wiley-Interscience, New York, 1979.

20. J.J. Christensen, D.J. Eatough, and R.M. Izatt, Chem. Rev., 74, 351 (1974).

21. I.M. Kolthoff, Anal. Chem., 51, 1R (1979).

22. J.M. Lehn, Pure and Appl. Chem., 50, 871 (1978) and 51, 979 (1979).

23. M. Shamsipur, Ph.D. Thesis, Michigan State University (1979).

24. C.J. Pedersen, J. Amer. Chem. Soc., 92, 386 (1970).

25. D.G. Parsons, M.R. Truter and J.N. Wingfield, Inorg. Chim. Acta, 14, 45 (1975).

26. M.A. Bush and M.R. Truter, J. Chem. Soc. Chem. Comm. 1439 (1970). J. Chem. Soc. (B) 1544 (1970), 1440 (1971) and J. Chem. Soc. Perkin II, 341 (1972).

27. M. Mercer and M.R. Truter, J. Chem. Soc. Dalton, 2215 (1973).

28. J.D. Dunitz, M. Dobler, P. Seiler and R.P. Phizackerley, Acta Cryst., B30, 2733 (1974).

29. C. Riche and C. Pascard-Billy, J. Chem. Soc. Chem. Comm., 183 (1977).

30. P.R. Mallison and M.R. Truter, J. Chem. Soc. Perkin II, 1818 (1972).

31. F.P. Remoortere and F.P. Boer, Inorg. Chem., 13, 2071 (1974).

32. F.P. Boer, M.A. Neuman, F.P. Remoortere and E.C. Steiner, Inorg. Chem., 13, 2826 (1974).

33. David Live and Sunney T. Chan, J. Amer. Chem. Soc., 98, 3769 (1976).

34. H.K. Frensdorff, J. Amer. Chem. Soc., 93, 600 (1971).

35. R.M. Izatt, J.H. Rytting, D.P. Nelson, B.L. Haymore, J.J. Christensen, Science, 164, 443 (1969).

36. R.M. Izatt, D.P. Nelson, J.H. Rytting, B.L. Haymore, and J.J. Christensen, J. Amer. Chem. Soc., 93, 1619 (1971).

37. J.J. Christensen, J.O. Hill, R.M. Izatt, Science, 29, 459 (1971).

38. R.M. Izatt, D.J. Eatough and J.J. Christensen, Struct. Bonding, 16, 161 (1973).

39. D.F. Evans, S.L. Wellington, J.A. Nadis, and E.L. Cussler, J. Solution Chem., 1, 499 (1972).

40. J. Koryta and M.L. Mittal, J. Eelectroanal. Chem. Interfacial Electrochem. 36, App. 14 (1972).

41. A. Hofmanova, J. Koryta, M. Brezina and M.L. Mittal, Inorg. Chim. Acta, 28, 73 (1978).

42. A. Agostiano, M. Caselli and M. Della Monica, J. Electroanal. Chem., 74, 95 (1976).

43. E. Schori, N. Nae and J.J. Grodzinski, J. Chem. Soc. Dalton, 2381 (1975).

44. A.J. Smetana and A.I. Popov, J. Chem. Thermodynamics, 11, 1145 (1979).

45. E. Shchori and J.J. Grodzinski, Isr., J. Chem., 11, 243 (1973).

46. R. Ungaro, B. El Haj and J. Smid, J. Amer. Chem. Soc., 98, 5198 (1976).

47. K.H. Pannell, W. Yee, G.S. Lewandos, and D.C. Hambrick, J. Amer. Chem. Soc., 99, 1457 (1977).

48. W.D. Curtis, D.A. Laidler and J.F. Stoddart, J. Chem. Soc. Perkin I, 1756 (1977).

49. R.M. Izatt, R.E. Terry, B.L. Haymore, L.D. Hansen, N.K. Dalley, A.G. Avondet, and J.J. Christensen, J. Amer. Chem. Soc., 98, 7620 (1976).

50. R.M. Izatt, R.E. Terry, D.P. Nelson, Y. Chan, D.J. Eatough, J.S. Bradshaw, L.D. Hansen, and J.J. Christensen, J. Amer. Chem. Soc., 98, 7626 (1976).

51. J.D. Lamb, R.M. Izatt, C.S. Swain and J.J. Christensen, J. Amer. Chem. Soc., 102, 475 (1980).

52. D.K. Cabbiness and D.W. Margerum, J. Amer. Chem. Soc., 91, 6540 (1969).

53. F.P. Hinz and D.W. Margerum, J. Amer. Chem. Soc., 96 (1974) and Inorg. Chem. 13, 2941 (1974).

54. M. Kodama and E. Kimura, J. Chem. Soc. Chem. Comm. 326 (1975).

55. A. Anichini, L. Fabbrizzi and P. Paoletti, R.M. Clay, J. Chem. Soc. Dalton, 577 (1978).

56. E. Mei, J.L. Dye, and A.I. Popov, J. Amer. Chem. Soc., 99, 5308 (1977).

57. E. Mei, A.I. Popov and J.L. Dye, J. Phy. Chem., 81, 1677 (1977).

58. V. Gutmann and E. Wychera, Inorg. Nucl. Chem. Lett, 2, 257 (1966).

59. V. Gutmann, Coordination Chemistry in Non-Aqueous Solutions, Springer-Verlag, Wien-New York (1969).

60. J.D. Lin, Ph.D. Thesis, Michigan State University, 1980.

61. A.J. Smetana, Ph.D. Thesis, Michigan State University, 1979.

62. E. Shchori, J.J.-Grodzinski, Z. Luz and M. Shporer, J. Amer. Chem. Soc., 93, 7133 (1971).

63. E. Shchori, J.J.-Grodzinski, and M. Shporer, J. Amer. Chem. Soc., 3842 (1973).

64. M. Shporer and Z. Luz, J. Amer. Chem. Soc., 97, 665 (1975).

65. G.W. Liesegang, M.M. Farrow, N. Purdie, and E.M. Eyring, J. Amer. Chem. Soc., 98, 6905 (1976).

66. G.W. Liesegang, M.M. Farrow, F.A. Vazquez, N. Purdie, and E.M. Eyring, J. Amer. Chem. Soc., 99, 3240 (1977).

67. L.J. Rodriguez, G.W. Liesegang, R.D. White, M.M. Farrow, N. Purdie, and E.M. Eyring, J. Phy. Chem., 81, 2118 (1977).

68. G.W. Liesegang, M.M. Farrow, L.J. Rodriguez, R.K. Burnham, and E.M. Eyring, Int. J. Chem. Kinetics, X, 471 (1978).

69. P.B. Chook, Proc. Natl. Acad. Sci., USA, 69, 1939 (1972).

70. D. Moras and R. Weiss, Acta Cryst., B29, 383, 396 and 400 (1973).

71. F. Mathieu, B. Metz, D. Moras, and R. Weiss, J. Amer. Chem. Soc., 100, 4412 (1978).

72. B. Metz, D. Moras and R. Weiss, Chem. Comm., 217 (1970) and 444 (1971) and Acta Cryst., B29, 388 (1973).

73. J.M. Lehn and J.P. Sauvage, Chem. Comm., 440 (1971) and J. Amer. Chem. Soc., 97, 6700 (1975).

74. B. Dietrich, J.M. Lehn and J.P. Sauvage, J.C.S. Chem. Comm., 15 (1973).

75. B. Dietrich, J.M. Lehn and J.P. Sauvage, J.C.S. Chem. Comm., 1055 (1970).

76. J.M. Lehn and F. Montavon, Helv. Chim. Acta, 61, 67 (1978).

77. E.L. Yee, J. Tabib and M.J. Weaver, J. Electroanal. Chem., 96, 241 (1979).

78. Y.M. Cahen, J.L. Dye and A.I. Popov, Inorg. Nucl. Chem. Letters, 10, 899 (1974) and J. Phy. Chem., 79, 1289 (1975).

79. A. Hourdakis and A.I. Popov, J. Solution Chem., 6, 299 (1977).

80. E. Kauffmann, J.M. Lehn and J.P. Sauvage, Helv. Chim. Acta, 59, 1099 (1976).

81. M.H. Abraham, A.F.D. Namor and W.H. Lee, J. Chem. Soc. Chem. Comm., 893 (1977).

82. E. Mei, L. Liu, J.L. Dye and A.I. Popov, J. Solution Chem., 6, 771 (1977).

83. E. Mei, J.L. Dye and A.I. Popov, J. Amer. Chem. Soc., 98, 1619 (1976).

84. N.M.-Desrosiers and J.P. Morel, Nouv. J. Chim., 3, 539 (1979).

85. J.M. Lehn, J.P. Suvage, B. Dietrich, J. Amer. Chem. Soc., 92, 2916 (1970).

86. Y.M. Cahen, J.L. Dye and A.I. Popov, J. Phys. Chem., 79, 1292 (1975).

87. J.M. Ceraso, J.L. Dye, J. Amer. Chem. Soc., 95, 4432 (1973).

88. J.M. Ceraso, P.B. Smith, J.S. Landers, and J.L. Dye, J. Phys. Chem., 81, 760 (1977).

89. B.G. Cox and H. Schneider, J. Amer. Chem. Soc., 99, 2809 (1977).

90. B.G. Cox, H. Schneider and J. Stroka, J. Amer. Chem. Soc., 100, 4746 (1978).

91. K. Henco, B. Tümmler and G. Maass, Angew. Chem., 89, 567 (1977).

92. G. Anderegg, Helv. Chim. Acta, 58, 1218 (1975).

93. J. Bessiere and M.F. Lejaille, Anal. Letters, 12 (A7), 753 (1979).

94. H. Høiland, J.A. Ringseth, and T.S. Brun, J. Solution Chem., 8, 779 (1979).

95. D.J. Sam and H.E. Simmons, J. Amer. Chem. Soc., 94, 4024 (1972).

96. E. Eyal and G.A. Rechnitz, Anal. Chem., 43, 1090 (1971).

97. D.C. Tosteson, Fed. Proc., 27, 1269 (1968).

98. G.W. Gokel, D.J. Cram, C.L. Liotta, H.P. Harris and F.L. Cook, J. Org. Chem, 39, 2445 (1974).

99. B. Dietrich, J.M. Lehn, J.P. Sauvage and J. Blanzat, Tetrahedron, 29, 1629 (1973).

100. R.H. Erlich, E. Roach and A.I. Popov, J. Amer. Chem. Soc., 92, 4989 (1970).

101. J.S. Shih, L. Liu, and A.I. Popov, J. Inorg. Nucl. Chem., 39, 552 (1977).

102. D.D. Traficante, J.A. Simms and M. Mulcay, J. Magn. Reson., 15, 484 (1974).

103. D. Wright, Ph.D. Thesis, Michigan State University, East Lansing, Michigan (1974).

104. D.H. Live and S.I. Chan, Anal. Chem., 42, 791 (1970).

105. G. Foex, C.J. Gorter and L.J. Smiths, "Constantes Selectionnees, Diamagnetisme et. Paramagnetisme, Relaxation Paramagnetique", Masson & Cie Editeurs, Paris (1957).

106. G.J. Templeman and A.L. Van Geet, J. Amer. Chem. Soc., 94, 5578 (1972).

107. Guild Corporation, R.D. 1 #384 Thomas-Venetia Rd. Eighty Four, PA 15330, USA.

108. E.M. Arnett, W.G. Bentrude, J.J. Burke, and P.M. Duggleby, J. Amer. Chem. Soc., 87, 1541 (1965).

109. V.A. Nicely and J.L. Dye, J. Chem. Educ., 48, 443 (1971).

110. C. Deverell and R.E. Richards, Mol. Phys., 10, 551 (1966) and 16, 421 (1969).

111. E.G. Bloor and R.G. Kidd, Can. J. Chem., 46, 3425 (1968).

112. A.L. Van Geet, J. Amer. Chem. Soc., 94, 5583 (1972).

113. J. Vaes, M. Chabanel, and M.L. Martin, J. Phys. Chem., 82, 2420 (1978).

114. C. Detellier, A. Gerstmans, and P. Laszlo, Inorg. Nucl. Chem. Letters, 15, 93 (1979).

115. M.S. Greenberg, Ph.D. Thesis, Michigan State University (1974).

116. Y. Cahen, Ph.D. Thesis, Michigan State University (1975).

117. E. Mei, Ph.D. Thesis, Michigan State University (1977).

118. J.S. Shih, Ph.D. Thesis, Michigan State University (1978).

119. E.D. Becker, High Resolution NMR, Academic Press, New York and London (1972).

120. N.K. Wilson, J. Phy. Chem., 83, 2649 (1979).

121. N. Ahmad and M.C. Day, J. Amer. Chem. Soc., 99, 941 (1977).

122. R.L. Kay, B.J. Hales and G.P. Cunningham, J. Phy. Chem., 71, 3925 (1967).

123. (a) D.P. Ames and P.G. Sears, J. Phys. Chem., 59, 16 (1955).
(b) P.G. Sears, G.R. Lester and L.R. Dawson, J. Phys. Chem., 60, 1433 (1956).

124. C. Carvajal, K.J. Tolle, J. Smid, and M. Szwarc, J. Amer. Chem. Soc., 87, 5548 (1965).

125. M.F.C. Ladd, Theoret. Chim. Acta (Berl.) 12, 333 (1968).

126. G.J. Janz and M.J. Tait, Can. J. Chem., 45, 1101 (1967).

127. W.J. Moore, Physical Chemistry, Prentice-Hall, Inc. Englewood Cliffs, N.J. (1972).

128. M.S. Greenberg and A.I. Popov, Spectrochim. Acta, 31A, 697 (1975)

129. T.R. Griffiths and D.C. Pugh, Coord. Chem. Rev., 29, 129 (1979)